TECHNISCHE UNIVERSITÄT WIEN
Vienna University of Technology

INSTITUTE OF MECHANICS
and MECHATRONICS

Aeroacoustics: Flow induced sound

Lecture notes for the
Summer School and Workshop
Waves in Flows

Univ. Prof. Manfred Kaltenbacher

Version: August 2018

Contents

1. Fluid Dynamics

We consider the motion of fluids in the continuum approximation, so that a body $\mathcal{B}$ is composed of particles $\mathcal{R}$ as displayed in Fig. 1.1. Thereby, a particle $\mathcal{R}$ already represents a macroscopic element. On the one hand a particle has to be small enough to describe the deformation accurately and on the other hand large enough to satisfy the assumptions of continuum theory. This means that the physical quantities density ρ, pressure p, velocity $\boldsymbol{v}$,

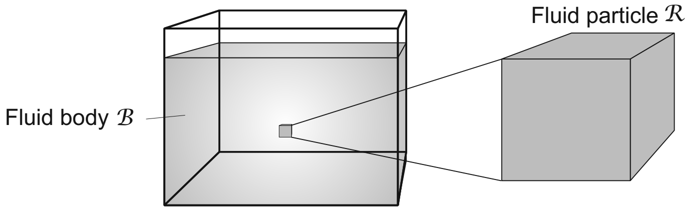

Figure 1.1.: A body $\mathcal{B}$ composed of particles $\mathcal{R}$.

temperature T, inner energy e and so on are functions of space and time, and are written as density $\rho(x_i, t)$, pressure $p(x_i, t)$, velocity $\boldsymbol{v}(x_i, t)$, temperature $T(x_i, t)$, inner energy $e(x_i, t)$, etc.. So, the total change of a scalar quantity like the density ρ is

$$\mathrm{d}\rho = \left(\frac{\partial \rho}{\partial t}\right) \mathrm{d}t + \left(\frac{\partial \rho}{\partial x_1}\right) \mathrm{d}x_1 + \left(\frac{\partial \rho}{\partial x_2}\right) \mathrm{d}x_2 + \left(\frac{\partial \rho}{\partial x_3}\right) \mathrm{d}x_3 \,. \tag{1.1}$$

Therefore, the total derivative (also called substantial derivative) computes by

$$\begin{aligned} \frac{\mathrm{d}\rho}{\mathrm{d}t} &= \frac{\partial \rho}{\partial t} + \frac{\partial \rho}{\partial x_1}\left(\frac{\mathrm{d}x_1}{\mathrm{d}t}\right) + \frac{\partial \rho}{\partial x_2}\left(\frac{\mathrm{d}x_2}{\mathrm{d}t}\right) + \frac{\partial \rho}{\partial x_3}\left(\frac{\mathrm{d}x_3}{\mathrm{d}t}\right) \\ &= \frac{\partial \rho}{\partial t} + \sum_1^3 \frac{\partial \rho}{\partial x_i}\left(\frac{\mathrm{d}x_i}{\mathrm{d}t}\right) = \frac{\partial \rho}{\partial t} + \frac{\partial \rho}{\partial x_i}\underbrace{\left(\frac{\mathrm{d}x_i}{\mathrm{d}t}\right)}_{v_i} \,. \end{aligned} \tag{1.2}$$

Note that in the last line of (1.2) we have used the summation rule of Einstein[1]. Furthermore, in literature the substantial derivative of a physical quantity is mainly denoted by the capital letter D and writes as

$$\frac{D}{Dt} = \frac{\partial}{\partial t} + \boldsymbol{v} \cdot \nabla \,. \tag{1.3}$$

1.1. Spatial Reference Systems

A spatial reference system defines how the motion of a continuum is described i.e., from which perspective an observer views the matter. In a Lagrangian frame of reference, the

[1] In the following, we use both vector and index notation; for details see App. B and C.

observer monitors the trajectory in space of each material point and measures its physical quantities. This can be understood by considering a measuring probe which moves together with the material, like a boat on a river. The advantage is that free or moving boundaries can be captured easily as they require no special effort. Therefore, the approach is suitable in the case of structural mechanics. However, its limitation is obtained dealing with large deformation, as in the case of fluid dynamics. In this case, a better choice is the Eulerian frame of reference, in which the observer monitors a single point in space when measuring physical quantities – the measuring probe stays at a fixed position in space. However, contrary to the Lagrangian approach, difficulties arise with deformations on the domain boundary, e.g., free boundaries and moving interfaces.
Formally, a deformation of a material body $\mathcal{B}$ is defined as a map ψ, which projects each point $\boldsymbol{X}$ at time $t \in \mathbb{R}$ to its current location $\boldsymbol{x}$, in mathematical terms

$$\boldsymbol{x} = \psi(\boldsymbol{X}, t), \qquad \psi : \mathcal{B} \times \mathbb{R} \to \mathbb{R}^3 \; .$$

By coupling structural and fluid mechanics an additional map between the different reference systems is necessary. In [1] a first method to solve the problem for an incompressible, viscous fluid has been presented. The so called Arbitrary-Lagrangian-Eulerian (ALE) method combines the advantages of both approaches. The concept is that the observer is neither fixed nor does move together with the material, but can move *arbitrarily*. Between each of the two reference systems a bijective mapping of the spatial variables $\boldsymbol{x}$ (Eulerian system), $\boldsymbol{X}$ (Lagrangian system) and $\boldsymbol{\chi}$ (ALE system) exists, as illustrated in Fig. 1.2. The choice of

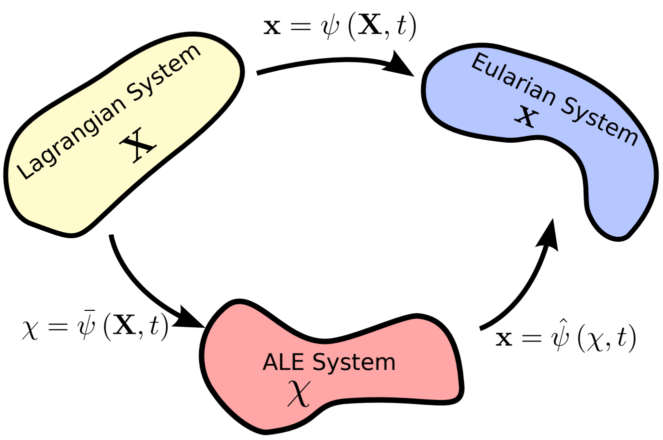

Figure 1.2.: Illustration of mapping between reference systems.

reference system effects the partial differential equations (PDEs) through its time derivative. Exemplified for a quantity f and its velocity $\boldsymbol{v}$, the total derivative results for the

- Lagrangian system to

$$\frac{Df}{Dt} = \left.\frac{\partial f}{\partial t}\right|_{\boldsymbol{X}}$$

- Eulerian system to

$$\frac{Df}{Dt} = \underbrace{\left.\frac{\partial f}{\partial t}\right|_{\boldsymbol{x}}}_{\text{local change}} + \underbrace{\left(\boldsymbol{v} \cdot \nabla_{\boldsymbol{x}}\right) f}_{\text{convective change}}$$

- ALE system to

$$\frac{Df}{Dt} = \left.\frac{\partial f}{\partial t}\right|_{\boldsymbol{\chi}} + (\boldsymbol{v}_c \cdot \nabla_{\boldsymbol{\chi}})\, f, \tag{1.4}$$

  with the convective velocity $\boldsymbol{v}_c = \boldsymbol{v} - \boldsymbol{v}_g$, the difference between material velocity $\boldsymbol{v}$ and grid velocity $\boldsymbol{v}_g$.

1.2. Reynolds' Transport Theorem

To derive the integral form of the balance equations the rate of change of integrals of scalar and vector functions has to be described, which is known as the Reynolds' transport theorem. The volume integral can change for two reasons: (1) scalar or vector functions change (2) the volume changes. The following discussion is directed to scalar valued functions.

Let's consider a scalar quantity $f(\boldsymbol{x}, t) : \Omega \times \mathbb{R} \to \mathbb{R}$, the change in time in a Lagrangian system of its volume integral

$$F(t) := \int\limits_{\Omega(t)} f(\boldsymbol{x}, t)\, \mathrm{d}\boldsymbol{x} \tag{1.5}$$

is given as

$$\frac{D}{Dt} F(t) = \frac{D}{Dt} \int\limits_{\Omega_L} f(\boldsymbol{X}, t)\, \mathrm{d}\boldsymbol{x} = \int\limits_{\Omega_L} \frac{\partial}{\partial t} f(\boldsymbol{X}, t)\, \mathrm{d}\boldsymbol{x}\,. \tag{1.6}$$

The simple transformation is due to the linearity of the integral and differential operators, and since the Lagrangian domain Ω_L conforms with the material movement, no additional terms are needed.
In an Eulerian context, time derivation must also take the time dependent domain $\Omega(t)$ into account by adding a surface flux term, which can be formulated as a volume term using the integral theorem of Gauß. This results in

$$\begin{aligned} \frac{D}{Dt} \int\limits_{\Omega(t)} f\, \mathrm{d}\boldsymbol{x} &= \int\limits_{\Omega(t)} \frac{\partial}{\partial t} f\, \mathrm{d}\boldsymbol{x} + \int\limits_{\Gamma(t)} f \boldsymbol{v} \cdot \boldsymbol{n}\, \mathrm{d}s \\ &= \int\limits_{\Omega(t)} \left(\frac{\partial}{\partial t} f + \nabla \cdot (f \boldsymbol{v}) \right) \mathrm{d}\boldsymbol{x}\,. \end{aligned} \tag{1.7}$$

1.3. Conservation Equations

The basic equations for the flow field are the conservation of mass, momentum and energy. Together with the constitutive equations and equations of state, a full set of PDEs is derived.

1.3.1. Conservation of Mass

The mass m of a body is the volume integral of its density ρ,

$$m = \int\limits_{\Omega(t)} \rho(\boldsymbol{x}, t)\, \mathrm{d}\boldsymbol{x}\,. \tag{1.8}$$

Mass conservation states that the mass of a body is conserved over time, assuming there is no source or drain. Therefore, applying Reynolds' transport theorem (1.7), results in

$$\begin{aligned} \frac{Dm}{Dt} &= \int\limits_{\Omega} \frac{\partial \rho}{\partial t} \,\mathrm{d}\boldsymbol{x} + \int\limits_{\Gamma} \rho \boldsymbol{v} \cdot \boldsymbol{n} \,\mathrm{d}s \\ &= \int\limits_{\Omega} \left(\frac{\partial \rho}{\partial t} + \nabla \cdot (\rho \boldsymbol{v}) \right) \mathrm{d}\boldsymbol{x} = 0. \end{aligned} \tag{1.9}$$

The integral in (1.9) can be dismissed, as it holds for arbitrary Ω and in the special case of an incompressible fluid ($\rho = const. \quad \forall (\boldsymbol{x}, t) \in \Omega \times \mathbb{R}$), which may be assumed for low Mach numbers (see Sec. 1.4), the time and space derivative of the density vanishes. This lead to the following form of mass conservation equations

$$\begin{aligned} \frac{\partial \rho}{\partial t} + \nabla \cdot (\rho \boldsymbol{v}) = 0 \qquad &\text{(compressible fluid)}, \\ \nabla \cdot \boldsymbol{v} = \nabla \cdot \boldsymbol{v}_{\mathrm{ic}} = 0 \qquad &\text{(incompressible fluid)}. \end{aligned} \tag{1.10}$$

Thereby, the subscript ic denotes that the physical quantity is incompressible.

1.3.2. Conservation of Momentum

The equation of momentum is implied by Newtons second law and states that momentum $\boldsymbol{I}_{\mathrm{m}}$ is the product of mass m and velocity $\boldsymbol{v}$

$$\boldsymbol{I}_{\mathrm{m}} = m\boldsymbol{v}\,. \tag{1.11}$$

Derivation in time gives the rate of change of momentum, which is equal to the force $\boldsymbol{F}$ and reveals the relation to Newtons second law in an Eulerian reference system

$$\boldsymbol{F} = \frac{D\boldsymbol{I}_{\mathrm{m}}}{Dt} = \frac{D}{Dt}(m\boldsymbol{v}) = \frac{\partial}{\partial t}(m\boldsymbol{v}) + \nabla \cdot (m\boldsymbol{v} \otimes \boldsymbol{v}), \tag{1.12}$$

where $\boldsymbol{v} \otimes \boldsymbol{v}$ is a tensor defined by the dyadic product $\otimes$ (see App. C). The last equality in (1.12) is derived from Reynolds transport theorem (1.7) and mass conservation (1.10).

The forces $\boldsymbol{F}$ acting on fluids can be split up into forces acting on the surface of the body $\boldsymbol{F}_{\Gamma}$, forces due to momentum of the molecules $D\boldsymbol{I}_{\mathrm{m}}/Dt$ and external forces $\boldsymbol{F}_{\mathrm{ex}}$ (e.g. gravity, electromagnetic forces)

$$\boldsymbol{F} = \boldsymbol{F}_{\Gamma} + \frac{D}{Dt}\boldsymbol{I}_{\mathrm{m}} + \boldsymbol{F}_{\mathrm{ex}}. \tag{1.13}$$

Thereby, the surface force computes by

$$\sum_{i=1}^{3} \boldsymbol{F}_{\Gamma_j} = -\sum_{i=1}^{3} \frac{\partial p}{\partial x_j} \Omega \boldsymbol{n}_j = -\Omega \nabla p. \tag{1.14}$$

and the total change of momentum $\boldsymbol{I}_{\mathrm{m}}$ by

$$\frac{D}{Dt}\boldsymbol{I}_{\mathrm{m}} = \Omega\, \nabla \cdot [\boldsymbol{\tau}] \tag{1.15}$$

with the viscous stress tensor $[\boldsymbol{\tau}]$ (see Fig. 1.3).

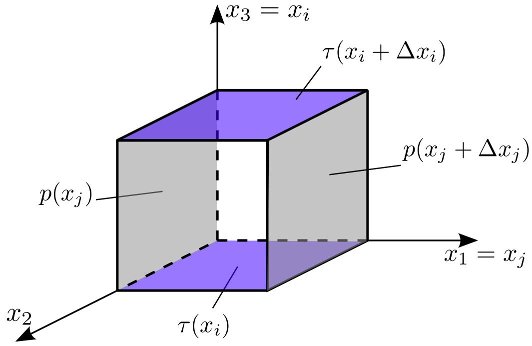

Figure 1.3.: Forces acting on a fluid element.

Now, we exploit the fact that $m = \rho\Omega$ and insert the pressure force (1.14), the viscous force (1.15) and any external forces per unit volume $\boldsymbol{f}$ acting on the fluid into (1.12). Thereby, we arrive at the momentum equation

$$\frac{\partial \rho \boldsymbol{v}}{\partial t} + \nabla \cdot (\rho\, \boldsymbol{v} \otimes \boldsymbol{v}) = -\nabla p + \nabla \cdot [\boldsymbol{\tau}] + \boldsymbol{f} \tag{1.16}$$

$$\frac{\partial \rho \boldsymbol{v}}{\partial t} + \nabla \cdot (\rho\, \boldsymbol{v} \otimes \boldsymbol{v} + p\,[\boldsymbol{I}] - [\boldsymbol{\tau}]) = \boldsymbol{f} \tag{1.17}$$

$$\frac{\partial \rho v_i}{\partial t} + \frac{\partial}{\partial x_j}(\rho v_j v_i + p\delta_{ij} - \tau_{ij}) = f_i\,, \tag{1.18}$$

with $[\boldsymbol{I}]$ the identity tensor. Furthermore, we introduce the momentum flux tensor $[\boldsymbol{\pi}]$ defined by

$$\pi_{ij} = \rho v_i v_j + p\delta_{ij} - \tau_{ij}\,, \tag{1.19}$$

and the fluid stress tensor $[\boldsymbol{\sigma}_{\mathrm{f}}]$ by

$$[\boldsymbol{\sigma}_{\mathrm{f}}] = -p\,[\boldsymbol{I}] + [\boldsymbol{\tau}]\,. \tag{1.20}$$

To arrive at an alternative formulation for the momentum equation, also called the non-conservative form, we exploit the following identities

$$\nabla \cdot (\rho \boldsymbol{v} \otimes \boldsymbol{v}) = \rho\, \boldsymbol{v} \cdot \nabla \boldsymbol{v} + \boldsymbol{v}\, \nabla \cdot (\rho \boldsymbol{v}) \tag{1.21}$$

$$\frac{\partial \rho \boldsymbol{v}}{\partial t} = \rho \frac{\partial \boldsymbol{v}}{\partial t} + \boldsymbol{v} \frac{\partial \rho}{\partial t} \tag{1.22}$$

and rewrite (1.16) by

$$\rho \frac{\partial \boldsymbol{v}}{\partial t} + \boldsymbol{v}\, \frac{\partial \rho}{\partial t} + \boldsymbol{v} \nabla \cdot (\rho \boldsymbol{v}) + \rho \boldsymbol{v} \cdot \nabla \boldsymbol{v} = -\nabla p + \nabla \cdot [\boldsymbol{\tau}] + \boldsymbol{f}\,. \tag{1.23}$$

Now, we use the mass conservation and arrive at

$$\rho \frac{\partial \boldsymbol{v}}{\partial t} + \rho\, \boldsymbol{v} \cdot \nabla \boldsymbol{v} = \rho\, \frac{D \boldsymbol{v}}{D t} = -\nabla p + \nabla \cdot [\boldsymbol{\tau}] + \boldsymbol{f} \tag{1.24}$$

$$\rho \frac{\partial v_i}{\partial t} + \rho v_j \frac{\partial v_i}{\partial x_j} = -\frac{\partial p}{\partial x_i} + \frac{\partial \tau_{ij}}{\partial x_j} + f_i\,.$$

1.3.3. Conservation of energy

The total balance of energy considers the inner, the kinetic and potential energies of a fluid. Since we do not consider gravity, the change of total energy e_{T} over time for a fluid element with mass m is given by

$$\frac{\mathrm{D}}{\mathrm{D}t}\left(m\left(\frac{1}{2}v^2+e\right)\right)=m\frac{\mathrm{D}}{\mathrm{D}t}\left(\frac{1}{2}v^2+e\right)+\left(\frac{1}{2}v^2+e\right)\frac{\mathrm{D}m}{\mathrm{D}t} \tag{1.25}$$

with e the inner energy and $v^2 = \boldsymbol{v}\cdot\boldsymbol{v}$. Due to mass conservation, the second term is zero and we obtain

$$\frac{\mathrm{D}}{\mathrm{D}t}\left(m\left(\frac{1}{2}v^2+e\right)\right)=\rho\Omega\frac{\mathrm{D}}{\mathrm{D}t}\left(\frac{1}{2}v^2+e\right). \tag{1.26}$$

This change of energy can be caused by [2]

- heat production per unit of volume: $q_{\mathrm{h}}\Omega$
- heat conduction energy due to heat flux $\boldsymbol{q}_{\mathrm{T}}$: $(-\partial q_{\mathrm{T}i}/\partial x_i)\,\Omega$
- energy due to surface pressure force: $(-\partial/\partial x_i(pv_i))\,\Omega$
- energy due to surface shear force: $(\partial/\partial x_i(\tau_{ij}v_j))\,\Omega$
- mechanical energy due to the force density $\boldsymbol{f}_i$ given by: $(f_i v_i)\,\Omega$

Thereby, we arrive at the conservation of energy given by

$$\rho\frac{\mathrm{D}}{\mathrm{D}t}\left(\frac{1}{2}v^2+e\right)=q_{\mathrm{h}}-\frac{\partial q_{\mathrm{T}i}}{\partial x_i}-\frac{\partial pv_i}{\partial x_i}+\frac{\partial \tau_{ij}v_j}{\partial x_i}+f_iv_i \tag{1.27}$$

or in vector notation by

$$\rho\frac{\mathrm{D}}{\mathrm{D}t}\left(\frac{1}{2}v^2+e\right)=q_{\mathrm{h}}-\nabla\cdot\boldsymbol{q}_{\mathrm{T}}-\nabla\cdot(p\boldsymbol{v})+\nabla\cdot([\boldsymbol{\tau}]\cdot\boldsymbol{v})+\boldsymbol{f}\cdot\boldsymbol{v}\,. \tag{1.28}$$

1.3.4. Constitutive equations

The conservation of mass, momentum and energy involve much more unknowns than equations. To close the system, additional information is provided by empirical information in form of constitutive equations. A good approximation is obtained by assuming the fluid to be in thermodynamic equilibrium. This implies for a homogeneous fluid that two *intrinsic* state variables fully determine the state of the fluid.

When we apply specific heat production q_{h} to a fluid element, then the specific inner energy e increases and at the same time the volume changes $\mathrm{d}\rho^{-1}$. Thereby, the first law of thermodynamics is expressed by

$$\mathrm{d}e=\mathrm{d}q_{\mathrm{h}}-p\,\mathrm{d}\rho^{-1}\,. \tag{1.29}$$

The second term in (1.29) considers a volumetric change which occurs at constant pressure. If the change occurs sufficiently slow, the fluid element is always in thermodynamic equilibrium, and we can express the heat input by the specific entropy s

$$\mathrm{d}q_{\mathrm{h}} = T\,\mathrm{d}s\,. \tag{1.30}$$

Therefore, we may rewrite (1.29) and arrive at the fundamental law of thermodynamics

$$\begin{aligned} \mathrm{d}e &= T\,\mathrm{d}s - p\,\mathrm{d}\rho^{-1} \\ &= T\,\mathrm{d}s + \frac{p}{\rho^2}\,\mathrm{d}\rho\,. \end{aligned} \tag{1.31}$$

In many cases we need to consider the change in pressure at constant volume. In this case, the particle increases its capacity to do work, which can be expressed by the enthalpy

$$h = e + \frac{p}{\rho}\,, \tag{1.32}$$

and using (1.29) we arrive at the relation for its total change

$$\mathrm{d}h = \mathrm{d}e + \frac{\mathrm{d}p}{\rho} + p\,\mathrm{d}\rho^{-1} = T\,\mathrm{d}s + \frac{\mathrm{d}p}{\rho}\,. \tag{1.33}$$

Towards acoustics, it is convenient to choose the mass density ρ and the specific entropy s as intrinsic state variables. Hence, the specific inner energy e is completely defined by a relation denoted as the thermal equation of state

$$e = e(\rho,\, s)\,. \tag{1.34}$$

Therefore, variations of e are given by

$$de = \left(\frac{\partial e}{\partial \rho}\right)_s \mathrm{d}\rho + \left(\frac{\partial e}{\partial s}\right)_\rho \mathrm{d}s\,. \tag{1.35}$$

A comparison with the fundamental law of thermodynamics (1.31) provides the thermodynamic equations for the temperature T and pressure p

$$T = \left(\frac{\partial e}{\partial s}\right)_\rho \;;\; p = \rho^2 \left(\frac{\partial e}{\partial \rho}\right)_s\,. \tag{1.36}$$

Since p is a function of ρ and s, we may write

$$dp = \left(\frac{\partial p}{\partial \rho}\right)_s \mathrm{d}\rho + \left(\frac{\partial p}{\partial s}\right)_\rho \mathrm{d}s\,. \tag{1.37}$$

As sound is defined as isentropic ($ds = 0$) pressure-density perturbations, the isentropic speed of sound is defined by

$$c = \sqrt{\left(\frac{\partial p}{\partial \rho}\right)_s}\,. \tag{1.38}$$

Since in many applications the fluid considered is air at ambient pressure and temperature, we may use the ideal gas law

$$p = \rho R T \tag{1.39}$$

with the specific gas constant R, which computes for an ideal gas as

$$R = c_p - c_\Omega \,. \tag{1.40}$$

In (1.40) c_p, c_Ω denote the specific heat at constant pressure and constant volume, respectively. Using (1.39) and computing the total derivative results in

$$\mathrm{d}p = \frac{\partial p}{\partial \rho}\,\mathrm{d}\rho + \frac{\partial p}{\partial T}\,\mathrm{d}T = RT\,\mathrm{d}\rho + \rho R\,\mathrm{d}T \,. \tag{1.41}$$

Diving this result by p and exploring (1.39) leads to

$$\frac{\mathrm{d}p}{p} = \frac{\mathrm{d}\rho}{\rho} + \frac{\mathrm{d}T}{T} \,. \tag{1.42}$$

Furthermore, the inner energy e depends for an ideal gas just on the temperature T via

$$\mathrm{d}e = c_\Omega\,\mathrm{d}T \,. \tag{1.43}$$

Substituting this relations in (1.31), assuming an isentropic state ($\mathrm{d}s = 0$) and using (1.39) results in

$$c_\Omega\,\mathrm{d}T = \frac{p}{\rho^2}\,\mathrm{d}\rho \;\rightarrow\; \frac{\mathrm{d}T}{T} = \frac{R}{c_\Omega}\frac{\mathrm{d}\rho}{\rho} \,. \tag{1.44}$$

This relation can be substituted in (1.42) to arrive at

$$\frac{\mathrm{d}p}{p} = \frac{\mathrm{d}\rho}{\rho} + \frac{R}{c_\Omega}\frac{\mathrm{d}\rho}{\rho} = \frac{c_p}{c_\Omega}\frac{\mathrm{d}\rho}{\rho} = \kappa\frac{\mathrm{d}\rho}{\rho} \tag{1.45}$$

with κ the specific heat ratio (also known as adiabatic exponent). A comparison of (1.45) with (1.38) yields

$$c = \sqrt{\kappa p/\rho} = \sqrt{\kappa RT} \,. \tag{1.46}$$

We see that the speed of sound c of an ideal gas depends only on the temperature. For air κ has a value of 1.402 so that we obtain a speed of sound c at $T = 15°\mathrm{C}$ of 341 m/s. For most practical applications, we can set the speed of sound to 340 m/s within a temperature range of 5°C to 25°C. Combining (1.45) and (1.46), we obtain the general pressure-density relation for an isentropic state

$$\mathrm{d}p = c^2\,\mathrm{d}\rho \,. \tag{1.47}$$

Furthermore, since we use an Eulerian frame of reference, we may rewrite (1.47) by

$$\frac{Dp}{Dt} = c^2\frac{D\rho}{Dt} \,. \tag{1.48}$$

As we consider local thermodynamic equilibrium, it is reasonable to assume that transport processes are determined by linear functions of the gradient of the flow state variables. This corresponds to *Newtonian fluid* behavior expressed by

$$\tau_{ij} = 2\mu\,\epsilon_{ij} + \lambda\epsilon_{ii}\delta_{ij} \tag{1.49}$$

with the rate of the strain tensor $\boldsymbol{\epsilon}$

$$\epsilon_{ij} = \frac{1}{2}\left(\frac{\partial v_i}{\partial x_j} + \frac{\partial v_j}{\partial x_i}\right) \,. \tag{1.50}$$

Note that the term $\epsilon_{ii} = \nabla \cdot \boldsymbol{v}$ takes into account the effect of dilatation. In thermodynamic equilibrium, the bulk viscosity λ is equal to $-(2/3)\mu$ (with μ being the dynamic viscosity) according to the hypothesis of Stokes, and we may write

$$\tau_{ij} = \mu \left(\frac{\partial v_i}{\partial x_j} + \frac{\partial v_j}{\partial x_i} \right) - \frac{2}{3} \mu \frac{\partial v_k}{\partial x_k} \delta_{ij} \,. \tag{1.51}$$

With this relation, we can also rewrite the divergence of the $[\boldsymbol{\tau}]$ as

$$. \tag{1.52}$$

Exploring the thermodynamic relations, we may rewrite the conservation of energy (see (1.28)) by the total change of the entropy. In doing so, we rewrite (1.31) by the substantial derivatives

$$\frac{De}{Dt} = T \frac{Ds}{Dt} - p \frac{D\rho^{-1}}{Dt} = T \frac{Ds}{Dt} + \frac{p}{\rho^2} \frac{D\rho}{Dt} \,. \tag{1.53}$$

In a next step, we incorporate the total energy $e_{\mathrm{T}} = e + v^2/2$ and multiply with the density

$$\rho \frac{De_{\mathrm{T}}}{Dt} = \rho T \frac{Ds}{Dt} + \frac{p}{\rho} \frac{D\rho}{Dt} + \rho \frac{D}{Dt} \left(\frac{v^2}{2} \right) \,. \tag{1.54}$$

In a next step, we use mass conservation rewritten with the substantial derivative

$$\frac{1}{\rho} \frac{D\rho}{Dt} = -\nabla \cdot \boldsymbol{v}$$

and arrive at

$$\rho \frac{De_{\mathrm{T}}}{Dt} = \rho T \frac{Ds}{Dt} - p \frac{\partial v_i}{\partial x_i} + \rho \frac{D}{Dt} \left(\frac{v^2}{2} \right) \tag{1.55}$$

Furthermore, we may rewrite the last term in (1.54) by

$$\rho \frac{D}{Dt} \left(\frac{v^2}{2} \right) = \boldsymbol{v} \cdot \rho \frac{D\boldsymbol{v}}{Dt} \,.$$

Now, we can use the conservation of momentum according to (1.24) and arrive at

$$\rho \frac{De_{\mathrm{T}}}{Dt} = \rho T \frac{Ds}{Dt} - p \frac{\partial v_i}{\partial x_i} + v_i \left(-\frac{\partial p}{\partial x_i} + \frac{\partial \tau_{ij}}{\partial x_j} + f_i \right) \,. \tag{1.56}$$

Finally, we substract from this relation the original conservation of energy according to (1.27) and obtain (not internal heat source, $q_{\mathrm{h}} = 0$)

$$\rho T \frac{Ds}{Dt} = \tau_{ij} \frac{\partial v_i}{\partial x_j} - \frac{\partial q_{\mathrm{T}i}}{\partial x_i} \,. \tag{1.57}$$

When heat transfer is neglected, the flow ist *adiabatic*. It is *isentropic*, when it is adiabatic and reversible, which means that the viscous dissipation can be neglected, which leads to

$$\rho T \frac{\mathrm{D}s}{\mathrm{D}t} = 0 \,. \tag{1.58}$$

Finally, when the fluid is homogeneous and the entropy uniform ($\mathrm{d}s = 0$), we call the flow *homentropic*.

1.4. Characterization of Flows by Dimensionless Numbers

Two flows around geometric similar models are physically similar if all characteristic numbers coincide [3]. Especially for measurement setups, these similarity considerations are important as it allows measuring of down sized geometries. Furthermore, the characteristic numbers are used to classify a flow situation. The Reynolds number is defined by

$$\mathrm{Re} = \frac{vl}{\nu} \tag{1.59}$$

with the characteristic flow velocity v, flow length l and kinematic viscosity ν. It provides the ratio between stationary inertia forces and viscous forces. Thereby, it allows to subdivide flows into laminar and turbulent ones. The Mach number allows for an approximate subdivision of a flow in compressible ($\mathrm{Ma} > 0.3$) and incompressible ($\mathrm{Ma} \leq 0.3$), and is defined by

$$\mathrm{Ma} = \frac{v}{c} \tag{1.60}$$

with c the speed of sound. In unsteady problems, periodic oscillating flow structures may occur, e.g. the Kármán vortex street in the wake of a cylinder. The dimensionless frequency of such an oscillation is denoted as the Strouhal number, and is defined by

$$\mathrm{St} = f\,\frac{l}{v} \tag{1.61}$$

with f the shedding frequency.

1.5. Vorticity

The motion of a fluid particle is a superposition of

- translational motion
- rotation
- distortion of shape, i.e. strain.

The rate of the strain tensor $\partial v_i/\partial x_j$ can be expressed as the sum of a symmetric and an anti-symmetric part

$$\frac{\partial v_i}{\partial x_j} = \frac{1}{2}\left(\frac{\partial v_i}{\partial x_j} + \frac{\partial v_j}{\partial x_i}\right) + \frac{1}{2}\left(\frac{\partial v_i}{\partial x_j} - \frac{\partial v_j}{\partial x_i}\right) . \tag{1.62}$$

The symmetric part defines the rate of strain tensor $\boldsymbol{\epsilon}$ (see (1.50)) and corresponds to a stretching of fluid particles along the principle axes. The anti-symmetric part

$$w_{ij} = \frac{1}{2}\left(\frac{\partial v_i}{\partial x_j} - \frac{\partial v_j}{\partial x_i}\right) \tag{1.63}$$

has only three independent components, since $w_{ii} = 0$, $w_{ij} = -w_{ji}$, and are combined into a vector, which is called the vorticity $\boldsymbol{w}$ and computes by

$$\boldsymbol{w} = \nabla \times \boldsymbol{v} . \tag{1.64}$$

The vorticity gives a measure of the angular rotation of fluid particles. E.g., a fluid particle with angular velocity about the origin, i.e. velocity $\boldsymbol{v}$ is given by $\boldsymbol{\Omega} \times \boldsymbol{r}$, has vorticity

$$\boldsymbol{\omega} = 2\boldsymbol{\Omega}\,.$$

Vorticity lines are always tangential to the vorticity vector and form closed field lines. These lines pass through every point of a simple closed curve and define the boundary of a *vortex tube*. For a tube of small cross-sectional area $\mathrm{d}\boldsymbol{s}$ the product $\boldsymbol{\omega}\cdot \mathrm{d}\boldsymbol{s}$ is called the tube strength, which has to be constant because of the following vector identity

$$\nabla \cdot \boldsymbol{\omega} = \nabla \cdot \nabla \times \boldsymbol{v} = 0\,.$$

Therefore the divergence theorem (also known as Gauss integral theorem, see App. B) leads to

$$\int\limits_{\Omega} \nabla \cdot \boldsymbol{\omega}\ \mathrm{d}\boldsymbol{x} = \oint\limits_{\Gamma(\Omega)} \boldsymbol{\omega}\cdot\ \mathrm{d}\boldsymbol{s} = 0\,. \tag{1.65}$$

We will now derive the PDE for vorticity and show that vorticity is transported by convection and molecular diffusion. Therefore, an initially confined region of vortex loops can frequently be assumed to remain within a bounded domain. We assume a Stokesian fluid (see (1.52)) and a homentropic flow, where the density ρ is only a function of pressure p. We start at the conservation of momentum (divided by the density) and use the vector identity (B.10) to arrive at

$$\frac{\partial \boldsymbol{v}}{\partial t} + \boldsymbol{v}\cdot\nabla\boldsymbol{v} + \frac{1}{\rho}\,\nabla p = -\nu\left(\nabla\times\boldsymbol{\omega} - \frac{4}{3}\nabla\nabla\cdot\boldsymbol{v}\right)\,. \tag{1.66}$$

In a next step, we use for the second term on the left hand side the vector identity according to (B.13) and for the third term the relation (A.1) to obtain *Crocco's form* of momentum conservation

$$\frac{\partial \boldsymbol{v}}{\partial t} + \boldsymbol{\omega}\times\boldsymbol{v} + \nabla B = -\nu\left(\nabla\times\boldsymbol{\omega} - \frac{4}{3}\nabla\nabla\cdot\boldsymbol{v}\right)\,. \tag{1.67}$$

Thereby, B denotes the total enthalpy in an homentropic flow

$$B = \int \frac{\mathrm{d}p}{\rho} + \frac{1}{2}v^2 \tag{1.68}$$

and the vector $\boldsymbol{\omega}\times\boldsymbol{v}$ is called the *Lamb vector*. When the flow is incompressible (denoted by the subscript ic), Crocco's equation reduces to

$$\frac{\partial \boldsymbol{v}_{\mathrm{ic}}}{\partial t} + \boldsymbol{\omega}\times\boldsymbol{v}_{\mathrm{ic}} + \nabla B = -\nu\nabla\times\boldsymbol{\omega}\,, \tag{1.69}$$

in which case dissipation occurs only for $\boldsymbol{\omega}\neq\boldsymbol{0}$. Applying the curl to (1.69) and considering the vector identity for $\boldsymbol{\omega}$

$$\nabla\times\nabla\times\boldsymbol{\omega} = \nabla\nabla\cdot\boldsymbol{\omega} - \nabla\cdot\nabla\boldsymbol{\omega} = \nabla\cdot\nabla\boldsymbol{\omega}$$

results in

$$\frac{\partial \boldsymbol{\omega}}{\partial t} + \nabla\times\big(\boldsymbol{\omega}\times\boldsymbol{v}_{\mathrm{ic}}\big) = \nu\nabla\cdot\nabla\boldsymbol{\omega}\,, \tag{1.70}$$

Finally, applying (B.11) and exploring the relation $\nabla\cdot\boldsymbol{v}_{\mathrm{ic}} = 0$, we arrive at the *vorticity equation*

$$\frac{D\boldsymbol{\omega}}{Dt} = \boldsymbol{\omega}\cdot\nabla\boldsymbol{v}_{\mathrm{ic}} + \nu\nabla\cdot\nabla\boldsymbol{\omega}\,. \tag{1.71}$$

The terms on the right hand side determine the mechanisms describing the change of vorticity:

- Term 1: $\boldsymbol{\omega} \cdot \nabla \boldsymbol{v}_{\mathrm{ic}}$
  In the absence of viscosity, vortex lines move with the fluid. They are rotated and stretched in a manner determined by the flow. When a vortex tube is stretched, the cross-sectional area is decreased and therefore the amplitude of vorticity has to increase in order to preserve the strength of the tube.

- Term 2: $\nu \nabla \cdot \nabla \boldsymbol{\omega}$
  This term is only important in regions of high shear, in particular near boundaries. Near walls the velocity becomes very small, so that (1.71) reduces to a diffusion equation

  $$\frac{\partial \boldsymbol{\omega}}{\partial t} = \nu \nabla \cdot \nabla \boldsymbol{\omega} \,. \tag{1.72}$$

  Vorticity is generated at solid boundaries and the viscosity is responsible for its diffusion into the fluid domain, where it may subsequently be convected by the flow.

On the other hand, if the vorticity within an incompressible flow is zero, we arrive at the *potential flow*. Then, we can describe the flow by a scalar potential ϕ (also called flow potential)

$$\boldsymbol{v}_{\mathrm{ic}} = \nabla \phi \,. \tag{1.73}$$

According to the incompressibility condition, we obtain the describing PDE

$$\nabla \cdot \boldsymbol{v}_{\mathrm{ic}} = \nabla \cdot \nabla \phi = 0 \,. \tag{1.74}$$

Please note that a potential flow is both, divergence- and curl-free. Therefore, according to the Helmholtz decomposition, the velocity field $\boldsymbol{v}_{\mathrm{ic}}$ in an incompressibel flow can be split into two vector fields

$$\boldsymbol{v}_{\mathrm{ic}} = \nabla \phi + \nabla \times \boldsymbol{\Psi} = \nabla \phi + \boldsymbol{v}_{\mathrm{v}} \,, \tag{1.75}$$

where ϕ describes the potential flow and $\boldsymbol{v}_{\mathrm{v}}$ the vortical flow with

$$\boldsymbol{\omega} = \nabla \times \boldsymbol{v}_{\mathrm{ic}} = \nabla \times \boldsymbol{v}_{\mathrm{v}} \,. \tag{1.76}$$

By applying the curl to (1.75), we obtain for the vector potential

$$\nabla \times \nabla \times \boldsymbol{\psi} = \nabla \times \boldsymbol{v}_{\mathrm{ic}} = \nabla \times \boldsymbol{v}_{\mathrm{v}} = \boldsymbol{\omega} \,. \tag{1.77}$$

Furthermore, by using the vector identity

$$\nabla \cdot \nabla \boldsymbol{\psi} = \nabla \nabla \cdot \boldsymbol{\psi} - \nabla \times \nabla \times \boldsymbol{\psi}$$

we may write

$$\nabla \cdot \nabla \boldsymbol{\psi} = -\boldsymbol{\omega} \,. \tag{1.78}$$

To obtain $\boldsymbol{\psi}$ we can use Green's function for the Laplace equation and arrive at

$$\boldsymbol{\psi}(\boldsymbol{x}) = \int_{\Omega} \frac{\boldsymbol{\omega}(\boldsymbol{y})}{4\pi |\boldsymbol{x} - \boldsymbol{y}|} \, \mathrm{d}\boldsymbol{y} \,. \tag{1.79}$$

On the other hand, knowing the vorticity $\boldsymbol{\omega}$, we may compute $\boldsymbol{v}_{\rm v}$ by

$$\boldsymbol{v}_{\rm v} = \nabla_x \times \int\limits_{\Omega} \frac{\boldsymbol{\omega}(\boldsymbol{y})}{4\pi|\boldsymbol{x}-\boldsymbol{y}|}\,{\rm d}\boldsymbol{y} = \int\limits_{\Omega} \frac{(\boldsymbol{y}-\boldsymbol{x})\times\boldsymbol{\omega}(\boldsymbol{y})}{4\pi|\boldsymbol{x}-\boldsymbol{y}|^3}\,{\rm d}\boldsymbol{y}\,, \tag{1.80}$$

which is a pure kinematic relation. Now, because vorticity is transported by convection and diffusion, an initially confined region of vorticity will tend to remain within a bounded body, so that it may be assumed that the *hydrodynamic field* $\boldsymbol{v}_{\rm v} \to 0$ as $|\boldsymbol{x}| \to \infty$ with $O(1/|\boldsymbol{x}|^3)$ [4].

Finally, let us consider a pulsating sphere as displayed in Fig. 1.4. Since there are no

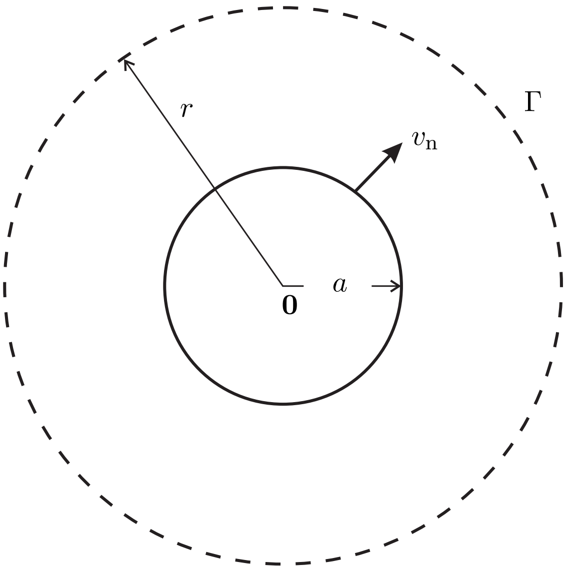

Figure 1.4.: Pulsating sphere.

sources in the fluid and we assume the fluid to be incompressible, we can model it by the Laplacian of the scalar velocity potential

$$\nabla \cdot \nabla\phi = \nabla^2\phi = 0\,. \tag{1.81}$$

Since the setup is radially symmetric, we obtain (using spherical coordinates)

$$\nabla^2\phi = \frac{1}{r^2}\frac{\partial}{\partial r}\left(r^2\frac{\partial}{\partial r}\right)\phi = 0\,;\quad r > a$$

and hence

$$\phi = \frac{A}{r} + B\,.$$

We assume that ϕ vanishes at ∞, so B can be set to zero. Furthermore, with the boundary condition $\partial\phi/\partial r = v_{\rm n}$ at $r = a$ we get

$$\phi(t) = -\frac{a^2}{r}\,v_{\rm n}(t) \text{ for } r > a\,. \tag{1.82}$$

Assuming a non-viscous fluid ($[\boldsymbol{\tau}] = \mathbf{0}$), no external forces ($\boldsymbol{f} = \mathbf{0}$) and neglecting the convective term, we may write the momentum conservation (see (1.24)) for an incompressible flow by

$$\rho_0 \frac{\partial \boldsymbol{v}_{\rm ic}}{\partial t} + \nabla p_{\rm ic} = 0\,. \tag{1.83}$$

Using the scalar potential ϕ, we arrive at the following linearized relation

$$p_{\rm ic} = -\rho_0 \frac{\partial \phi}{\partial t}\,. \tag{1.84}$$

With (1.82) we can compute the resulting pressure $p_{\rm ic}$ to

$$p_{\rm ic}(t) = -\rho_0 \frac{\partial \phi}{\partial t} = \rho_0\, \frac{a^2}{r}\, \frac{\partial v_{\rm n}}{\partial t}\,. \tag{1.85}$$

The volume flux $q_\Omega(t)$ at any time computes as

$$q_\Omega(t) = \oint_\Gamma \nabla\phi \cdot \, \mathrm{d}\boldsymbol{s} = \oint_\Gamma \underbrace{\nabla\phi \cdot \boldsymbol{e}_{\rm r}}_{\partial\phi/\partial r = v_{\rm n}} \,\mathrm{d}s = 4\pi a^2\, v_{\rm n}(t)\,,$$

and so we can rewrite (1.82) by

$$\phi(t) = -\frac{q_\Omega(t)}{4\pi r} \text{ for } r > a\,. \tag{1.86}$$

This solution also holds for $r \to 0$ (see [4]).

1.6. Towards Acoustics

In the previous section, we have demonstrated the decomposition of an incompressible flow into its potential flow described by the scalar potential ϕ and its vortical flow described by the vector potential Ψ. Now, we consider conservation of mass for a compressible fluid

$$\frac{1}{\rho}\frac{D\rho}{Dt} \;=\; -\nabla\cdot\boldsymbol{v} \tag{1.87}$$

and again applying a Helmholtz decomposition according to

$$\boldsymbol{v} = \nabla\tilde{\phi} + \nabla\times\tilde{\boldsymbol{\Psi}}\,, \tag{1.88}$$

Thereby, we obtain

$$\begin{aligned} \frac{1}{\rho}\frac{D\rho}{Dt} &= -\nabla\cdot\nabla\tilde{\phi} - \underbrace{\nabla\cdot\nabla\times\tilde{\boldsymbol{\Psi}}}_{=0} \\ &= -\nabla\cdot\nabla\tilde{\phi}\,. \end{aligned} \tag{1.89}$$

In this case, the scalar potential $\tilde{\phi}$ also includes compressible effects, which may include wave propagation, since this is just possible in a compressible fluid. Indeed, as already described in [5], the overall compressible flow may be decomposed into three parts:

- Irrotational deformation without volume change (see Fig. 1.5a):
  The classical theory of potential flow equations describes this velocity field and is well known in fluid dynamics. The resulting flow field is both, divergence-free and curl-free.
- A rigid-body rotation at an angular velocity (see Fig. 1.5b):
  Typical vortical flow structures can be described by the vorticity $\boldsymbol{\omega}$ and its dynamics.
- Isotropic expansion (see Fig. 1.5c):
  This part is proportional to the volumetric rate of expansion $\nabla\cdot\boldsymbol{v}$. The field component can be described by a scalar potential associated with the compressibility of the fluid.

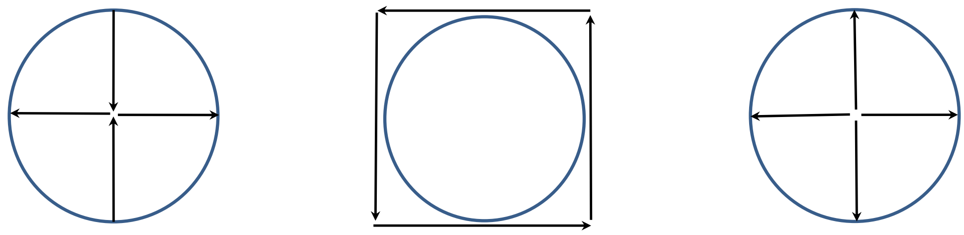

(a) Irrotational deformation without volume change.

(b) A rigid-body rotation.

(c) Isotropic expansion.

Figure 1.5.: General decomposition of a flow field.

The extension of the classical Helmholtz decomposition is the *Helmholtz-Hodge decomposition*, which also considers the topology of a domain, and in special considers the decomposition on a bounded domain Ω_r (bounded by $\Gamma(\Omega_\mathrm{r})$). According to an compressible flow, we may write

$$\boldsymbol{v} = \boldsymbol{v}_\mathrm{v} + \nabla\tilde{\phi} = \nabla\times\boldsymbol{A} + \nabla\tilde{\phi}\,. \tag{1.90}$$

Thereby, the vortical field $\boldsymbol{v}_\mathrm{v}$ has zero divergence and has to be parallel to the boundary $\Gamma(\Omega_\mathrm{r})$. These two properties are necessary to obtain the uniqueness and orthogonallity between the two vector fields. The orthogonallity requires

$$\int\limits_{\Omega_\mathrm{r}} \nabla\tilde{\phi}\cdot\boldsymbol{v}_\mathrm{v}\;\mathrm{d}\boldsymbol{x} = 0\,. \tag{1.91}$$

By applying the Gauss theorem, we obtain

$$\int\limits_{\Omega_\mathrm{r}} \left(\nabla(\tilde{\phi}\boldsymbol{v}_\mathrm{v}) - \tilde{\phi}\nabla\cdot\boldsymbol{v}_\mathrm{v}\right)\;\mathrm{d}\boldsymbol{x} - \oint\limits_{\Gamma} \tilde{\phi}\,\boldsymbol{v}_\mathrm{v}\cdot\boldsymbol{n}\;\mathrm{d}s = 0\,. \tag{1.92}$$

Therefore, the orthogonality condition (1.91) holds, if

$$\nabla\cdot\boldsymbol{v}_\mathrm{v} = 0\,;\quad \boldsymbol{v}_\mathrm{v}\cdot\boldsymbol{n} = 0\,. \tag{1.93}$$

This implies that the normal component of $\boldsymbol{v}$ on Γ comes entirely from the potential field. Hence, the following PDEs for the potentials have to be fulfilled

$$\nabla\times\nabla\times\boldsymbol{A} \;=\; \boldsymbol{\omega}\ \text{ in } \Omega_\mathrm{r}\,;\quad \boldsymbol{n}\times\boldsymbol{A} = 0\ \text{ on } \Gamma \tag{1.94}$$

$$\nabla\cdot\nabla\tilde{\phi} \;=\; \nabla\cdot\boldsymbol{v}\ \text{ in } \Omega_\mathrm{r}\,;\quad \frac{\partial\tilde{\phi}}{\partial\boldsymbol{n}} = \boldsymbol{n}\cdot\boldsymbol{v}\ \text{ on } \Gamma\,. \tag{1.95}$$

Note that from the scalar potential $\tilde{\phi}$ one can further separate a harmonic function ϕ, which fulfills

$$\nabla \cdot \nabla \phi = 0\,, \tag{1.96}$$

such that $\nabla \phi$ is orthogonal to both $\nabla(\tilde{\phi} - \phi)$ and $\boldsymbol{v}_\mathrm{v}$. So, we end up in a triple orthogonal decomposition

$$\boldsymbol{v} = \boldsymbol{v}_\mathrm{v} + \boldsymbol{v}_\mathrm{c} + \boldsymbol{v}_\mathrm{h} = \nabla \times \boldsymbol{A} + \nabla \phi_\mathrm{c} + \nabla \phi\,. \tag{1.97}$$

Thereby, the following physical interpretation can be drawn:

- vortical field, described by $\boldsymbol{v}_\mathrm{v} = \nabla \times \boldsymbol{A}$, which has to solve

$$\nabla \times \nabla \times \boldsymbol{A} = \boldsymbol{\omega} \;\text{ in } \Omega_\mathrm{r}\,; \quad \boldsymbol{n} \times \boldsymbol{A} = 0 \;\text{ on } \Gamma \tag{1.98}$$

- compressible, radiating (acoustic field) field, described by $\boldsymbol{v}_\mathrm{c} = \nabla \phi_\mathrm{c}$

$$\nabla \cdot \nabla \phi_\mathrm{c} = \nabla \cdot \boldsymbol{v} \;\text{ in } \Omega_\mathrm{r}\,; \quad \frac{\partial \phi_\mathrm{c}}{\partial \boldsymbol{n}} = 0 \;\text{ on } \Gamma\,. \tag{1.99}$$

- potential flow field, described by $\boldsymbol{v}_\mathrm{h} = \nabla \phi$.

$$\nabla \cdot \nabla \phi = 0 \;\text{ in } \Omega_\mathrm{r}\,; \quad \frac{\partial \phi}{\partial \boldsymbol{n}} = \boldsymbol{n} \cdot \boldsymbol{v} \;\text{ on } \Gamma\,. \tag{1.100}$$

2. Acoustics

2.1. Wave equation

We assume an isentropic case, where the total variation of the entropy is zero and the pressure is only a function of the density. For linear acoustics, this results in the well known relation between the acoustic pressure p_a and density ρ_a

$$p_\mathrm{a} = c_0^2 \rho_\mathrm{a} \tag{2.1}$$

with a constant speed of sound c_0. Furthermore, the acoustic field can be seen as a perturbation of the mean flow field

$$p = p_0 + p_\mathrm{a}\,; \quad \rho = \rho_0 + \rho_\mathrm{a}\,; \quad \boldsymbol{v} = \boldsymbol{v}_0 + \boldsymbol{v}_\mathrm{a} \tag{2.2}$$

with the following relations

$$p_\mathrm{a} \ll p_0\,; \quad \rho_\mathrm{a} \ll \rho_0\,. \tag{2.3}$$

In addition, we assume the viscosity to be zero, so that the viscous stress tensor $[\boldsymbol{\tau}]$ can be neglected, and the force density $\boldsymbol{f}$ is zero. We call ρ_a the acoustic density and $\boldsymbol{v}_\mathrm{a}$ the acoustic particle velocity.

For a quiescent fluid, the mean velocity $\boldsymbol{v}_0$ is zero, and furthermore we assume a spatial and temporal constant mean density ρ_0 and pressure p_0. Using the perturbation ansatz (2.2) and substituting it into (1.10) and (1.24), results in

$$\frac{\partial(\rho_0 + \rho_\mathrm{a})}{\partial t} + \nabla \cdot \Big((\rho_0 + \rho_a)\boldsymbol{v}_\mathrm{a} \Big) = 0 \tag{2.4}$$

$$(\rho_0 + \rho_\mathrm{a})\frac{\partial \boldsymbol{v}_\mathrm{a}}{\partial t} + \Big((\rho_0 + \rho_\mathrm{a})\boldsymbol{v}_\mathrm{a} \Big) \cdot \nabla \boldsymbol{v}_\mathrm{a} = -\nabla \big(p_0 + p_\mathrm{a} \big)\,. \tag{2.5}$$

In a next step, since we derive linear acoustic conservation equations, we are allowed to cancel second order terms (e.g., such as $\rho_\mathrm{a}\boldsymbol{v}_\mathrm{a}$), and arrive at conservation of mass and momentum

$$\frac{\partial \rho_\mathrm{a}}{\partial t} + \rho_0 \nabla \boldsymbol{v}_\mathrm{a} = 0 \tag{2.6}$$

$$\rho_0 \frac{\partial \boldsymbol{v}_\mathrm{a}}{\partial t} + \nabla p_\mathrm{a} = \boldsymbol{0}\,. \tag{2.7}$$

Applying the curl-operation to (2.7) results in

$$\nabla \times \frac{\partial \boldsymbol{v}_\mathrm{a}}{\partial t} = \boldsymbol{0}\,, \tag{2.8}$$

which allows us to introduce the scalar acoustic potential ψ_a via

$$\boldsymbol{v}_\mathrm{a} = -\nabla \psi_\mathrm{a}\,. \tag{2.9}$$

Substituting (2.9) into (2.7) results in the well known relation between acoustic pressure and scalar potential

$$p_{\mathrm{a}} = \rho_0 \frac{\partial \psi_{\mathrm{a}}}{\partial t} \,. \tag{2.10}$$

Now, we substitute this relation into (2.6), use (2.1) and arrive at the well known acoustic wave equation

$$\frac{1}{c_0^2} \frac{\partial^2 \psi_{\mathrm{a}}}{\partial t^2} - \Delta \psi_{\mathrm{a}} = 0 \,. \tag{2.11}$$

On the other hand, we also obtain the wave equation for the acoustic pressure p_{a} exploring (2.6), (2.7) and (2.1)

$$\frac{1}{c_0^2} \frac{\partial^2 p_{\mathrm{a}}}{\partial t^2} - \Delta p_{\mathrm{a}} = 0 \,. \tag{2.12}$$

2.2. Simple solutions

In order to get some physical insight in the propagation of acoustic sound, we will consider two special cases: plane and spherical waves. Let's start with the simpler case, the propagation of a plane wave as displayed in Fig. 2.1. Thus, we can express the acoustic pressure by

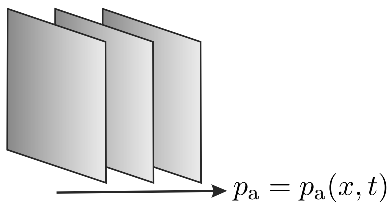

Figure 2.1.: Propagation of a plane wave.

$p_{\mathrm{a}} = p_{\mathrm{a}}(x,t)$ and the particle velocity by $\boldsymbol{v}_{\mathrm{a}} = v_{\mathrm{a}}(x,t)\boldsymbol{e}_x$. Using these relations together with the linear pressure-density law (assuming constant mean density, see (2.1)), we arrive at the following 1D linear wave equation

$$\frac{\partial^2 p_{\mathrm{a}}}{\partial x^2} - \frac{1}{c_0^2} \frac{\partial^2 p_{\mathrm{a}}}{\partial t^2} = 0 \,, \tag{2.13}$$

which can be rewritten in factorized version as

$$\left(\frac{\partial}{\partial x} - \frac{1}{c_0} \frac{\partial}{\partial t} \right) \left(\frac{\partial}{\partial x} + \frac{1}{c_0} \frac{\partial}{\partial t} \right) p_{\mathrm{a}} = 0 \,. \tag{2.14}$$

This version of the linearized, 1D wave equation motivates us to introduce the following two functions (solution according to d'Alembert)

$$\xi \;=\; t - x/c_0 \,; \quad \eta = t + x/c_0$$

with properties

$$\begin{aligned} \frac{\partial}{\partial t} &= \frac{\partial}{\partial \xi} \frac{\partial \xi}{\partial t} + \frac{\partial}{\partial \eta} \frac{\partial \eta}{\partial t} = \frac{\partial}{\partial \xi} + \frac{\partial}{\partial \eta} \\ \frac{\partial}{\partial x} &= \frac{\partial}{\partial \xi} \frac{\partial \xi}{\partial x} + \frac{\partial}{\partial \eta} \frac{\partial \eta}{\partial x} = \frac{1}{c_0} \left(\frac{\partial}{\partial \eta} - \frac{\partial}{\partial \xi} \right) \,. \end{aligned}$$

Therewith, we obtain for the factorized operator

$$\frac{\partial}{\partial x} - \frac{1}{c_0}\frac{\partial}{\partial t} \quad = \quad -\frac{2}{c_0}\frac{\partial}{\partial \xi}\,; \qquad \frac{\partial}{\partial x} + \frac{1}{c_0}\frac{\partial}{\partial t} = \frac{2}{c_0}\frac{\partial}{\partial \eta}$$

and the linear, 1D wave equation transfers to

$$-\frac{4}{c_0^2}\frac{\partial}{\partial \xi}\frac{\partial}{\partial \eta}p_\mathrm{a} = 0\,.$$

The general solution computes as a superposition of arbitrary functions of ξ and η

$$p_\mathrm{a} = f(\xi) + f(\eta) = f(t - x/c_0) + g(t + x/c_0)\,. \tag{2.15}$$

This solution describes waves moving with the speed of sound c_0 in $+x$ and $-x$ direction, respectively. In a next step, we use the linearized conservation of momentum according to (2.5), and rewrite it for the 1D case (assuming zero source term)

$$\rho_0 \frac{\partial v_\mathrm{a}}{\partial t} + \frac{\partial p_\mathrm{a}}{\partial x} = 0\,. \tag{2.16}$$

Now, we use just consider a forward propagating wave, i.e. $g(t) = 0$, substitute (2.15) into (2.16) and obtain

$$\begin{aligned} v_\mathrm{a} &= -\frac{1}{\rho_0}\int \frac{\partial p_\mathrm{a}}{\partial x}\,\mathrm{d}t = -\frac{1}{\rho_0}\int \frac{\partial f(t-x/c_0)}{\partial x}\,\mathrm{d}t = -\frac{1}{\rho_0}\int \frac{\partial f(t-x/c_0)}{\partial t}\,\frac{\partial (t-x/c_0)}{\partial x}\,\mathrm{d}t \\ &= \frac{1}{\rho_0 c_0}\int \frac{\partial f(t-x/c_0)}{\partial t}\,\mathrm{d}t \frac{1}{\rho_0 c_0}\,f(t-x/c_0) = \frac{p_\mathrm{a}}{\rho_0 c_0}\,. \end{aligned} \tag{2.17}$$

Therewith, the value of the acoustic pressure over acoustic particle velocity for a plane wave is constant. To allow for a general orientation of the coordinate system, a free field plane wave may be expressed by

$$p_\mathrm{a} = f(\boldsymbol{n}\cdot\boldsymbol{x} - c_0 t)\,; \quad \boldsymbol{v}_\mathrm{a} = \frac{\boldsymbol{n}}{\rho_0 c_0}\,f(\boldsymbol{n}\cdot\boldsymbol{x} - c_0 t)\,, \tag{2.18}$$

where the direction of propagation is given by the unit vector $\boldsymbol{n}$. A time harmonic plane wave of angular frequency $\omega = 2\pi f$ is usually written as

$$p_\mathrm{a}\,,\ \boldsymbol{v}_\mathrm{a} \sim e^{j(\omega t - \boldsymbol{k}\cdot\boldsymbol{x})} \tag{2.19}$$

with the wave number (also called wave vector) $\boldsymbol{k}$, which computes by

$$\boldsymbol{k} = k\boldsymbol{n} = \frac{\omega}{c_0}\,\boldsymbol{n}\,. \tag{2.20}$$

The second case of investigation will be a spherical wave, where we assume a point source located at the origin. In the first step, we rewrite the linearized wave equation in spherical coordinates and consider that the pressure p_a will just depend on the radius r. Therewith, the Laplace-operator reads as

$$\nabla\cdot\nabla p_\mathrm{a}(r,t) = \frac{\partial^2 p_\mathrm{a}}{\partial r^2} + \frac{2}{r}\frac{\partial p_\mathrm{a}}{\partial r} = \frac{1}{r}\frac{\partial^2 r p_\mathrm{a}}{\partial r^2}$$

and we obtain

$$\frac{1}{r}\frac{\partial^2 r p_\mathrm{a}}{\partial r^2} - \frac{1}{c_0^2}\underbrace{\frac{\partial^2 p_\mathrm{a}}{\partial t^2}}_{\frac{1}{r}\frac{\partial^2 r p_\mathrm{a}}{\partial t^2}} = 0\,. \tag{2.21}$$

A multiplication of (2.21) with r results in the same wave equation as obtained for the plane case (see (2.13)), just instead of p_a we have rp_a. Therefore, the solution of (2.21) reads as

$$p_\mathrm{a}(r,t) = \frac{1}{r}\,\left(f(t - r/c_0) + g(t + r/c_0)\right)\,, \tag{2.22}$$

which means that the pressure amplitude will decrease according to the distance r from the source. The acoustic intensity is defined by the product of the two primary acoustic quantities

$$\boldsymbol{I}_\mathrm{a} = p_\mathrm{a}\,\boldsymbol{v}_\mathrm{a}\,. \tag{2.23}$$

The assumed symmetry requires that all quantities will just exhibit a radial component. Therewith, we can express the time averaged acoustic intensity $\boldsymbol{I}_\mathrm{a}^\mathrm{av}$ in normal direction $\boldsymbol{n}$ by a scalar value just depending on r

$$\boldsymbol{I}_\mathrm{a}^\mathrm{av}\cdot\boldsymbol{n} = I_r^\mathrm{av}$$

and as a function of the time averaged acoustic power P_a^av of our source

$$I_r^\mathrm{av} = \frac{P_\mathrm{a}^\mathrm{av}}{4\pi r^2}\,. \tag{2.24}$$

According to (2.24), the acoustic intensity decreases with the squared distance from the source. This relation is known as the *spherical spreading law.*

In order to obtain the acoustic velocity $\boldsymbol{v}_\mathrm{a} = v_\mathrm{a}(r,t)\boldsymbol{e}_r$ as a function of the acoustic pressure p_a, we substitute the general solution for p_a (see (2.22), in which we set without loss of generality $g = 0$) into the linear momentum equation (see (2.7))

$$\begin{aligned}\frac{\partial v_\mathrm{a}}{\partial t} &= -\frac{1}{\rho_0}\frac{\partial p_\mathrm{a}}{\partial r} = -\frac{1}{\rho_0}\frac{\partial}{\partial r}\left(\frac{f(t-r/c_0)}{r}\right)\\ v_\mathrm{a} &= -\frac{1}{\rho_0}\frac{\partial}{\partial r}\left(\frac{F(t-r/c_0)}{r}\right)\end{aligned} \tag{2.25}$$

with $f(t) = \partial F(t)/\partial t$. Using the relation

$$\frac{\partial F(t-r/c_0)}{\partial r} = -\frac{1}{c_0}\frac{\partial F(t-r/c_0)}{\partial t}$$

and performing the differentiation with respect to r results in

$$v_\mathrm{a}(r,t) = -\frac{1}{\rho_0}\frac{1}{r}\frac{\partial F(t-r/c_0)}{\partial r} + \frac{F(t-r/c_0)}{\rho_0 r^2} \tag{2.26}$$

$$= \frac{1}{\rho_0 c_0}\underbrace{\frac{1}{r}\frac{\partial F(t-r/c_0)}{\partial t}}_{f/r = p_\mathrm{a}} + \frac{F(t-r/c_0)}{\rho_0 r^2} \tag{2.27}$$

$$= \frac{p_\mathrm{a}}{\rho_0 c_0} + \frac{F(t-r/c_0)}{\rho_0 r^2}\,. \tag{2.28}$$

Therewith, spherical waves show in the limit $r \to \infty$ the same acoustic behaviour as plane waves.

Now with this acoustic velocity-pressure relation, we may rewrite the acoustic intensity for spherical waves as

$$I_r = \frac{{p_\mathrm{a}}^2}{\rho_0 c_0} + \frac{p_\mathrm{a}}{\rho_0 r^2} F(t - r/c_0)$$

With the relation (just outgoing waves)

$$p_\mathrm{a} = \frac{f}{r} = \frac{1}{r}\frac{\partial F}{\partial t}$$

we obtain

$$I_r = \frac{{p_\mathrm{a}}^2}{\rho_0 c_0} + \frac{1}{2\rho_0 r^3}\frac{\partial F^2(t - r/c_0)}{\partial t},$$

which results for the time averaged quantity (assuming $F(t - r/c)$ is a periodic function) in the same expression as for the plane wave

$$I_r^\mathrm{av} = \frac{({p_\mathrm{a}}^2)_\mathrm{av}}{\rho_0 c_0}.$$

2.3. Acoustic quantities and order of magnitudes

Let us consider a loudspeaker generating sound at a fixed frequency f and a number of microphones recording the sound as displayed in Fig. 2.2. In a first step, we measure the sound with one microphone fixed at $\boldsymbol{x}_0$, and we will obtain a periodic signal in time with the same frequency f and period time $T = 1/f$. In a second step, we use all microphones

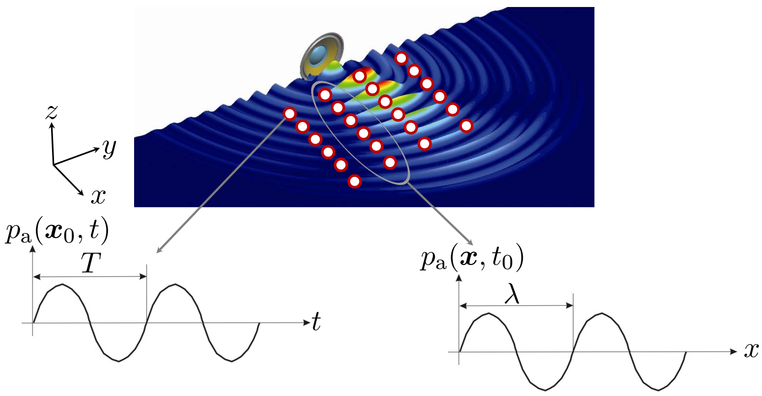

Figure 2.2.: Sound generated by a loudspeaker and measured by microphones.

and record the pressure at a fixed time t_0. Drawing the obtained values along the individual positions of the microphone, e.g. along the coordinate x, we again obtain a periodic signal, which is now periodic in space. This periodicity is characterized by the wavelength λ and is uniquely defined by the frequency f and the speed of sound c_0 via the relation

$$\lambda = \frac{c_0}{f}. \tag{2.29}$$

Assuming a frequency of 1 kHz, the wavelength in air takes on the value of 0.343 m ($c_0 = 343$ m/s).

Strictly speaking, each acoustic wave has to be considered as transient, having a beginning and an end. However, for some long duration sound, we speak of continuous wave (cw) propagation and we define for the acoustic pressure p_a a mean square pressure $(p_\mathrm{a})^2_\mathrm{av}$ as well as a root mean squared (rms) pressure $p_\mathrm{a,rms}$

$$p_\mathrm{a,rms} = \sqrt{\frac{1}{T}\int\limits_{t_0}^{t_0+T} (p-p_0)^2 \,\mathrm{d}t} = \sqrt{\frac{1}{T}\int\limits_{t_0}^{t_0+T} p_\mathrm{a}^2 \,\mathrm{d}t}\,. \tag{2.30}$$

In (2.30) T denotes the period time of the signal or if we cannot strictly speak of a periodic signal, an interminable long time interval. Now, it has to be mentioned that the threshold of hearing of an average human is at about 20 μPa and the threshold of pain at about 20 Pa, which differs 10^6 orders of magnitude. Thus, logarithmic scales are mainly used for acoustic quantities. The most common one is the *decibel* (dB), which expresses the quantity as a ratio relative to a reference value. Thereby, the sound pressure level $L_{\mathrm{p_a}}$ (SPL) is defined by

$$L_{\mathrm{p_a}} = 20\,\log_{10}\frac{p_\mathrm{a,rms}}{p_\mathrm{a,ref}} \qquad p_\mathrm{a,ref} = 20\,\mu\mathrm{P}a\,. \tag{2.31}$$

The reference pressure $p_\mathrm{a,ref}$ corresponds to the sound at 1 kHz that an average person can just hear.

In addition, the acoustic intensity $\boldsymbol{I}_\mathrm{a}$ is defined by the product of the acoustic pressure and particle velocity

$$\boldsymbol{I}_\mathrm{a} = p_\mathrm{a}\boldsymbol{v}_\mathrm{a}\,. \tag{2.32}$$

The intensity level $L_{\mathrm{I_a}}$ is then defined by

$$L_{\mathrm{I_a}} = 10\,\log_{10}\frac{I_\mathrm{a}^\mathrm{av}}{I_\mathrm{a,ref}} \qquad I_\mathrm{a,ref} = 10^{-12}\,\mathrm{W/m^2}\,, \tag{2.33}$$

with $I_\mathrm{a,ref}$ the reference sound intensity corresponding to $p_\mathrm{a,ref}$. Again, we use an averaged value for defining the intensity level, which computes by

$$I_\mathrm{a}^\mathrm{av} = |\boldsymbol{I}_\mathrm{a}^\mathrm{av}| = \left|\frac{1}{T}\int\limits_{t_0}^{t_0+T} \boldsymbol{v}_\mathrm{a}p_\mathrm{a}\,\mathrm{d}t\,.\right| \tag{2.34}$$

Finally, we compute the acoustic power by integrating the acoustic intensity (unit W/m^2) over a closed surface

$$P_\mathrm{a} = \oint\limits_\Gamma \boldsymbol{I}_\mathrm{a}\cdot \mathrm{d}\boldsymbol{s} = \oint\limits_\Gamma \boldsymbol{I}_\mathrm{a}\cdot\boldsymbol{n}\,\mathrm{d}s\,. \tag{2.35}$$

Then, the sound-power level $L_{\mathrm{P_a}}$ computes as

$$L_{\mathrm{P_a}} = 10\,\log_{10}\frac{P_\mathrm{a}^\mathrm{av}}{P_\mathrm{a,ref}} \qquad P_\mathrm{a,ref} = 10^{-12}\,\mathrm{W}\,, \tag{2.36}$$

with $P_\mathrm{a,ref}$ the reference sound power corresponding to $p_\mathrm{a,ref}$. In Tables 2.1 and 2.2 some typical sound pressure and sound power levels are listed.

Table 2.1.: Typical sound pressure levels SPL.

Threshold of hearing	Voice at 5 m	Car at 20 m	Pneumatic hammer at 2 m	Jet at 3 m
0 dB	60 dB	80 dB	100 dB	140 dB

Table 2.2.: Typical sound power levels and in parentheses the absolute acoustic power P_a.

Voice	Fan	Loudspeaker	Jet airliner
30 dB (25 μW)	110 dB (0.05 W)	128 dB (60 W)	170 dB (50 kW)

A useful quantity in the acoustics is impedance, which is a measure of the amount by which the motion induced by a pressure applied to a surface is impeded. However, a quantity that varies with time and depends on initial values is not of interest. Thus the specific acoustic impedance is defined via the Fourier transform by

$$\hat{Z}_\mathrm{a}(\boldsymbol{x},\omega) = \frac{\hat{p}_\mathrm{a}(\boldsymbol{x},\omega)}{\hat{\boldsymbol{v}}_\mathrm{a}(\boldsymbol{x},\omega)\cdot\boldsymbol{n}(\boldsymbol{x})} \tag{2.37}$$

at a point $\boldsymbol{x}$ on the surface Γ with unit normal vector $\boldsymbol{n}$. It is in general a complex number and its real part is called *resistance*, its imaginary part *reactance* and its inverse the *specific acoustic admittance* denoted by $\hat{Y}_\mathrm{a}(\boldsymbol{x},\omega)$. For a plane wave (see Sec. 2.2) the acoustic impedance $\hat{Z}_\mathrm{a}$ is constant

$$\hat{Z}_\mathrm{a}(\boldsymbol{x},\omega) = \rho_0 c_0\,. \tag{2.38}$$

For a quiescent fluid the acoustic power across a surface Γ computes for time harmonic fields by

$$\begin{aligned} P_\mathrm{a}^\mathrm{av} &= \int_\Gamma \left(\frac{1}{T}\int_0^T \mathrm{Re}\left(\hat{p}_\mathrm{a}e^{j\omega t}\right)\,\mathrm{Re}\left(\hat{\boldsymbol{v}}_\mathrm{a}\cdot\boldsymbol{n}e^{j\omega t}\right)\,\mathrm{d}t\right)\mathrm{d}s \\ &= \frac{1}{4}\int_\Gamma \left(\hat{p}_\mathrm{a}\hat{\boldsymbol{v}}_\mathrm{a}^* + \hat{p}_\mathrm{a}^*\hat{\boldsymbol{v}}_\mathrm{a}\right)\cdot\boldsymbol{n}\,\mathrm{d}s \\ &= \frac{1}{2}\int_\Gamma \mathrm{Re}\left(\hat{p}_\mathrm{a}^*\hat{\boldsymbol{v}}_\mathrm{a}\right)\cdot\boldsymbol{n}\,\mathrm{d}s \end{aligned} \tag{2.39}$$

with * denoting the conjugate complex. Now, we use the impedance $\hat{Z}_\mathrm{a}$ of the surface and arrive at

$$P_\mathrm{a}^\mathrm{av} = \frac{1}{2}\int_\Gamma \mathrm{Re}\left(\hat{Z}_\mathrm{a}\right)\,|\hat{\boldsymbol{v}}_\mathrm{a}\cdot\boldsymbol{n}|^2\,\mathrm{d}s\,. \tag{2.40}$$

Hence, the real part of the impedance (equal to the resistance) is related to the energy flow. If $\mathrm{Re}\left(\hat{Z}_\mathrm{a}\right) > 0$ the surface is *passive* and absorbs energy, and if $\mathrm{Re}\left(\hat{Z}_\mathrm{a}\right) < 0$ the surface is *active* and produces energy.

In a next step, we analyze what happens, when an acoustic wave propagates from one fluid medium to another one. For simplicity, we restrict to a plane wave, which is described by (see (2.15))

$$p_\mathrm{a}(t) = f(t - x/c_0) + g(t + x/c_0) \tag{2.41}$$

In the frequency domain, we may write

$$\hat{p}_\mathrm{a} = \hat{f}e^{-j\omega x/c_0} + \hat{g}e^{j\omega x/c_0} = p^+ e^{j\omega t - jkx} + p^- e^{j\omega t + jkx}\,. \tag{2.42}$$

Thereby, p^+ is the amplitude of the wave incident at $x = 0$ from $x < 0$ and p^- the amplitude of the reflected wave at $x = 0$ by an impedance $\hat{Z}_\mathrm{a}$. Using the linear conservation of momentum, we obtain the particle velocity

$$\hat{v}_\mathrm{a}(x) = \frac{1}{\rho_0 c_0}\left(p^+ e^{-jkx} - p^- e^{jkx}\right)\,. \tag{2.43}$$

Defining the reflection coefficient R by

$$R = \frac{p^-}{p^+}\,, \tag{2.44}$$

we arrive with $\hat{Z}_\mathrm{a} = \hat{p}(0)/\hat{v}(0)$ at

$$R = \frac{\hat{Z}_\mathrm{a} - \rho_0 c_0}{\hat{Z}_\mathrm{a} + \rho_0 c_0}\,. \tag{2.45}$$

In two dimensions, we consider a plane wave with direction $(\cos\theta, \sin\theta)$, where θ is the angle with the y-axis and the wave approaches from $y < 0$ and hits an impedance $\hat{Z}$ at $y = 0$. The overall pressure may be expressed by

$$\hat{p}_\mathrm{a}(x,y) = e^{-jkx\sin\theta}\left(p^+ e^{-ky\cos\theta} + p^- e^{jky\cos\theta}\right)\,. \tag{2.46}$$

Furthermore, the y-component of the particle velocity computes to

$$\hat{v}_\mathrm{a}(x,y) = \frac{\cos\theta}{\rho_0 c_0} e^{-jkx\sin\theta}\left(p^+ e^{-ky\cos\theta} - p^- e^{jky\cos\theta}\right)\,. \tag{2.47}$$

Thereby, the impedance is

$$\hat{Z}_\mathrm{a} = \frac{\hat{p}(x,0)}{\hat{v}(x,0)} = \frac{\rho_0 c_0}{\cos\theta}\frac{p^+ + p^-}{p^+ - p^-} = \frac{\rho_0 c_0}{\cos\theta}\frac{1+R}{1-R} \tag{2.48}$$

so that the reflection coefficient computes as

$$R = \frac{\hat{Z}_\mathrm{a}\cos\theta - \rho_0 c_0}{\hat{Z}_\mathrm{a}\cos\theta + \rho_0 c_0}\,. \tag{2.49}$$

2.4. Impulsive sound sources

The sound being generated by a unit, impulsive point source $\delta(\boldsymbol{x})\delta(t)$ is the solution of

$$\frac{1}{c_0^2}\frac{\partial^2 \psi_{\mathrm{a}}}{\partial t^2} - \nabla\cdot\nabla\psi_{\mathrm{a}} = \delta(\boldsymbol{x})\delta(t) \tag{2.50}$$

with ψ_{a} the scalar acoustic potential. Now, since the source exists only for an infinitesimal instant of time $t = 0$, the scalar potential ψ_{a} will be zero for $t < 0$. Due to the radially symmetry, we may rewrite (2.50) in cylindrical coordinates for $r = |\boldsymbol{x}| > 0$ by

$$\frac{1}{c_0^2}\frac{\partial^2 \psi_{\mathrm{a}}}{\partial t^2} - \frac{1}{r^2}\frac{\partial}{\partial r}\left(r^2\frac{\partial}{\partial r}\right)\psi_{\mathrm{a}} = 0 \quad \text{for } r > 0\,. \tag{2.51}$$

According to Sec. 2.2 (see (2.22)) the solution is

$$\psi_{\mathrm{a}} = \frac{f(t - r/c_0)}{r} + \frac{g(t + r/c_0)}{r}\,. \tag{2.52}$$

The first term represents a spherically symmetric wave propagating in the direction of increasing values of r (outgoing wave) and the second term describes an incoming wave. Physically, we have to set g to zero, since according to *causality* (also known as the radiation condition) sound produced by a source must radiate away from this source.

To complete the solution, we have to determine the function f, which results in (see [4])

$$f(t - r/c_0) = \frac{1}{4\pi}\,\delta(t - r/c_0) \tag{2.53}$$

and the solution becomes

$$\psi_{\mathrm{a}}(\boldsymbol{x},t) = \frac{1}{4\pi r}\,\delta(t - r/c_0) = \frac{1}{4\pi|\boldsymbol{x}|}\,\delta(t - |\boldsymbol{x}|/c_0)\,. \tag{2.54}$$

This represents a spherical pulse that is nonzero only on the surface of the sphere with $r = c_0 t > 0$, whose radius increases with the speed of sound c_0. It clearly vanishes everywhere for $t < 0$. Compared to the solution of a potential flow generated by a pulsating sphere (see Sec. 1.6) we have as an argument the retarded time.

2.5. Free space Green's functions

The *free-space Green's function* $G(\boldsymbol{x},\boldsymbol{y},t-\tau)$ is the *causal* solution of the wave equation by an impulsive point source with strength $\delta(\boldsymbol{x}-\boldsymbol{y})\delta(t-\tau)$ located at $\boldsymbol{x} = \boldsymbol{y}$ at time $t = \tau$. The expression for G is simply obtained from (2.54), when we replace the source position $\boldsymbol{x} = 0$ at time $t = 0$ by $\boldsymbol{x} - \boldsymbol{y}$ at $t - \tau$. This substitutions result in

$$\left(\frac{1}{c_0^2}\frac{\partial^2}{\partial t^2} - \nabla\cdot\nabla\right) G = \delta(\boldsymbol{x}-\boldsymbol{y})\delta(t-\tau) \quad \text{where } G = 0 \text{ for } t < \tau \tag{2.55}$$

with

$$G(\boldsymbol{x},\boldsymbol{y},t) = \frac{1}{4\pi|\boldsymbol{x}-\boldsymbol{y}|}\,\delta\left(t - \tau - \frac{|\boldsymbol{x}-\boldsymbol{y}|}{c_0}\right)\,. \tag{2.56}$$

This describes an impulsive, spherical symmetric wave expanding from the source at $\boldsymbol{y}$ (therefore $\boldsymbol{y}$ are called the source coordinates) with the speed of sound c_0. The wave amplitude decreases inversely with the distance to the observation point $\boldsymbol{x}$.

Now, Green's function is the fundamental building block for the computation of the inhomogeneous wave equation with any generalized source distribution $\mathcal{F}(\boldsymbol{x}, t)$

$$\left(\frac{1}{c_0^2} \frac{\partial^2}{\partial t^2} - \nabla \cdot \nabla \right) p_\mathrm{a} = \mathcal{F}(\boldsymbol{x}, t) \, . \tag{2.57}$$

The key idea is that the source distribution is regarded as a distribution of impulsive point sources

$$\mathcal{F}(\boldsymbol{x}, t) = \int_0^T \int_{-\infty}^{\infty} \mathcal{F}(\boldsymbol{y}, \tau) \delta(\boldsymbol{x} - \boldsymbol{y}) \delta(t - \tau) \, \mathrm{d}\boldsymbol{y} \, \mathrm{d}\tau \, .$$

Therefore, the outgoing wave solution for each constituent source strength

$$\mathcal{F}(\boldsymbol{y}, \tau) \delta(\boldsymbol{x} - \boldsymbol{y}) \delta(t - \tau)$$

is given by

$$\mathcal{F}(\boldsymbol{y}, \tau) G(\boldsymbol{x}, \boldsymbol{y}, t - \tau) \, .$$

Therefore, the overall solution is obtained by adding up all the individual contributions

$$\begin{aligned} p_\mathrm{a}(\boldsymbol{x}, t) &= \int_0^T \int_{-\infty}^{\infty} \mathcal{F}(\boldsymbol{y}, \tau) G(\boldsymbol{x}, \boldsymbol{y}, t - \tau) \, \mathrm{d}\boldsymbol{y} \, \mathrm{d}\tau \\ &= \frac{1}{4\pi} \int_0^T \int_{-\infty}^{\infty} \frac{\mathcal{F}(\boldsymbol{y}, \tau)}{|\boldsymbol{x} - \boldsymbol{y}|} \, \delta \left(t - \tau - \frac{|\boldsymbol{x} - \boldsymbol{y}|}{c_0} \right) \mathrm{d}\boldsymbol{y} \, \mathrm{d}\tau \\ &= \frac{1}{4\pi} \int_{-\infty}^{\infty} \frac{\mathcal{F}\left(\boldsymbol{y}, t - \frac{|\boldsymbol{x} - \boldsymbol{y}|}{c_0} \right)}{|\boldsymbol{x} - \boldsymbol{y}|} \, \mathrm{d}\boldsymbol{y} \, . \end{aligned} \tag{2.58}$$

This integral formula is called a **retarded** formula, since it represents the pressure at position $\boldsymbol{x}$ (observation point) and time t as a linear superposition of sources at $\boldsymbol{y}$ radiated at earlier times $t - |\boldsymbol{x} - \boldsymbol{y}|/c_0$. Thereby, the time of travel for the sound waves from the source point $\boldsymbol{y}$ to the observer point $\boldsymbol{x}$ is $|\boldsymbol{x} - \boldsymbol{y}|/c_0$.

In general, finding a (tailored) Green's function of given configuration (including, e.g., scatterer) is only marginally easier than the full solution of the inhomogeneous wave equation.Therefore, it is not possible to give a general recipe. However, it is important to note that often we can simplify a problem already by the corresponding integral formulation (as done above) using free field Green's function. Furthermore, the delta-function source may be rendered into a more easily treated from by spatial Fourier transform. Thereby, (2.56) leads to the free field Green's function in the frequency domain (setting $\tau = 0$)

$$\begin{aligned} \hat{G}(\boldsymbol{x}, \omega) &= \int_{-\infty}^{\infty} \frac{1}{4\pi |\boldsymbol{x} - \boldsymbol{y}|} \, \delta \left(t - \frac{|\boldsymbol{x} - \boldsymbol{y}|}{c_0} \right) e^{-j\omega t} \, \mathrm{d}t \\ &= \frac{e^{-jkr}}{4\pi r} \end{aligned} \tag{2.59}$$

with $r = |\boldsymbol{x} - \boldsymbol{y}|$ and $k = \omega / c_0$.

2.6. Monopoles, dipoles and quadrupoles

A volume point source $q(t)\delta(\boldsymbol{x})$ as a model of a pulsating sphere (as considered in Sec. 1.6) is called a *monopole* point source. Now, we consider a compressible fluid and the corresponding wave equation

$$\left(\frac{1}{c_0}\frac{\partial^2}{\partial t^2} - \nabla\cdot\nabla\right)\psi_{\mathrm{a}} = q(t)\delta(\boldsymbol{x})\,.$$

The solution can be simply obtained by using (2.58), replacing p^{a} by ψ_{a} and setting $\mathcal{F}(\boldsymbol{y},\tau) = q(\tau)\delta(\boldsymbol{y})$

$$\psi_{\mathrm{a}}(\boldsymbol{x},t) = \frac{q(t-|\boldsymbol{x}|/c_0)}{4\pi|\boldsymbol{x}|} = \frac{q(t-r/c_0)}{4\pi r}\,. \tag{2.60}$$

This differs from the solution obtained within an incompressible fluid (see (1.86)) by the dependence on the retarded time $t - r/c_0$. Any change at the source is now communicated to a fluid element at distance r after an appropriate estimated delay r/c_0 required for sound to travel outward from the source.

In a next step, we will investigate in a *point dipole*. Then, a source on the right hand side of the wave equation (2.57) of the following type

$$\mathcal{F}(\boldsymbol{x},t) = \nabla\cdot(\boldsymbol{f}(t)\delta(\boldsymbol{x})) = \frac{\partial}{\partial x_j}\left(f_j(t)\delta(\boldsymbol{x})\right) \tag{2.61}$$

is called a *point dipole* located at the origin. The sound generated by such a source computes according to (2.58)

$$p_{\mathrm{a}}(\boldsymbol{x},t) \;=\; \frac{1}{4\pi}\int\limits_{-\infty}^{\infty}\frac{\partial}{\partial y_j}\left(f_j(t-|\boldsymbol{x}-\boldsymbol{y}|/c_0)\;\delta(\boldsymbol{y})\right)\frac{\delta\left(t-\frac{|\boldsymbol{x}-\boldsymbol{y}|}{c_0}\right)}{|\boldsymbol{x}-\boldsymbol{y}|}\,\mathrm{d}\boldsymbol{y}\,. \tag{2.62}$$

In a first step, we perform an integration by parts and arrive at

$$\begin{aligned} p_{\mathrm{a}}(\boldsymbol{x},t) \;=\; & -\frac{1}{4\pi}\int\limits_{-\infty}^{\infty} f_j(t-|\boldsymbol{x}-\boldsymbol{y}|/c_0)\;\delta(\boldsymbol{y})\,\frac{\partial}{\partial y_j}\left(\frac{\delta\left(t-\frac{|\boldsymbol{x}-\boldsymbol{y}|}{c_0}\right)}{|\boldsymbol{x}-\boldsymbol{y}|}\right)\mathrm{d}\boldsymbol{y} \\ & +\frac{1}{4\pi}\int\limits_{\Gamma}\left(f_j(t-|\boldsymbol{x}-\boldsymbol{y}|/c_0)\;\delta(\boldsymbol{y})\right)\frac{\delta\left(t-\frac{|\boldsymbol{x}-\boldsymbol{y}|}{c_0}\right)}{|\boldsymbol{x}-\boldsymbol{y}|}\,\boldsymbol{n}\cdot\boldsymbol{e}_j\,\mathrm{d}s\,. \end{aligned} \tag{2.63}$$

Thereby the second integral has to be evaluated at a surface for which $y_j = \pm\infty$, so that due to the property of the delta function $\delta(\boldsymbol{y}) = 0$ at $y_j = \pm\infty$, it vanishes. Furthermore, we explore the relation

$$\frac{\partial}{\partial y_j}\left(\frac{\delta\left(t-\frac{|\boldsymbol{x}-\boldsymbol{y}|}{c_0}\right)}{|\boldsymbol{x}-\boldsymbol{y}|}\right) = -\frac{\partial}{\partial x_j}\left(\frac{\delta\left(t-\frac{|\boldsymbol{x}-\boldsymbol{y}|}{c_0}\right)}{|\boldsymbol{x}-\boldsymbol{y}|}\right)\,, \tag{2.64}$$

and arrive at

$$
\begin{aligned}
p_\mathrm{a}(\boldsymbol{x},t) &= \frac{1}{4\pi}\int\limits_{-\infty}^{\infty} f_j(t-|\boldsymbol{x}-\boldsymbol{y}|/c_0)\ \delta(\boldsymbol{y})\ \frac{\partial}{\partial x_j}\left(\frac{\delta\left(t-\frac{|\boldsymbol{x}-\boldsymbol{y}|}{c_0}\right)}{|\boldsymbol{x}-\boldsymbol{y}|}\right)\ \mathrm{d}\boldsymbol{y} \\
&= \frac{1}{4\pi}\frac{\partial}{\partial x_j}\int\limits_{-\infty}^{\infty} f_j(t-|\boldsymbol{x}-\boldsymbol{y}|/c_0)\ \delta(\boldsymbol{y})\ \frac{\delta\left(t-\frac{|\boldsymbol{x}-\boldsymbol{y}|}{c_0}\right)}{|\boldsymbol{x}-\boldsymbol{y}|}\ \mathrm{d}\boldsymbol{y}\,. \qquad (2.65)
\end{aligned}
$$

Due to the property of the delta function, we can directly obtain the solution for the acoustic pressure by

$$
p_\mathrm{a}(\boldsymbol{x},t) = \frac{\partial}{\partial x_j}\left(\frac{f_j(t-|\boldsymbol{x}|/c_0)}{4\pi|\boldsymbol{x}|}\right). \qquad (2.66)
$$

Therefore, a distributed dipole source $\mathcal{F}(\boldsymbol{x},t) = \nabla\cdot\boldsymbol{f}(\boldsymbol{x},t)$ results in the following expression for the acoustic pressure

$$
p_\mathrm{a}(\boldsymbol{x},t) = \frac{1}{4\pi}\frac{\partial}{\partial x_j}\int\limits_{-\infty}^{\infty}\frac{f_j(\boldsymbol{y},t-|\boldsymbol{x}-\boldsymbol{y}|/c_0)}{|\boldsymbol{x}-\boldsymbol{y}|}\ \mathrm{d}\boldsymbol{y}\,. \qquad (2.67)
$$

A point dipole at the origin oriented in the direction of the unit vector $\boldsymbol{n}$ is entirely equivalent to two point monopoles of equal but opposite strengths placed a short distance apart (much smaller as the wavelength). Furthermore, a combination of four monopole sources, whose net volume source strength is zero, is called a *quadrupole*. A general quadrupole is a source distribution being characterized by a second space derivative of the form

$$
\mathcal{F}(\boldsymbol{x},t) = \frac{\partial^2 L_{ij}}{\partial x_i \partial x_j}\,. \qquad (2.68)
$$

Here, L_{ij} are the components of an arbitrary tensor. In the context of aeroacoustics, $[\boldsymbol{L}]$ will denote the Lighthill tensor (see Sec. 3.1). Applying the procedure as in the case of the dipole source two times results in the corresponding acoustic pressure

$$
p_\mathrm{a}(\boldsymbol{x},t) = \frac{1}{4\pi}\frac{\partial^2}{\partial x_i \partial x_j}\int\limits_{-\infty}^{\infty}\frac{L_{ij}(\boldsymbol{y},t-|\boldsymbol{x}-\boldsymbol{y}|/c_0)}{|\boldsymbol{x}-\boldsymbol{y}|}\ \mathrm{d}\boldsymbol{y}\,. \qquad (2.69)
$$

2.7. Calculation of acoustic far field

We will now discuss useful approximations for the evaluation of

$$
p_\mathrm{a}(\boldsymbol{x},t) = \frac{1}{4\pi}\int\limits_{-\infty}^{\infty}\frac{\mathcal{F}\left(\boldsymbol{y},t-\frac{|\boldsymbol{x}-\boldsymbol{y}|}{c_0}\right)}{|\boldsymbol{x}-\boldsymbol{y}|}\ \mathrm{d}\boldsymbol{y}\,, \qquad (2.70)
$$

when computing the sound in the far field. Thereby, as mostly true for practical applications, we assume that $\mathcal{F}(\boldsymbol{x},t)$ is nonzero only in a finite source region, as displayed in Fig. 2.3. Furthermore, the source region contains the origin O of the coordinate system. In a first step,

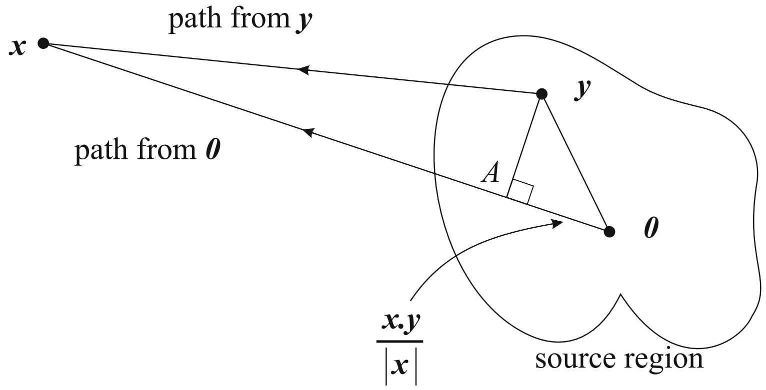

Figure 2.3.: Acoustic far field calculation.

we assume $|\boldsymbol{x}| \gg |\boldsymbol{y}|$, so that the following approximation will hold

$$\begin{aligned}
|\boldsymbol{x}-\boldsymbol{y}| &= \left(|\boldsymbol{x}|^2 - 2\boldsymbol{x}\cdot\boldsymbol{y} + |\boldsymbol{y}|^2\right)^{\frac{1}{2}} \\
&= |\boldsymbol{x}| \left(1 - \frac{2\boldsymbol{x}\cdot\boldsymbol{y}}{|\boldsymbol{x}|^2} + \frac{|\boldsymbol{y}|^2}{|\boldsymbol{x}|^2}\right)^{\frac{1}{2}} \\
&\approx |\boldsymbol{x}| \left(1 - \frac{2\boldsymbol{x}\cdot\boldsymbol{y}}{|\boldsymbol{x}|^2}\right)^{\frac{1}{2}} \\
&\approx |\boldsymbol{x}| - \frac{\boldsymbol{x}\cdot\boldsymbol{y}}{|\boldsymbol{x}|} \quad \text{for} \quad \frac{|\boldsymbol{y}|}{|\boldsymbol{x}|} \ll 1 \,. \qquad (2.71)
\end{aligned}$$

In a second step, we investigate in the term $1/|\boldsymbol{x}-\boldsymbol{y}|$ using the above result

$$\frac{1}{|\boldsymbol{x}-\boldsymbol{y}|} \approx \frac{1}{|\boldsymbol{x}| - \frac{\boldsymbol{x}\cdot\boldsymbol{y}}{|\boldsymbol{x}|}} = \frac{1}{|\boldsymbol{x}|}\left(\frac{1}{1-\frac{\boldsymbol{x}\cdot\boldsymbol{y}}{|\boldsymbol{x}|^2}}\right) \qquad (2.72)$$

Now, we develop the term in the parenthesis in a Taylor series up to first order and arrive at

$$\frac{1}{|\boldsymbol{x}-\boldsymbol{y}|} \approx \frac{1}{|\boldsymbol{x}|}\left(1 + \frac{\boldsymbol{x}\cdot\boldsymbol{y}}{|\boldsymbol{x}|^2}\right) = \frac{1}{|\boldsymbol{x}|} + \frac{\boldsymbol{x}\cdot\boldsymbol{y}}{|\boldsymbol{x}|^3} \,.$$

This approximation demonstrates that in order to obtain the far field approximation of (2.70), which solution behaves like $1/r = 1/|\boldsymbol{x}|$ as $|\boldsymbol{x}| \to \infty$, it is sufficient to replace $|\boldsymbol{x}-\boldsymbol{y}|$ in the denominator of the integrand by $|\boldsymbol{x}|$. However, in the argument of the source strength $\mathcal{F}$ it is important to retain possible phase differences between the sound waves generated by the source distribution at location $\boldsymbol{y}$. Therefore, we replace $|\boldsymbol{x}-\boldsymbol{y}|$ in the source argument by the approximation obtained in (2.71) and arrive at

$$p_{\mathrm{a}}(\boldsymbol{x},t) \approx \frac{1}{4\pi|\boldsymbol{x}|}\int\limits_{-\infty}^{\infty} \mathcal{F}\left(\boldsymbol{y}, t - \frac{|\boldsymbol{x}|}{c_0} + \frac{\boldsymbol{x}\cdot\boldsymbol{y}}{c_0|\boldsymbol{x}|}\right)\,\mathrm{d}\boldsymbol{y}\,, \quad |\boldsymbol{x}| \to \infty\,. \qquad (2.73)$$

This approximation when computing the acoustic far field is known as *Fraunhofer approximation.* The source region may extend over many characteristic wavelengths of the sound. By retaining the contribution $\boldsymbol{x} \cdot \boldsymbol{y}/(c_0|\boldsymbol{x}|)$ to the retarded time, we ensure that the interference between waves generated at different positions within the source region is correctly described by this far-field approximation. Let's consider the setup as displayed in Fig. 2.3. The acoustic travel time from a source point $\boldsymbol{y}$ to a far-field point $\boldsymbol{x}$ is equal to that from the point labelled by A to $\boldsymbol{x}$ when $\boldsymbol{x}$ goes to infinity. The travel time over the distance OA computes by

$$t_{OA} = \frac{1}{c_0} \boldsymbol{y} \cdot \boldsymbol{e}_{\boldsymbol{x}} = \frac{1}{c_0} \boldsymbol{y} \cdot \frac{\boldsymbol{x}}{|\boldsymbol{x}|} .$$

Therefore, the time obtained by $|\boldsymbol{x}|/c_0 - \boldsymbol{x} \cdot \boldsymbol{y}/(c_0|\boldsymbol{x}|)$ is the correct value of the retarded time when $\boldsymbol{x}$ goes to infinity.

Let's apply the above approximation for a dipole source distribution. In doing so, we use the far-field formula according to (2.73) to a dipole source $\mathcal{F}(\boldsymbol{x}, t) = \nabla \cdot \boldsymbol{f}(\boldsymbol{x}, t)$ and obtain

$$p_{\mathrm{a}}(\boldsymbol{x}, t) \approx \frac{1}{4\pi|\boldsymbol{x}|} \frac{\partial}{\partial x_j} \left(\int_{-\infty}^{\infty} f_j \left(\boldsymbol{y}, t - \frac{|\boldsymbol{x}|}{c_0} + \frac{\boldsymbol{x} \cdot \boldsymbol{y}}{c_0|\boldsymbol{x}|} \right) \mathrm{d}\boldsymbol{y} \right) . \tag{2.74}$$

In a next step we replace the space derivative with a time derivative, which is usually more easily estimated in practical applications. This operation is done as follows

$$\frac{\partial}{\partial x_j} f_j \left(\boldsymbol{y}, t - \frac{|\boldsymbol{x}|}{c_0} + \frac{\boldsymbol{x} \cdot \boldsymbol{y}}{c_0|\boldsymbol{x}|} \right) = \frac{\partial f_j}{\partial t} \frac{\partial}{\partial x_j} \left(t - \frac{|\boldsymbol{x}|}{c_0} + \frac{\boldsymbol{x} \cdot \boldsymbol{y}}{c_0|\boldsymbol{x}|} \right) .$$

Now, the second term evaluates as

$$\begin{aligned} \frac{\partial}{\partial x_j} \left(t - \frac{|\boldsymbol{x}|}{c_0} + \frac{\boldsymbol{x} \cdot \boldsymbol{y}}{c_0|\boldsymbol{x}|} \right) &= -\frac{1}{c_0} \frac{\partial |\boldsymbol{x}|}{\partial x_j} + \frac{1}{c_0} \frac{\partial}{\partial x_j} \left(\frac{\boldsymbol{x} \cdot \boldsymbol{y}}{|\boldsymbol{x}|} \right) \\ &= -\frac{1}{c_0} \frac{x_j}{|\boldsymbol{x}|} + \frac{1}{c_0} \frac{y_j |\boldsymbol{x}| - \boldsymbol{x} \cdot \boldsymbol{y}\, x_j |\boldsymbol{x}|^{-1}}{|\boldsymbol{x}|^2} \\ &= -\frac{1}{c_0} \frac{x_j}{|\boldsymbol{x}|} + \frac{y_j}{c_0|\boldsymbol{x}|} - \frac{\boldsymbol{x} \cdot \boldsymbol{y}\, x_j}{|\boldsymbol{x}|^3} \\ &\approx -\frac{1}{c_0} \frac{x_j}{|\boldsymbol{x}|} \quad \text{for } |\boldsymbol{y}| \ll |\boldsymbol{x}| . \end{aligned}$$

Collecting these results, we can provide the far-field approximation for a source dipole $\mathcal{F} = \nabla \cdot \boldsymbol{f}(\boldsymbol{x}, t)$ as follows (cancelling all terms which are proportional to $1/|\boldsymbol{x}|^2$ as well as $\boldsymbol{x} \cdot \boldsymbol{y}\, x_j/|\boldsymbol{x}|^4$)

$$p_{\mathrm{a}}(\boldsymbol{x}, t) \approx \frac{-x_j}{4\pi c_0 |\boldsymbol{x}|^2} \frac{\partial}{\partial t} \left(\int_{-\infty}^{\infty} f_j \left(\boldsymbol{y}, t - \frac{|\boldsymbol{x}|}{c_0} + \frac{\boldsymbol{x} \cdot \boldsymbol{y}}{c_0|\boldsymbol{x}|} \right) \mathrm{d}\boldsymbol{y} \right) \tag{2.75}$$

Please note that the term

$$\frac{x_j}{|\boldsymbol{x}|^2} = \frac{x_j}{|\boldsymbol{x}|} \frac{1}{|\boldsymbol{x}|} = \frac{x_j}{|\boldsymbol{x}|} \frac{1}{r}$$

is not changing the rate of the amplitude decay, which is still given by $1/r$. The first term $x_j/|\boldsymbol{x}|$ is the jth component of the unit vector $\boldsymbol{x}/|\boldsymbol{x}|$ and so it does just influence the directivity pattern (see Fig. 2.4 for the directivity of a dipole).

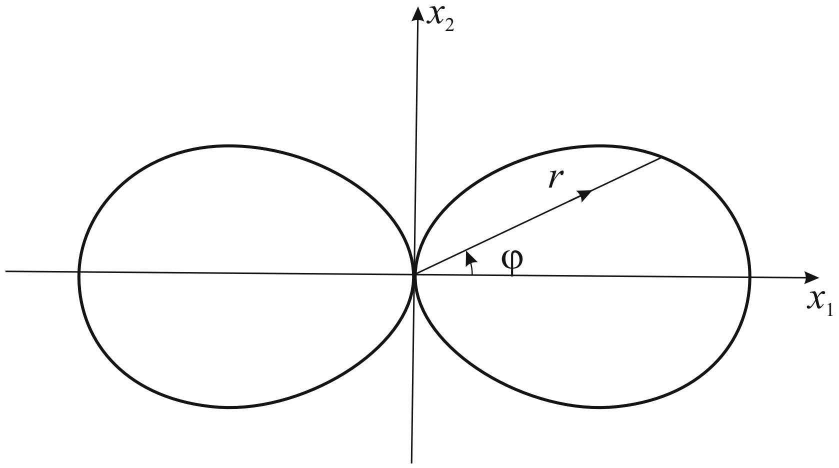

Figure 2.4.: Directivity of a dipole source. The plotted directivity is $\propto p^2$ (proportional to the intensity).

Furthermore, it is necessary to realize that the rule of interchanging a space derivative with a time derivative is given by

$$\frac{\partial}{\partial x_j} \approx -\frac{1}{c_0}\frac{x_j}{|\boldsymbol{x}|}\frac{\partial}{\partial t}\,. \tag{2.76}$$

We will now explore this relation, when deriving the far-field approximation for a quadrupole source given by

$$\mathcal{F}(\boldsymbol{x},t) = \frac{\partial^2 L_{ij}(\boldsymbol{x},t)}{\partial x_i \partial x_j}\,. \tag{2.77}$$

According to (2.76) we directly arrive at

$$p_{\mathrm{a}}(\boldsymbol{x},t) \approx \frac{x_i x_j}{4\pi c_0^2 |\boldsymbol{x}|^3}\frac{\partial^2}{\partial t^2}\left(\int\limits_{-\infty}^{\infty} L_{ij}\left(\boldsymbol{y}, t - \frac{|\boldsymbol{x}|}{c_0} + \frac{\boldsymbol{x}\cdot\boldsymbol{y}}{c_0|\boldsymbol{x}|}\right)\,\mathrm{d}\boldsymbol{y}\right) \tag{2.78}$$

Now, for a point quadrupole in the x_1-x_2 plane

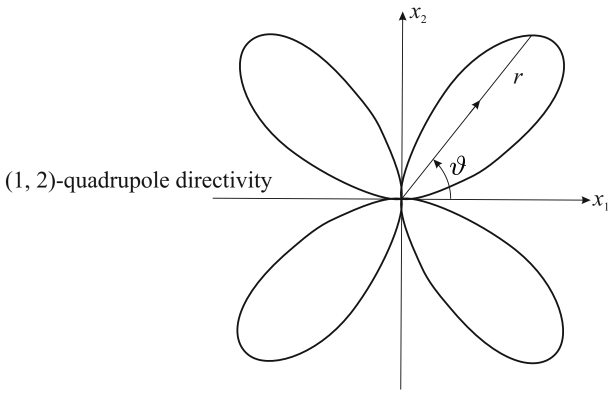

Figure 2.5.: Directivity of a quadrupole source: radiation in the x_1-x_2 plane ($\varphi = 0, \pi$).

$$\mathcal{F}(\boldsymbol{x},t) = \frac{\partial^2}{\partial x_1 \partial x_2}\,\left(L(t)\delta(\boldsymbol{x})\right)$$

we obtain by exploring (2.78) the following far-field pressure

$$p_{\rm a}(\boldsymbol{x},t) \approx \frac{x_1 x_2}{4\pi c_0^2 |\boldsymbol{x}|^3} \frac{\partial^2}{\partial t^2} L\left(t - \frac{|\boldsymbol{x}|}{c_0}\right) \qquad \boldsymbol{x} \to \infty\,. \tag{2.79}$$

If we use spherical coordinates, such that

$$x_1 = r\cos\vartheta\,;\quad x_2 = r\sin\vartheta\cos\varphi\,;\quad x_3 = r\sin\vartheta\cos\varphi$$

we may rewrite the pressure by

$$p_{\rm a}(\boldsymbol{x},t) \approx \frac{\sin 2\vartheta\,\cos\varphi}{8\pi c_0^2 |\boldsymbol{x}|} \frac{\partial^2}{\partial t^2} L\left(t - \frac{|\boldsymbol{x}|}{c_0}\right) \qquad \boldsymbol{x} \to \infty\,. \tag{2.80}$$

The directivity pattern of the sound intensity, which is given by $\propto (p^{\rm a})^2$, is therefore represented by $\sin^2 2\vartheta\,\cos^2\varphi$. Its shape is displayed in Fig. 2.5.

2.8. Compactness

We consider a rigid sphere of radius a oscillating at a small amplitude of velocity $U\boldsymbol{e}_{x_1}$, as displayed in Fig. 2.6. Assuming that a is very small, we may model the source as a point

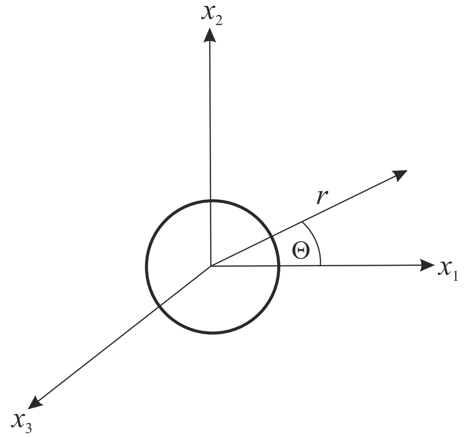

Figure 2.6.: Oscillating sphere.

dipole of amplitude $2\pi a^3 U(t)$, so that the acoustic potential $\psi_{\rm a}$ computes by solving

$$\left(\frac{1}{c_0^2}\frac{\partial^2}{\partial t^2} - \nabla\cdot\nabla\right)\psi_{\rm a} = \frac{\partial}{\partial x_1}\big(2\pi a^3 U(t)\delta(\boldsymbol{x})\big)\,. \tag{2.81}$$

According to (2.66), the solution is given by

$$\psi_{\rm a}(\boldsymbol{x},t) = \frac{\partial}{\partial x_1}\left(\frac{2\pi a^3 U(t - |\boldsymbol{x}|/c_0)}{4\pi|\boldsymbol{x}|}\right)\,. \tag{2.82}$$

With the following two relations

$$\begin{aligned} \frac{\partial}{\partial x_1}\left(\frac{1}{|\boldsymbol{x}|}\right) &= -\frac{x_1}{|\boldsymbol{x}|^3} \\ \frac{\partial}{\partial x_1}(U(t - |\boldsymbol{x}|/c_0) &= -\frac{\partial U(t)}{\partial t}\frac{1}{c_0}\frac{x_1}{|\boldsymbol{x}|} \end{aligned}$$

and $r = |\boldsymbol{x}|$, $x_1 = r\cos\Theta$, we arrive at

$$\psi_\mathrm{a}(\boldsymbol{x},t) = \underbrace{-\frac{a^3\cos\Theta}{2r^2}U(t-|\boldsymbol{x}|/c_0)}_{\text{near field}} \underbrace{-\frac{a^3\cos\Theta}{2c_0 r}\frac{\partial U(t-|\boldsymbol{x}|/c_0)}{\partial t}}_{\text{far field}} \,. \tag{2.83}$$

Thereby, we observe that the near-field term is dominant at sufficiently small distances r from the origin

$$\frac{1}{r} \gg \frac{1}{c_0}\frac{1}{U}\frac{\partial U}{\partial t} \sim \frac{f}{c_0} = \frac{1}{\lambda}\,. \tag{2.84}$$

Hence, the near-field term is dominated when

$$r \ll \lambda\,. \tag{2.85}$$

The motion becomes incompressible when $c_0 \to \infty$. In this limit, the solution reduces entirely to the near-field term, which we also call the *hydrodynamic near-field* and its amplitude decreases like $1/r^2$ as $r \to \infty$. Thereby, the retarded time can be neglected and the near-field coincide with that of the incompressible potential flow.

In regions, e.g. at boundaries, where the acoustic potential ψ_a varies significantly over a distance l, which is short compared to the wavelength λ, the acoustic field can be approximated by the incompressible potential flow. We call such a region *compact*, and a source size much smaller than λ is a *compact source*. For a precise definition, we define a typical time scale τ (or angular frequency ω) and a length scale l. Then, the dimensionless form of the wave equation reads

$$\frac{\partial^2\psi_\mathrm{a}}{\partial\tilde{x}_i^2} = \mathrm{He}^2\,\frac{\partial^2\psi_\mathrm{a}}{\partial\tilde{t}^2} \tag{2.86}$$

with $\tilde{t} = t/\tau = \omega t$ and $\tilde{x}_i = x_i/l$. In (2.86) He denotes the Helmholtz number and computes by

$$\mathrm{He} = \frac{l}{c_0\tau} = \frac{\omega l}{c_0} = \frac{2\pi l}{\lambda} \ll 1\,.$$

Note that the time derivative term in (2.86) is multiplied by the square of a Helmholtz-number. Therefore, if He is small, we may neglect this term and the wave equation reduces to

$$\nabla\cdot\nabla\psi_\mathrm{a} = 0\,. \tag{2.87}$$

Hence, we can describe the acoustic field by the incompressible potential flow, which allows us to use incompressible potential flow theory to derive the local behaves of acoustic fields in compact regions.

2.9. Solution of wave equation using Green's function

We consider a stationary medium, in which the acoustic field is computed by the linear wave equation. The domain may include surfaces generating sound and surfaces, where the sound waves are scattered, as displayed in Fig. 2.7. Our goal is to compute the acoustic pressure

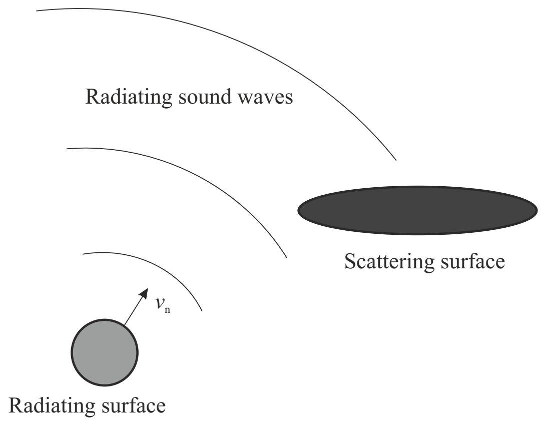

Figure 2.7.: Radiating and scattering surfaces in a sound field.

p_a at observer position $\boldsymbol{x}$ and time t due to some sources in space $\boldsymbol{y}$ and time τ. In doing so, we write the wave equation in terms of $\boldsymbol{y}$ and τ

$$\frac{1}{c_0^2}\frac{\partial^2 p_\mathrm{a}(\boldsymbol{y},\tau)}{\partial\tau^2} - \frac{\partial^2 p_\mathrm{a}(\boldsymbol{y},\tau)}{\partial y_i^2} = 0\,. \tag{2.88}$$

In a next step, we introduce the Green's function G being the solution of the inhomogeneous wave equation

$$\frac{1}{c_0^2}\frac{\partial^2 G}{\partial\tau^2} - \frac{\partial^2 G}{\partial y_i^2} = \delta(\boldsymbol{x}-\boldsymbol{y})\,\delta(t-\tau)\,. \tag{2.89}$$

Thereby, the Green's function is distributed in space as a function of $\boldsymbol{y}$ and τ, but also depends on the observer position $\boldsymbol{x}$ and time t, and so we write $G = G(\boldsymbol{x},t|\boldsymbol{y},\tau)$. Now, we multiply (2.89) by $p_\mathrm{a}(\boldsymbol{y},\tau)$, (2.88) by $G(\boldsymbol{x},t|\boldsymbol{y},\tau)$ and subtract the so obtained equations to achieve at

$$\frac{1}{c_0^2}\left(p_\mathrm{a}\frac{\partial^2 G}{\partial\tau^2} - G\frac{\partial^2 p_\mathrm{a}}{\partial\tau^2}\right) - \left(p_\mathrm{a}\frac{\partial^2 G}{\partial y_i^2} - G\frac{\partial^2 p_\mathrm{a}}{\partial y_i^2}\right) = \delta(\boldsymbol{x}-\boldsymbol{y})\,\delta(t-\tau)\,p_\mathrm{a}(\boldsymbol{y},\tau)\,. \tag{2.90}$$

Next, we integrate over τ and the volume $\Omega(\boldsymbol{y})$ and explore the property of the delta function

$$p_\mathrm{a}(\boldsymbol{x},t) = \int_\Omega\int_0^T \frac{1}{c_0^2}\left(p_\mathrm{a}\frac{\partial^2 G}{\partial\tau^2} - G\frac{\partial^2 p_\mathrm{a}}{\partial\tau^2}\right) - \left(p_\mathrm{a}\frac{\partial^2 G}{\partial y_i^2} - G\frac{\partial^2 p_\mathrm{a}}{\partial y_i^2}\right)\mathrm{d}\tau\,\mathrm{d}\boldsymbol{y}\,. \tag{2.91}$$

The first integrand in (2.91) may be rearranged as follows

$$\left(p_\mathrm{a}\frac{\partial^2 G}{\partial\tau^2} - G\frac{\partial^2 p_\mathrm{a}}{\partial\tau^2}\right) = \frac{\partial}{\partial\tau}\left(p_\mathrm{a}\frac{\partial G}{\partial\tau} - G\frac{\partial p_\mathrm{a}}{\partial\tau}\right) \tag{2.92}$$

from which follows

$$\int_\Omega\int_0^T \frac{\partial}{\partial\tau}\left(p_\mathrm{a}\frac{\partial G}{\partial\tau} - G\frac{\partial p_\mathrm{a}}{\partial\tau}\right)\mathrm{d}\tau\,\mathrm{d}\boldsymbol{y} = \int_\Omega \left(p_\mathrm{a}\frac{\partial G}{\partial\tau} - G\frac{\partial p_\mathrm{a}}{\partial\tau}\right)_{\tau=0}^{\tau=T}\mathrm{d}\boldsymbol{y}\,. \tag{2.93}$$

The integrand is zero at the lower limit $\tau = 0$, when we specify p_a and $\partial p_\mathrm{a}/\partial\tau$ to be zero at $\tau = 0$. Furthermore, we explore the *causality condition* that sound heard at time t must be generated at time $\tau < t$. This implies that the Green's function $G(\boldsymbol{x}, t|\boldsymbol{y}, \tau)$ and its time derivative $\partial G(\boldsymbol{x}, t|\boldsymbol{y}, \tau)/\partial\tau$ is zero for $\tau \geq t$, so that the integrand at the upper limit is also zero for $t < T$.

A similar expansion is done for the second term in (2.93) obtaining

$$\int\limits_\Omega \left(p_\mathrm{a} \frac{\partial^2 G}{\partial y_i^2} - G \frac{\partial^2 p_\mathrm{a}}{\partial y_i^2} \right) \mathrm{d}\boldsymbol{y} = \int\limits_\Omega \frac{\partial}{\partial y_i} \left(p_\mathrm{a} \frac{\partial G}{\partial y_i} - G \frac{\partial p_\mathrm{a}}{\partial y_i} \right) \mathrm{d}\boldsymbol{y} \,. \tag{2.94}$$

Here, we can use the divergence theorem to turn the volume integral over the enclosing surface integral with normal vector pointing into the volume

$$p_\mathrm{a}(\boldsymbol{x}, t) = \int\limits_\Gamma \int\limits_0^T \left(p_\mathrm{a}(\boldsymbol{y}, \tau) \frac{\partial G(\boldsymbol{x}, t|\boldsymbol{y}, \tau)}{\partial y_i} - G(\boldsymbol{x}, t|\boldsymbol{y}, \tau) \frac{\partial p_\mathrm{a}(\boldsymbol{y}, \tau)}{\partial y_i} \right) n_i \, \mathrm{d}s(\boldsymbol{y}) \, \mathrm{d}\tau \,. \tag{2.95}$$

In free field application, the Sommerfeld radiation condition eliminates the need to include the exterior boundary in the surface integral. The resulting integral equation (2.95) solves the linear acoustic wave equation and can be evaluated from knowledge of the pressure and the pressure gradient on surfaces that bound the region of interest as well as other surfaces, i.e scattering surfaces or sound generating surfaces. Furthermore, we need to know the Green's function, which must satisfy the inhomogeneous wave equation (2.89) and a causality condition, e.g. free field Green's function according to (2.56). Then we can use (2.95) for both sound radiation and scattering problems involving prescribed surface motion and / or surface pressure as displayed in Fig. 2.7. For radiating surfaces, the pressure gradient term can be obtained by the acoustic momentum equation (2.7) as

$$\frac{\partial p_\mathrm{a}}{\partial y_i} n_i = -\rho_0 \frac{\partial \boldsymbol{v}_{\mathrm{a},i}}{\partial \tau} n_i = -\rho_0 \frac{\partial v_\mathrm{n}}{\partial \tau} \,. \tag{2.96}$$

Then, (2.95) may be rewritten as

$$p_\mathrm{a}(\boldsymbol{x}, t) = \int\limits_\Gamma \int\limits_0^T \left(p_\mathrm{a}(\boldsymbol{y}, \tau) \frac{\partial G(\boldsymbol{x}, t|\boldsymbol{y}, \tau)}{\partial y_i} \right) n_i \, \mathrm{d}s(\boldsymbol{y}) \, \mathrm{d}\tau + \int\limits_\Gamma \int\limits_0^T \left(\rho_0 \frac{\partial v_\mathrm{n}}{\partial \tau} \, G(\boldsymbol{x}, t|\boldsymbol{y}, \tau) \right) \mathrm{d}s(\boldsymbol{y}) \, \mathrm{d}\tau \,. \tag{2.97}$$

Since for many cases, we perform computations in the frequency domain, we also provide (2.95) in the frequency domain via a Fourier transform. Thereby, we obtain

$$\hat{p}_\mathrm{a}(\boldsymbol{x}, \omega) = \int\limits_\Gamma \left(\hat{p}_\mathrm{a}(\boldsymbol{y}, \omega) \frac{\partial \hat{G}(\boldsymbol{x}|\boldsymbol{y})}{\partial y_i} - \hat{G}(\boldsymbol{x}|) \frac{\partial \hat{p}_\mathrm{a}(\boldsymbol{y}, \omega)}{\partial y_i} \right) n_i \, \mathrm{d}s(\boldsymbol{y}) \tag{2.98}$$

and for our special case of an radiating surface according to (2.97)

$$\hat{p}_\mathrm{a}(\boldsymbol{x}, \omega) = \int\limits_\Omega \left(\hat{p}_\mathrm{a}(\boldsymbol{y}, \omega) \frac{\partial \hat{G}(\boldsymbol{x}|\boldsymbol{y})}{\partial y_i} \right) n_i \, \mathrm{d}s(\boldsymbol{y}) + \int\limits_\Gamma \left(j\omega\rho_0 \hat{v}_\mathrm{n} \, \hat{G}(\boldsymbol{x}|\boldsymbol{y}) \right) \mathrm{d}s(\boldsymbol{y}) \tag{2.99}$$

with $\hat{G}$, i.e. using free field Green's function according to (2.59).

As an example, let us compute the acoustic pressure generated by an pulsating sphere with radius a and vibration velocity $\hat{v}_\mathrm{n}$. Assuming the radius a to be very small, the spatial dependency of $\hat{G}$ and $\partial\hat{G}/\partial y_i$ becomes negligible, and we may write for the far field solution

$$\hat{p}_\mathrm{a}(\boldsymbol{x},\omega) = \left[\frac{\partial \hat{G}}{\partial y_i}\right]_{y_i=0} \int\limits_{\Gamma} p_\mathrm{a} n_i \,\mathrm{d}s(\boldsymbol{y}) + [\hat{G}]_{y_i=0} \int\limits_{\Gamma} j\omega\rho_0\hat{v}_\mathrm{n} \;\mathrm{d}s(\boldsymbol{y})\,. \tag{2.100}$$

The first term represents the net force exerted on the fluid by the sphere, and is zero because the pressure is constant on the surface. Therefore, we obtain

$$\hat{p}_\mathrm{a}(\boldsymbol{x},\omega) = \frac{j\omega\rho_0 a^2 \hat{v}_\mathrm{n}}{|\boldsymbol{x}|}\, e^{jk|\boldsymbol{x}|}\,. \tag{2.101}$$

For the general case, we often do not know $p_\mathrm{a}(\boldsymbol{y})$ on the surfaces and (2.98) or (2.98) cannot be directly solved. So, a numerical method, i.e. the boundary element method has to be applied. However, in cases that the surface is a rigid scatterer, we get rid of the first term, when we force $n_i\partial\hat{G}/\partial y_i$ to be zero. Such Green's functions are called *tailored* (modified) Green's functions [4, 6]

3. Aeroacoustics

3.1. Lighthill's Acoustic Analogy

The sound generated by a flow in an unbounded fluid is usually called *aerodynamic sound*. Most unsteady flows in technical applications are of high Reynolds number, and the acoustic radiation is a very small by-product of the motion. Thereby, the turbulence is usually produced by fluid motion over a solid body and/or by flow instabilities. Lighthill transformed the general equations of mass and momentum conservation to an exact inhomogeneous wave equation whose source terms are important only within the turbulent region [7].

Lighthill was initially interested in solving the problem, illustrated in Fig. 3.1a, of the sound produced by a turbulent nozzle and arrived at the inhomogeneous wave equation. However, at this time a volume discretization by numerical schemes was not feasible and so a

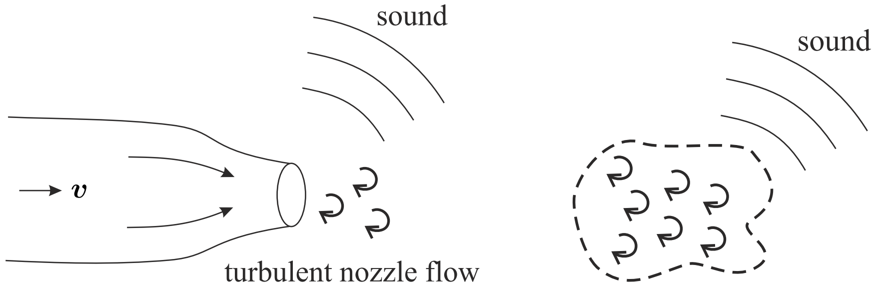

(a) Turbulent nozzle flow. (b) Isolated turbulent region.

Figure 3.1.: Sound generation by turbulent flows.

transformation of the PDE into an integral representation was performed, which can just be achieved for a free field setup, for which Green's function is available. Therefore, Lighthill's theory in its integral formulation just applies to the simple situation as given in Fig. 3.1b. This avoids complications caused by the presence of the nozzle. The fluid is assumed to be at rest at the observer position, where a mean pressure, density and speed of sound are respectively equal to p_0, ρ_0 and c_0. So Lighthill compared the equations for the production of density fluctuations in the real flow with those in an ideal linear acoustic medium (quiescent fluid).

For the derivation, we start at Reynolds form of the momentum equation, as given by (1.18) neglecting any force density $\boldsymbol{f}$

$$\frac{\partial \rho \boldsymbol{v}}{\partial t} + \nabla \cdot [\boldsymbol{\pi}] \quad = \quad 0\,, \tag{3.1}$$

with the momentum flux tensor $\pi_{ij} = \rho v_i v_j + (p - p_0)\delta_{ij} - \tau_{ij}$, where the constant pressure p_0 is inserted for convenience. In an ideal, linear acoustic medium, the momentum flux tensor contains only the pressure

$$\pi_{ij} \to \pi^0_{ij} = (p - p_0)\delta_{ij} = c_0^2(\rho - \rho_0)\delta_{ij} \tag{3.2}$$

and Reynolds momentum equation reduces to

$$\frac{\partial \rho v_i}{\partial t} + \frac{\partial}{\partial x_i}\left(c_0^2(\rho - \rho_0)\right) = 0\,. \tag{3.3}$$

Rewriting the conservation of mass in the form

$$\frac{\partial}{\partial t}(\rho - \rho_0) + \frac{\partial \rho v_i}{\partial x_i} = 0 \tag{3.4}$$

allows us to eliminate the momentum density ρv_i in (3.3). Therefore, we perform a time derivative on (3.4), a spatial derivative on (3.3) and subtract the two resulting equations. These operations leads to the equation of linear acoustics satisfied by the perturbation density

$$\left(\frac{1}{c_0^2}\frac{\partial^2}{\partial t^2} - \nabla\cdot\nabla\right)\left(c_0^2(\rho - \rho_0)\right) = 0\,. \tag{3.5}$$

Because flow is neglected, the unique solution of this equation satisfying the radiation condition and we obtain $\rho - \rho_0 = 0$.

Now, it can be asserted that the sound generated by the turbulence in the *real fluid* is exactly equivalent to that produced in the ideal, stationary acoustic medium forced by the stress distribution

$$L_{ij} = \pi_{ij} - \pi_{ij}^0 = \rho v_i v_j + \left((p - p_0) - c_0^2(\rho - \rho_0)\right)\delta_{ij} - \tau_{ij}\,, \tag{3.6}$$

where $[\boldsymbol{L}]$ is called the *Lighthill stress tensor*.

Indeed, we can rewrite (3.1) as the momentum equation for an ideal, stationary acoustic medium of mean density ρ_0 and speed of sound c_0 subjected to the externally applied stress L_{ij}

$$\frac{\partial \rho v_i}{\partial t} + \frac{\partial \pi_{ij}^0}{\partial x_j} = -\frac{\partial}{\partial x_j}\left(\pi_{ij} - \pi_{ij}^0\right)\,, \tag{3.7}$$

or equivalent

$$\frac{\partial \rho v_i}{\partial t} + \frac{\partial}{\partial x_j}\left(c_0^2(\rho - \rho_0)\right) = -\frac{\partial L_{ij}}{\partial x_j}\,. \tag{3.8}$$

By eliminating the momentum density ρv_i using (3.4) we arrive at **Lighthill's equation**

$$\left(\frac{1}{c_0^2}\frac{\partial^2}{\partial t^2} - \nabla\cdot\nabla\right)\left(c_0^2(\rho - \rho_0)\right) = \frac{\partial^2 L_{ij}}{\partial x_i \partial x_j}\,. \tag{3.9}$$

It has to be noted that $(\rho - \rho_0) = \rho'$ is a fluctuating density not being equal to the acoustic density ρ^{a}, but a superposition of flow and acoustic parts within flow regions.

The problem of calculating the flow generated sound is equivalent to solving this wave equation, which is possible when the source term $\partial^2 L_{ij}/\partial x_i \partial x_j$ is provided, e.g., by a CFD computation. This type of source term can just be interpreted as a quadrupole term, when free field conditions are assumed, i.e. no solid bodies are present. Therefore, the free field turbulence is an extremely weak sound source, and so in low Mach number flows, just a very small portion of the flow energy is converted into sound. However, in the presence of walls the sound radiation by turbulence can be dramatically enhanced. In the next section, we will see that compact bodies will radiate a dipole sound field associated to the force which they exert on the flow as a reaction to the dynamic force of the flow applied to them. Sharp edges are particularly efficient radiators.

In the definition of the Lighthill tensor according to (3.6) the term $\rho v_i v_j$ is called the Reynolds stress. It is a nonlinear term and can be neglected except where the motion is turbulent. The second term $\left((p - p_0) - c_0^2(\rho - \rho_0)\right)\delta_{ij}$ represents the *excess of* moment transfer by the pressure over that in the ideal fluid of density ρ_0 and speed of sound c_0. This is produced by wave amplitude nonlinearity, and by mean density variations in the source flow. The viscous stress tensor τ_{ij} properly accounts for the attenuation of the sound. In most applications the Reynolds number in the source region is high and we can neglect this contribution.

The solution of (3.9) for free field radiation condition with outgoing wave behaviour can be rewritten in integral form as follows (see sec. 2.6)

$$c_0^2(\rho - \rho_0)(\boldsymbol{x}, t) = \frac{1}{4\pi} \frac{\partial^2}{\partial x_i \partial x_j} \int\limits_{-\infty}^{\infty} \frac{L_{ij}(\boldsymbol{y}, t - |\boldsymbol{x} - \boldsymbol{y}|/c_0)}{|\boldsymbol{x} - \boldsymbol{y}|} \, \mathrm{d}\boldsymbol{y} \,. \tag{3.10}$$

Thereby, $\boldsymbol{y}$ defines the source coordinate and $\boldsymbol{x}$ the coordinate at which we compute the acoustic density fluctuation. This provides a useful prediction of the sound, if L_{ij} is known. Please note that the terms in L_{ij} not only account for the generation of sound, but also includes acoustic *self modulation* caused by

- acoustic nonlinearity,
- the convection of sound waves by the turbulent flow velocity,
- refraction caused by sound speed variations,
- and attenuation due to thermal and viscous actions.

The influence of acoustic nonlinearity and thermoviscous dissipation is usually sufficiently small to be neglected within the source region. Convection and refraction of sound within the flow region can be important, e.g., in the presence of a mean shear layer (when the Reynolds stress will include terms like $\rho v_{0i} v'_j$, where $\boldsymbol{v}_0$ and $\boldsymbol{v}'$ respectively denote the mean and fluctuating components of $\boldsymbol{v}$). Such effects are described by the presence of unsteady linear terms in L_{ij}. Furthermore, since for practical applications the source term is obtained by numerically solving Navier-Stokes equation, the question of how accurate the source term is resolved, is always present.

In summary, the whole set of compressible flow dynamics equations have to be solved in order to be able to calculate Lighthill's tensor. However, this means that we have to resolve both the flow structures and acoustic waves, which is an enormous challenge for any numerical scheme and the computational noise itself may strongly disturb the physical radiating wave components [8]. Therefore, in the theories of Phillips and Lilley interaction effects have been, at least to some extend, moved to the wave operator [9, 10]. These equations predict certain aspects of the sound field surrounding a jet quite accurately, which are not accounted for Lighthill's equation due to the restricted numerical resolution of the source term need in

(3.9) [11].

Now, let's consider the situation for which the mean density and speed of sound are uniform throughout the fluid. The variations in the density ρ within a low Mach number, high Reynolds number source flow are then of order $O(\rho_0 \mathrm{Ma}^2)$. Thus, $\rho v_i v_j = \rho_0 \left(1 + O(\mathrm{Ma}^2)\right) v_i v_j \approx \rho_0 v_i v_j$. Furthermore, if $c(\boldsymbol{x}, t)$ is the local speed of sound in the source region, it can be shown that $c_0^2/c^2 = 1 + O(\mathrm{Ma}^2)$, so that we obtain

$$p - p_0 - c_0^2(\rho - \rho_0) = (p - p_0)(1 - c_0^2 \underbrace{\frac{\rho - \rho_0}{p - p_0}}_{1/c^2}) \approx (p - p_0)(1 - c_0^2/c^2) \sim O(\rho_0 v^2 \mathrm{Ma}^2)\,. \quad (3.11)$$

Therefore, if viscous dissipation is neglected, we may approximate the Lighthill tensor by

$$L_{ij} \approx \rho_0 v_i v_j \quad \text{for } \mathrm{Ma}^2 \ll 1\,. \quad (3.12)$$

With this result we obtain for the pressure fluctuation using the isentropic pressure-density relation the following integral representation

$$p'(\boldsymbol{x}, t) \approx \frac{\partial^2}{\partial x_i \partial x_j} \int \frac{\rho_0 v_i v_j (\boldsymbol{y}, t - |\boldsymbol{x} - \boldsymbol{y}|/c_0)}{4\pi |\boldsymbol{x} - \boldsymbol{y}|} \,\mathrm{d}\boldsymbol{y} \quad (3.13)$$

$$\approx \frac{x_i x_j}{4\pi c_0^2 |\boldsymbol{x}|^3} \frac{\partial^2}{\partial t^2} \int \rho_0 v_i v_j \left(\boldsymbol{y}, t - \frac{|\boldsymbol{x}|}{c_0} + \frac{\boldsymbol{x} \cdot \boldsymbol{y}}{c_0 |\boldsymbol{x}|}\right) \,\mathrm{d}\boldsymbol{y}\,. \quad (3.14)$$

To obtain (3.14), we have used the far field approximation, which allows the following substitution (see Sec. 2.7)

$$\frac{\partial}{\partial x_j} \approx -\frac{1}{c_0} \frac{x_j}{|\boldsymbol{x}|} \frac{\partial}{\partial t}\,. \quad (3.15)$$

Now, we want to derive the order of the magnitude of the acoustic pressure as a function of the flow velocity $\boldsymbol{v}$. In doing so, we introduce a characteristic velocity v and length scale l of a single vortex as displayed in Fig. 3.2. Fluctuations in $v_i v_j$ occurring in different turbulent

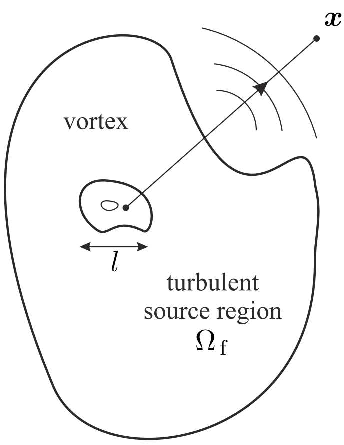

Figure 3.2.: Single vortex in a turbulent flow region at its acoustic radiation towards the far field.

regions by distances larger than $O(l)$ will be treated to be statistically independent. So the sound may be considered to be generated by a collection of $\Omega_{\rm f}/l^3$ independent vortices. The characteristic frequency of the turbulent fluctuations can be estimated by $f \sim v/l$ so that the wavelength λ of sound will result in

$$\lambda = \frac{c_0}{f} \sim \frac{c_0 l}{v} = \frac{l}{\mathrm{Ma}} \gg l \text{ for } \mathrm{Ma} = v/c_0 \ll 1\,.$$

Hence, we arrive at the quite important conclusion that the turbulent vortices are all acoustically compact. This means that in the relation (3.14) the retarded time variation $\boldsymbol{x}\cdot\boldsymbol{y}/(c_0|\boldsymbol{x}|)$ can be neglected. Therefore, the value of the integral over one source vortex in (3.14) can be estimated to be of order $\rho_0 v^2 l^3$. The order of the magnitude for the time derivative in (3.14) is estimated to be

$$\frac{\partial}{\partial t} \sim \frac{v}{l}\,.$$

Collecting all this estimates, we may now state that the acoustic pressure in the far-field, generated by one vortex, satisfies

$$p_{\rm a} \sim \frac{l}{|\boldsymbol{x}|}\,\frac{\rho_0 v^4}{c_0^2} = \frac{l}{|\boldsymbol{x}|}\,\rho_0 v^2 \mathrm{Ma}^2\,. \tag{3.16}$$

The acoustic power defined by

$$P_{\rm a} = \oint_\Gamma p_{\rm a}\boldsymbol{v}_{\rm a}\cdot \mathrm{d}\boldsymbol{s} = \oint_\Gamma p_{\rm a}\boldsymbol{v}_{\rm a}\cdot\boldsymbol{n}\;\mathrm{d}s \tag{3.17}$$

can be computed in the far-field with the relation $\boldsymbol{v}_{\rm a}\cdot\boldsymbol{n} = p_{\rm a}/(\rho_0 c_0)$ as follows

$$P_{\rm a} = \oint_\Gamma \frac{{p_{\rm a}}^2}{\rho_0 c_0}\;\mathrm{d}s\,. \tag{3.18}$$

This formula allows us to estimate the acoustic power generated by one vortex

$$P_{\rm a} \sim 4\pi|\boldsymbol{x}|^2\frac{{p_{\rm a}}^2}{\rho_0 c_0} \sim \frac{l^2\rho_0 v^8}{c_0^5} = \rho_0\, l^2\, v^3\, \mathrm{Ma}^5\,. \tag{3.19}$$

This is the famous **eighth power law**.

For practical applications of Lighthill's analogy, it would be quite beneficial to know the leading order term of Lighthill's tensor. This analysis has been done in [12] for low Mach number flows in an isentropic medium by applying method of matched asymptotic expansion (see, e.g., [8]). Sound emission from an eddy region involves three length scales: the eddy size l, the wavelength λ of the sound, and a dimension L of the region. The problem is solved for $\mathrm{Ma} \ll 1$ and $L/l \sim 1$ by matching the compressible eddy core scaled by l to a surrounding acoustic field scaled by λ. Thereby, Lighthill's solution is shown to be adequate in both regions, if L_{ij} is approximated by

$$L_{ij} \approx \rho_0 v_{{\rm ic},i} v_{{\rm ic},j} \tag{3.20}$$

with $\boldsymbol{v}_{\rm ic} = \nabla\times\boldsymbol{\psi}(\boldsymbol{\omega})$ and vorticity $\boldsymbol{\omega} = \nabla\times\boldsymbol{v}_{\rm ic}$. Such a flow field is described by solving the incompressible flow dynamics equations. Thereby, we obtain an incompressible flow velocity

$\boldsymbol{v}_{\mathrm{ic}}$ and pressure p_{ic}. For an incompressible flow, the divergence of $\boldsymbol{v}_{\mathrm{ic}}$ is zero, which allows to rewrite the second spatial derivative of (3.20) by

$$\frac{\partial^2}{\partial x_i x_j}\left(\rho_0 v_{\mathrm{ic},i} v_{\mathrm{ic},j}\right) = \rho_0 \frac{\partial v_{\mathrm{ic},j}}{\partial x_i}\frac{\partial v_{\mathrm{ic},i}}{\partial x_j}\,. \tag{3.21}$$

Furthermore, applying the divergence to (1.18) provides the following equivalence (using $\nabla \cdot \boldsymbol{v}_{\mathrm{ic}} = 0$ and assuming $\boldsymbol{f} = 0$)

$$\nabla \cdot \nabla p_{\mathrm{ic}} = -\rho_0 \frac{\partial^2 v_{\mathrm{ic},i} v_{\mathrm{ic},j}}{\partial x_i \partial x_j}\,. \tag{3.22}$$

With such an approach, we totally separate the flow from the acoustic field, which also means that any influence of the acoustic field on the flow field is neglected.

3.2. Curle's Theory

The main restriction of Lighthill's integral formulation is that it can just consider free radiation. Therewith, it can not consider situations where there is any solid body within the region. In [13] this problem was solved by deriving an integral formulation for the sound generated by turbulence in the vicinity of an arbitrary, fixed surface Γ_{s} as displayed in Fig. 3.3a. Thereby the surface Γ_{s} is defined by the function $f(\boldsymbol{x})$, which has the following property (see Fig. 3.3b).

$$f(\boldsymbol{x}) = \begin{cases} 0 & \text{for } \boldsymbol{x} \text{ on } \Gamma_{\mathrm{s}} \\ < 0 & \text{for } \boldsymbol{x} \text{ within the surface} \\ > 0 & \text{for } \boldsymbol{x} \text{ in } \Omega\,. \end{cases}$$

This surface may either be a solid body, or just an artificial control surface used to isolate a

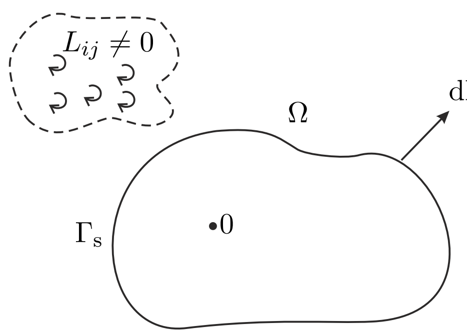

(a) Turbulent source region with solid body.

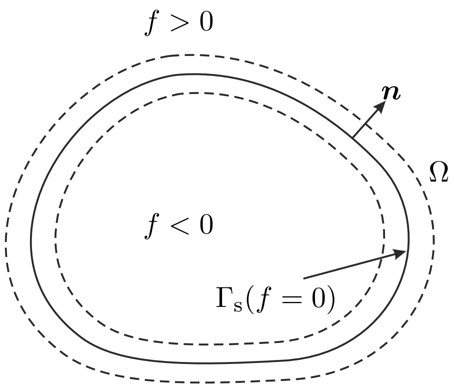

(b) Solid body.

Figure 3.3.: Setup for deriving Curle's equation.

fixed region of space containing both solid bodies and fluid or just fluid.

To derive Curle's equation we start with the momentum equation according to (3.8) and multiply it with the Heaviside function $H(f)$

$$H(f)\,\frac{\partial \rho v_i}{\partial t} + H(f)\,\frac{\partial}{\partial x_i}\left(c_0^2(\rho - \rho_0)\right) \;=\; -H(f)\,\frac{\partial L_{ij}}{\partial x_j}\,. \tag{3.23}$$

Now, we use the product rule for differentiation (noting that the time derivative of the Heaviside function, which just depends on space, is zero) and obtain by also writing L_{ij} by its individual components

$$\frac{\partial}{\partial t}\left(\rho v_i H(f)\right) + \frac{\partial}{\partial x_j}\left(c_0^2(\rho-\rho_0)H(f)\right) - c_0^2(\rho-\rho_0)\,\frac{\partial H(f)}{\partial x_i} \tag{3.24}$$
$$= -\frac{\partial}{\partial x_j}\left(L_{ij}H(f)\right) + \underbrace{\left(\rho v_i v_j + \left((p-p_0) - c_0^2(\rho-\rho_0)\right)\delta_{ij} - \tau_{ij}\right)}_{L_{ij}}\,\frac{\partial H(f)}{\partial x_j}\,.$$

We can cancel out the term $c_0^2(\rho-\rho_0)\,\partial H(f)/\partial x_i$ being at both sides of the equation and arrive at

$$\frac{\partial}{\partial t}\left(\rho v_i H(f)\right) + \frac{\partial}{\partial x_j}\left(c_0^2(\rho-\rho_0)H(f)\right)$$
$$= -\frac{\partial}{\partial x_j}\left(L_{ij}H(f)\right) + \left(\rho v_i v_j + (p-p_0)\,\delta_{ij} - \tau_{ij}\right)\frac{\partial H(f)}{\partial x_j}\,. \tag{3.25}$$

The same procedure is now applied to the mass conservation according to (3.4) and so we obtain

$$\frac{\partial}{\partial t}\left((\rho-\rho_0)H(f)\right) + \frac{\partial}{\partial x_i}\left(\rho v_i H(f)\right) - \rho v_i \frac{\partial H(f)}{\partial x_i} = 0\,. \tag{3.26}$$

Now, we perform a time derivative to this equation and rearrange it for $\rho v_i H(f)$

$$\frac{\partial^2}{\partial t \partial x_i}\left(\rho v_i H(f)\right) = \frac{\partial}{\partial t}\left(\rho v_i \frac{\partial H(f)}{\partial x_i}\right) - \frac{\partial^2}{\partial t^2}\left((\rho-\rho_0)H(f)\right)\,. \tag{3.27}$$

In a last step, we apply the divergence operation to (3.25) and substitute the expression for $\rho v_i H(f)$ from (3.27)

$$\left(\frac{1}{c_0^2}\frac{\partial^2}{\partial t^2} - \nabla\cdot\nabla\right)\left(c_0^2(\rho-\rho_0)H(f)\right) \tag{3.28}$$
$$= \frac{\partial^2 L_{ij}H(f)}{\partial x_i \partial x_j}$$
$$- \frac{\partial}{\partial x_i}\left(\left(\rho v_i v_j + (p-p_0)\delta_{ij} - \tau_{ij}\right)\frac{\partial H(f)}{\partial x_j}\right)$$
$$+ \frac{\partial}{\partial t}\left(\rho v_j \frac{\partial H(f)}{\partial x_j}\right)\,.$$

This equation is now valid throughout the space, including the region enclosed by Γ_s. Furthermore, compared to Lighthill's equation, we have obtained two additional terms on the right hand side of the wave equation including space derivatives of the Heaviside function $H(f)$. Thereby, according to our previous investigation the second term on the right hand side corresponds to a dipole and the third term to a monopole with the following interpretation:

- Γ_s is the boundary of a solid body:
  In this case the surface dipole represents the production of sound by the unsteady force that the body exerts on the exterior fluid, whereas the monopole is responsible for the sound generated by volume pulsations (if any) of the body.

- Γ_s is just an artificial control surface:
  The dipole and monopole sources account for the presence of solid bodies and turbulences within Γ_s (when L_{ij} is different from zero in Γ_s) and also for the interaction of sound generated outside Γ_s with the fluid and solid bodies inside Γ_s.

To transform (3.28) to the corresponding integral representation is a straight forward operation. According to the wave equation and its integral representation we obtain for the monopole term

$$\frac{1}{4\pi} \int_{-\infty}^{\infty} \frac{\partial}{\partial t} \langle \rho v_j \rangle \, \frac{\partial H(f)}{\partial y_j} \, \frac{1}{|\boldsymbol{x} - \boldsymbol{y}|} \, \mathrm{d}\boldsymbol{y} \,, \tag{3.29}$$

where $\langle \; \rangle$ indicates that the terms have to be evaluated at retarted time $(t - |\boldsymbol{x} - \boldsymbol{y}|/c_0)$. For the dipole term we obtain the following integral representation

$$\frac{1}{4\pi} \frac{\partial}{\partial x_i} \int_{-\infty}^{\infty} \langle \rho v_i v_j + (p - p_0)\delta_{ij} - \tau_{ij} \rangle \, \frac{\partial H(f)}{\partial y_j} \, \frac{1}{|\boldsymbol{x} - \boldsymbol{y}|} \, \mathrm{d}\boldsymbol{y} \,. \tag{3.30}$$

The last step is the handling of the Heaviside function, which has according to generalized function theory the following property for an arbitrary smooth function $\Phi(\boldsymbol{x})$ [4]

$$\int_{-\infty}^{\infty} \Phi(\boldsymbol{y}) \frac{\partial H(f)}{\partial y_j} \, \mathrm{d}\boldsymbol{y} = \oint_{\Gamma_\mathrm{s}} \Phi(\boldsymbol{y}) n_j \, \mathrm{d}s = \oint_{\Gamma_\mathrm{s}} \Phi(\boldsymbol{y}) \, \mathrm{d}s_j \,. \tag{3.31}$$

Exploring this property, we finally arrive at Curle's equation in integral form

$$\begin{aligned} c_0^2(\rho - \rho_0)\, H(f) \;&=\; \frac{\partial^2}{\partial x_i \partial x_j} \int_{\Omega} \frac{\langle L_{ij} \rangle}{4\pi |\boldsymbol{x} - \boldsymbol{y}|} \, \mathrm{d}\boldsymbol{y} \\ &\quad - \frac{\partial}{\partial x_i} \oint_{\Gamma_\mathrm{s}} \frac{\langle \rho v_i v_j + (p - p_0)\delta_{ij} - \tau_{ij} \rangle}{4\pi |\boldsymbol{x} - \boldsymbol{y}|} \, \mathrm{d}s_j(\boldsymbol{y}) \\ &\quad + \frac{\partial}{\partial t} \oint_{\Gamma_\mathrm{s}} \frac{\langle \rho v_j \rangle}{4\pi |\boldsymbol{x} - \boldsymbol{y}|} \, \mathrm{d}s_j(\boldsymbol{y}) \,. \end{aligned} \tag{3.32}$$

Now, let us restrict to a rigid body for which the flow velocity in normal direction on this body is zero, so that (3.32) reduces to

$$\begin{aligned} c_0^2(\rho - \rho_0)\, H(f) \;&=\; \frac{\partial^2}{\partial x_i \partial x_j} \int_{\Omega} \frac{\langle L_{ij} \rangle}{4\pi |\boldsymbol{x} - \boldsymbol{y}|} \, \mathrm{d}\boldsymbol{y} \\ &\quad - \frac{\partial}{\partial x_i} \oint_{\Gamma_\mathrm{s}} \frac{\langle (p - p_0)\delta_{ij} - \tau_{ij} \rangle}{4\pi |\boldsymbol{x} - \boldsymbol{y}|} \, \mathrm{d}s_j(\boldsymbol{y}) \,. \end{aligned} \tag{3.33}$$

Furthermore, we assume the body to be acoustically compact, which means that $\mathrm{Ma} = v/c_0 \ll 1$. In the following investigation, we want to estimate the order of the sound generation by the dipole term. With the characteristic velocity v and scale length l of a vortex, we have the following relations

$$(p - p_0) \sim \rho_0 v^2 \,; \quad \tau \sim \mu \frac{v}{l} \,. \tag{3.34}$$

Therefore, we can compute the ratio

$$\frac{p - p_0}{\tau} \sim \frac{\rho_0 v l}{\mu} = \frac{v l}{\nu}$$

with $\nu = \mu/\rho_0$ the kinematic viscosity, which is just the definition of the Reynolds number $\mathrm{Re} = vl/\nu$. Since in turbulent flows Re is quite high, we can neglect the viscous contribution. In the far-field, the acoustic pressure p_a is equal to $c_0^2(\rho - \rho_0)H(f)$ ($H(f)$ is there just 1), and exploring the compactness which allows us to neglect the retarded time variation $\boldsymbol{x} \cdot \boldsymbol{y}/(c_0|\boldsymbol{x}|)$ results for the second term in (3.33) using (3.15) in

$$p_\mathrm{a} \approx \frac{x_i}{4\pi c_0 |\boldsymbol{x}|^2} \frac{\partial}{\partial t} \oint\limits_{\Gamma_\mathrm{s}} (p - p_0) \left(\boldsymbol{y}, t - \frac{|\boldsymbol{x}|}{c_0} \right) \mathrm{d}s_i = \frac{x_i}{4\pi c_0 |\boldsymbol{x}|^2} \frac{\partial F_i}{\partial t} \left(t - \frac{|\boldsymbol{x}|}{c_0} \right) \tag{3.35}$$

with $\boldsymbol{F}$ the total unsteady surface force. For a surface element with a diameter of l, the contribution to the acoustic pressure p_a can be estimated by

$$p_\mathrm{a} \sim \frac{1}{c_0 |\boldsymbol{x}|} \frac{v}{l} \rho_0 v^2 l^2 = \frac{l}{|\boldsymbol{x}|} \rho_0 v^2 \mathrm{Ma} \,. \tag{3.36}$$

Assuming to have Γ_s/l^2 independently radiating surface elements, we can estimate the acoustic power (see also (3.19))

$$\begin{aligned} P_\mathrm{a} \sim 4\pi |\boldsymbol{x}|^2 \frac{{p_\mathrm{a}}^2}{\rho_0 c_0} \frac{\Gamma_\mathrm{s}}{l^2} &= \left(4\pi |\boldsymbol{x}|^2 \frac{l^2}{\rho_0 c_0 |\boldsymbol{x}|^2} \rho_0^2 v^4 \mathrm{Ma}^2 \right) \frac{\Gamma_\mathrm{s}}{l^2} \\ &\sim \rho_0 \Gamma_\mathrm{s} v^3 \mathrm{Ma}^3 \,. \end{aligned} \tag{3.37}$$

So, we see that in case of a dipole we arrive at a **sixth power law** and compared to the quadrupole we have a factor of $1/\mathrm{Ma}^2$ being stronger.

Therefore, we can summarize that Lighthills' inhomogeneous wave equation is a quite general model to describe flow-induced sound. Solving this partial differential equation by the correct boundary conditions, i.e. $\partial p'/\partial \boldsymbol{n} = 0$ at the surface of solid bodies, using a volume discretization method includes all sources of the sound. The additional source terms, as given in (3.32) just come up, because the partial differential equation is converted to an integral representation for which Greens' function is needed. Furthermore, the solution is a fluctuating pressure (density), which approaches the acoustic pressure (density) outside the flow region.

In a final step, we will demonstrate that Curle's equation according to (3.32) can be also obtained by solving Lighthill's equation using the method of Green's function as described in Sec. 2.9. The detailed derivation can be found in [6]. Thereby, the the following integral equation is obtained

$$
\begin{aligned}
c_0^2(\rho - \rho_0) &= \int_0^T \int_\Omega \frac{\partial^2 G}{\partial y_i \partial y_j} L_{ij}(\boldsymbol{y}, \tau) \, \mathrm{d}\boldsymbol{y} \, \mathrm{d}\tau \\
&+ \int_0^T \int_\Gamma \left(\big((p - p_0)\delta_{ij} - \tau_{ij} + \rho v_i v_j \big) \frac{\partial G}{\partial y_i} + G \frac{\partial(\rho v_j)}{\partial \tau} \right) \mathrm{d}s_j(\boldsymbol{y}) \, \mathrm{d}\tau \,. \quad (3.38)
\end{aligned}
$$

Now, we apply the free field Green's function

$$
G(\boldsymbol{x}, t|\boldsymbol{y}, \tau) = \frac{\delta(t - \tau - |\boldsymbol{x} - \boldsymbol{y}|/c_0)}{4\pi|\boldsymbol{x} - \boldsymbol{y}|} \quad (3.39)
$$

with the properties

$$
\frac{\partial G}{\partial y_i} = -\frac{\partial G}{\partial x_i}\,; \quad \frac{\partial^2 G}{\partial y_i y_j} = \frac{\partial^2 G}{\partial x_i x_j} \quad (3.40)
$$

and we may rewrite (3.38) by

$$
\begin{aligned}
c_0^2(\rho - \rho_0) &= \frac{\partial^2}{\partial x_i \partial x_j} \int_0^T \int_\Omega G \, L_{ij}(\boldsymbol{y}, \tau) \, \mathrm{d}\boldsymbol{y} \, \mathrm{d}\tau \\
&+ \int_0^T \int_\Gamma \left(G \frac{\partial(\rho v_j)}{\partial \tau} \right) \mathrm{d}s_j(\boldsymbol{y}) \, \mathrm{d}\tau \\
&- \frac{\partial}{\partial x_i} \int_0^T \int_\Omega \big((p - p_0)\delta_{ij} - \tau_{ij} + \rho v_i v_j \big) G \, \mathrm{d}s_j(\boldsymbol{y}) \, \mathrm{d}\tau \,. \quad (3.41)
\end{aligned}
$$

Now, we substitute the Green's function according to (3.39) and perform the integration over time to arrive at

$$
\begin{aligned}
c_0^2(\rho - \rho_0) &= \frac{\partial^2}{\partial x_i \partial x_j} \int_\Omega \frac{\langle L_{ij} \rangle}{4\pi|\boldsymbol{x} - \boldsymbol{y}|} \, \mathrm{d}\boldsymbol{y} \\
&+ \frac{\partial}{\partial t} \int_\Gamma \frac{\langle \rho v_j \rangle}{4\pi|\boldsymbol{x} - \boldsymbol{y}|} \, \mathrm{d}s_j(\boldsymbol{y}) \\
&- \frac{\partial}{\partial x_i} \int_\Omega \frac{\langle (p - p_0)\delta_{ij} - \tau_{ij} + \rho v_i v_j \rangle}{4\pi|\boldsymbol{x} - \boldsymbol{y}|} \, \mathrm{d}s_j(\boldsymbol{y}) \,, \quad (3.42)
\end{aligned}
$$

where $\langle \; \rangle$ indicates that the terms have to be evaluated at retarted time $(t - |\boldsymbol{x} - \boldsymbol{y}|/c_0)$. It is easy to see that this equation fully coincide with (3.32).

Finally, we want to note that starting from Lighthill's inhomogeneous wave equation, see (3.9), we may also arrive at an internal equation, which not only takes into account stationary scattering objects but also moving surfaces as occurring for propellers and helicopter rotor noise. The resulting formulation is known as *Ffowcs Williams and Hawkings equation* and a detailed derivation can be found in the original publication [14], or by a description being more easily understandable, e.g., in [6].

3.3. Vortex Sound

For many applications at low Mach number it is more convenient to rewrite the noise producing parts of Lighthill's tensor $[\boldsymbol{L}]$ by its local vorticity. The main advantage is that vortical regions of the flow are much more concentrated then the region over which $[\boldsymbol{L}]$ is nonzero.

An eddy of size l with typical velocity U generates sound with frequencies of the order U/l. The wavelength of the sound, $\lambda = O(l/\mathrm{Ma})$, greatly exceeds the eddy size l of a low Mach number flow. As shown in [12] (see Sec. 3.1) the leading order term at low Mach number flows of Lighthill's tensor is

$$\tilde{L}_{ij} = \rho_0 v_{\mathrm{ic},i} v_{\mathrm{ic},j} \,. \tag{3.43}$$

As discussed in Sec. 1.5, the incompressible flow velocity is defined by the vorticty $\boldsymbol{\omega}$ according to

$$\boldsymbol{v}_{\mathrm{ic}} = \nabla_x \times \int_\Omega \frac{\boldsymbol{\omega}(\boldsymbol{y})}{4\pi|\boldsymbol{x}-\boldsymbol{y}|}\,\mathrm{d}\boldsymbol{y} \,. \tag{3.44}$$

Using the vector identities (B.13), (B.14) and the property $\nabla \cdot \boldsymbol{v}_{\mathrm{ic}} = 0$, the reduced source term of Lighthill's inhomogenoeus wave equation can be written as

$$\nabla \cdot \nabla \cdot [\tilde{\boldsymbol{L}}] = \rho_0 \nabla \cdot \nabla \cdot (\boldsymbol{v}_{\mathrm{ic}} \otimes \boldsymbol{v}_{\mathrm{ic}}) = \rho_0 \nabla \cdot (\boldsymbol{\omega} \times \boldsymbol{v}_{\mathrm{ic}}) + \rho_0 \underbrace{\nabla \cdot \nabla \Big(\frac{1}{2} \boldsymbol{v}_{\mathrm{ic}} \cdot \boldsymbol{v}_{\mathrm{ic}}\Big)}_{(\nabla^2 \frac{1}{2} v_{\mathrm{ic}}^2)} \,. \tag{3.45}$$

Substituting this result into Lighthill's integral form results for $(\rho - \rho_0)(\boldsymbol{x},t) = \rho'(\boldsymbol{x},t)$ in

$$\rho'(\boldsymbol{x},t) = \frac{\rho_0}{4\pi c_0^2} \int_{-\infty}^{\infty} \int_\Omega \left(\nabla \cdot (\boldsymbol{\omega} \times \boldsymbol{v}_{\mathrm{ic}}) + \nabla^2 \left(\frac{v_{\mathrm{ic}}^2}{2} \right) \right) \frac{\delta(t - \tau - |\boldsymbol{x}-\boldsymbol{y}|/c_0)}{|\boldsymbol{x}-\boldsymbol{y}|}\,\mathrm{d}\boldsymbol{y}\,\mathrm{d}\tau \,. \tag{3.46}$$

In the usual way, we integrate by parts to transfer the derivatives to the Green's function (note that the surface integral vanishes)

$$\begin{aligned} \rho'(\boldsymbol{x},t) &= \frac{\rho_0}{4\pi c_0^2} \int_{-\infty}^{\infty} \int_\Omega \left(-(\boldsymbol{\omega} \times \boldsymbol{v}_{\mathrm{ic}})_i \frac{\partial}{\partial y_i} \left(\frac{\delta(t - \tau - |\boldsymbol{x}-\boldsymbol{y}|/c_0)}{|\boldsymbol{x}-\boldsymbol{y}|} \right) \right) \mathrm{d}\boldsymbol{y}\,\mathrm{d}\tau \\ &+ \frac{\rho_0}{4\pi c_0^2} \int_{-\infty}^{\infty} \int_\Omega \left(\frac{v_{\mathrm{ic}}^2}{2} \right) \frac{\partial^2}{\partial y_i \partial y_j} \left(\frac{\delta(t - \tau - |\boldsymbol{x}-\boldsymbol{y}|/c_0)}{|\boldsymbol{x}-\boldsymbol{y}|} \right) \mathrm{d}\boldsymbol{y}\,\mathrm{d}\tau \,. \end{aligned} \tag{3.47}$$

The Green's function depend on $|\boldsymbol{x}-\boldsymbol{y}|$ and so we can using the relation (2.64) and arrive at

$$\begin{aligned} \rho'(\boldsymbol{x},t) &= \frac{\rho_0}{4\pi c_0^2} \frac{\partial}{\partial x_i} \int_{-\infty}^{\infty} \int_\Omega (\boldsymbol{\omega} \times \boldsymbol{v}_{\mathrm{ic}})_i \frac{\delta(t - \tau - |\boldsymbol{x}-\boldsymbol{y}|/c_0)}{|\boldsymbol{x}-\boldsymbol{y}|}\,\mathrm{d}\boldsymbol{y}\,\mathrm{d}\tau \\ &+ \frac{\rho_0}{4\pi c_0^2} \frac{\partial^2}{\partial x_i \partial x_j} \int_{-\infty}^{\infty} \int_\Omega \frac{v_{\mathrm{ic}}^2}{2} \frac{\delta(t - \tau - |\boldsymbol{x}-\boldsymbol{y}|/c_0)}{|\boldsymbol{x}-\boldsymbol{y}|}\,\mathrm{d}\boldsymbol{y}\,\mathrm{d}\tau \,. \end{aligned} \tag{3.48}$$

Next, we use the δ-property to evaluate the τ-integral

$$\begin{aligned}\rho'(\boldsymbol{x},t) &= \frac{\rho_0}{4\pi c_0^2}\frac{\partial}{\partial x_i}\int\limits_\Omega \frac{(\boldsymbol{\omega}\times\boldsymbol{v}_{\rm ic})_i(\boldsymbol{y},t-|\boldsymbol{x}-\boldsymbol{y}|/c_0)}{|\boldsymbol{x}-\boldsymbol{y}|}\,\mathrm{d}\boldsymbol{y}\\ &+ \frac{\rho_0}{4\pi c_0^2}\frac{\partial^2}{\partial x_i\partial x_j}\int\limits_\Omega \frac{\frac{1}{2}v_{\rm ic}^2(\boldsymbol{y},t-|\boldsymbol{x}-\boldsymbol{y}|/c_0)}{|\boldsymbol{x}-\boldsymbol{y}|}\,\mathrm{d}\boldsymbol{y}\,. \end{aligned} \tag{3.49}$$

Further simplifications can be performed by turning to the far-field approximation. For the case $|\boldsymbol{x}| \gg |\boldsymbol{y}|$we may use (see Sec. 2.7)

$$|\boldsymbol{x}-\boldsymbol{y}| \approx |\boldsymbol{x}| - \frac{\boldsymbol{x}\cdot\boldsymbol{y}}{|\boldsymbol{x}|}\,; \quad \frac{1}{|\boldsymbol{x}-\boldsymbol{y}|} \approx \frac{1}{|\boldsymbol{x}|}\,; \quad \frac{\partial}{\partial x_i} \approx -\frac{x_i}{c_0|\boldsymbol{x}|}\frac{\partial}{\partial t}$$

and obtain

$$\begin{aligned}\rho'(\boldsymbol{x},t) &= \frac{-\rho_0 x_i}{4\pi c_0^3|\boldsymbol{x}|^2}\frac{\partial}{\partial t}\int\limits_\Omega (\boldsymbol{\omega}\times\boldsymbol{v}_{\rm ic})_i\Big(\boldsymbol{y},t-\frac{|\boldsymbol{x}|}{c_0}+\frac{\boldsymbol{x}\cdot\boldsymbol{y}}{c_0|\boldsymbol{x}|}\Big)\,\mathrm{d}\boldsymbol{y}\\ &+ \frac{\rho_0}{8\pi c_0^4}\frac{\partial^2}{\partial t^2}\int\limits_\Omega v_{\rm ic}^2\Big(\boldsymbol{y},t-\frac{|\boldsymbol{x}|}{c_0}+\frac{\boldsymbol{x}\cdot\boldsymbol{y}}{c_0|\boldsymbol{x}|}\Big)\,\mathrm{d}\boldsymbol{y}\,. \end{aligned} \tag{3.50}$$

The variation in retarted time can be expanded in a Taylor series

$$(\cdot)\Big(\boldsymbol{y},t-\frac{|\boldsymbol{x}|}{c_0}+\frac{\boldsymbol{x}\cdot\boldsymbol{y}}{c_0|\boldsymbol{x}|}\Big) = (\cdot)\Big(\boldsymbol{y},t-\frac{|\boldsymbol{x}|}{c_0}\Big) + \frac{\boldsymbol{x}\cdot\boldsymbol{y}}{c_0|\boldsymbol{x}|}\frac{\partial}{\partial t}(\cdot)\Big(\boldsymbol{y},t-\frac{|\boldsymbol{x}|}{c_0}\Big) + \ldots\ . \tag{3.51}$$

Since at low Mach number flows an eddy is compact, we can expect that the largest contribution to the sound field is generated by the lowest-order term in the expansion. Thereby, the total source strength

$$\frac{1}{2}\int\limits_\Omega v_{\rm ic}^2\Big(\boldsymbol{y},t-\frac{|\boldsymbol{x}|}{c_0}\Big)\,\mathrm{d}\boldsymbol{y}$$

is constant and therefore its time derivative zero. This can be readily proofed from the inviscid, incompressible momentum equation (see Sec. 1.5)

$$\frac{\partial\boldsymbol{v}_{\rm ic}}{\partial t} + \nabla\left(\frac{p_{\rm ic}}{\rho_0}+\frac{1}{2}(v_{\rm ic})^2\right) = -\boldsymbol{\omega}\times\boldsymbol{v}_{\rm ic} \tag{3.52}$$

by taking the scalar product with $\boldsymbol{v}_{\rm ic}$ and exploring $\nabla\cdot\boldsymbol{v}_{\rm ic}=0$

$$\frac{1}{2}\frac{\partial v_{\rm ic}^2}{\partial t} + \nabla\cdot\left(\boldsymbol{v}_{\rm ic}\left(\frac{p_{\rm ic}}{\rho_0}+\frac{v_{\rm ic}^2}{2}\right)\right) = 0\,. \tag{3.53}$$

Integrating over all space and applying the divergence theorem shows that the second term tends to zero at least as fast as $|\boldsymbol{y}|^{-3}$ as $|\boldsymbol{y}|\to\infty$. So a contribution to the far-field is just provided by the effect of retarted time variation over the source region. However, this leads to a contribution of order $\rho_0\mathrm{Ma}^5 l/|\boldsymbol{x}|$, which is negligible.

Let us now consider the first integral in (3.50) and apply the expansion of retarted time variation according to (3.51). This step results in

$$\begin{aligned}\frac{x_i}{|\boldsymbol{x}|^2}\frac{\partial}{\partial t}\int\limits_{\Omega}(\boldsymbol{\omega}\times\boldsymbol{v}_{\mathrm{ic}})_i\Big(\boldsymbol{y},t-\frac{|\boldsymbol{x}|}{c_0}+\frac{\boldsymbol{x}\cdot\boldsymbol{y}}{c_0|\boldsymbol{x}|}\Big)\,\mathrm{d}\boldsymbol{y} &= \frac{x_i}{|\boldsymbol{x}|^2}\frac{\partial}{\partial t}\int\limits_{\Omega}(\boldsymbol{\omega}\times\boldsymbol{v}_{\mathrm{ic}})_i\Big(\boldsymbol{y},t-\frac{|\boldsymbol{x}|}{c_0}\Big)\,\mathrm{d}\boldsymbol{y} \\ &+ \frac{x_ix_j}{c_0|\boldsymbol{x}|^3}\frac{\partial^2}{\partial t^2}\int\limits_{\Omega}y_i(\boldsymbol{\omega}\times\boldsymbol{v}_{\mathrm{ic}})_i\Big(\boldsymbol{y},t-\frac{|\boldsymbol{x}|}{c_0}\Big)\,\mathrm{d}\boldsymbol{y}\,.\end{aligned} \tag{3.54}$$

Because the first integrand in (3.54) can be expressed via (B.13) as a divergence, it will vanish. Therefore, the leading term in the far-field for the density fluctuation can be computed by

$$\rho'(\boldsymbol{x},t) = \frac{-\rho_0}{4\pi c_0^4|\boldsymbol{x}|^3}\frac{\partial^2}{\partial t^2}\int\limits_{\Omega}(\boldsymbol{x}\cdot\boldsymbol{y})\,(\boldsymbol{x}\cdot\boldsymbol{\omega}\times\boldsymbol{v}_{\mathrm{ic}})\Big(\boldsymbol{y},t-\frac{|\boldsymbol{x}|}{c_0}\Big)\,\mathrm{d}\boldsymbol{y}\,. \tag{3.55}$$

As an example, we consider the radiation by an elliptical vortex [8]. The equation of the ellipse can be written by

$$\sigma = a\left(1+\epsilon\cos\left(2\psi-\frac{1}{2}\Omega t\right)\right)\,. \tag{3.56}$$

Thereby, (σ,ψ) are the polar coordinates, $(x_1,x_2.x_3)$ the Cartesian coordinates, ϵ a small parameter and $\boldsymbol{\omega}=\Omega\boldsymbol{e}_z$ the uniform vortivity. When ϵ is small but finite, the elliptic cross-section of the cylinder spins around its axis with angular velocity $\Omega/4$, and the unsteadiness induced in the flow radiates as sound. Lamb determined the velocity field with in the core given by [15]

$$\boldsymbol{v}_{\mathrm{ic}} = \frac{1}{2}\Omega\sigma\Big(\big(-\sin\psi-\epsilon\sin(\psi-\Omega t/2)\big)\boldsymbol{e}_x+\big(\cos\psi-\epsilon\cos(\psi-\Omega t/2)\big)\boldsymbol{e}_y\Big)\,. \tag{3.57}$$

Hence, inside the vortex core we obtain

$$\boldsymbol{\omega}\times\boldsymbol{v}_{\mathrm{ic}} = \frac{1}{2}\Omega^2\sigma\Big(\big(-\cos\psi-\epsilon\cos(\psi-\Omega t/2)\big)\boldsymbol{e}_x+\big(-\sin\psi-\epsilon\sin(\psi-\Omega t/2)\big)\boldsymbol{e}_y\Big)\,. \tag{3.58}$$

and outside the term $\boldsymbol{\omega}\times\boldsymbol{v}_{\mathrm{ic}}$ is zero. To compute the sound field, we will use (3.55). However, this two-dimensional problem has a source extended in y_3-direction and so the source is certainly not compact. So, the dependency of $|\boldsymbol{x}-\boldsymbol{y}|$ has to be retained in y_3, and we modify (3.55) for our problem as follows

$$\rho'(\boldsymbol{x},t) = -\frac{\rho_0}{4\pi c_0^4}\frac{\partial^2}{\partial t^2}\int\limits_{\Omega}\frac{(x_1y_1+x_2y_2)(\boldsymbol{x}\cdot\boldsymbol{\omega}\times\boldsymbol{v}_{\mathrm{ic}})\Big(\boldsymbol{y},t-\left(R^2+y_3^2\right)^{1/2}/c\Big)}{\left(R^2+y_3^2\right)^{3/2}}\,\mathrm{d}\boldsymbol{y}\,, \tag{3.59}$$

where $R=\left(x_1^2+x_2^2\right)^{1/2}$. Substituting the expression for $\boldsymbol{\omega}\times\boldsymbol{v}_{\mathrm{ic}}$, the integral can be evaluated over σ and ψ

$$\rho'(\boldsymbol{x},t) = -\frac{\rho_0\epsilon\Omega^4a^4R^2}{128c_0^4}\int\limits_{-\infty}^{\infty}\frac{1}{(R^2+y_3^2)^{3/2})}\cos\left(2\theta-\frac{1}{2}\Omega t+\frac{\Omega}{2c_0}\left(R^2+y_3^2\right)^{1/2}\right)\mathrm{d}y_3 \tag{3.60}$$

with $x_1 = R\cos\theta$, $x_2 = R\sin\theta$. For far-field points, for which $\Omega R \gg c_0$, the y_3-integral may be evaluated by changing the integration variable to y_3/R and using the method of stationary phase [8]. Thereby, we obtain

$$\rho'(\boldsymbol{x},t) = -\frac{\rho_0 \epsilon \Omega^{7/2} a^{7/2}}{64 c_0^{7/2}} \left(\frac{\pi a}{R}\right)^{1/2} \cos\left(2\theta + \frac{\pi}{4} - \frac{\Omega}{2}\left(t - \frac{R}{c_0}\right)\right) . \tag{3.61}$$

A general equation for vortex sound has been derived based on Lighthill's equation in [4] and is well known as the *equation of vortex sound*. Thereby, the total enthalpy (see Sec. 1.5)

$$B = \int \frac{\mathrm{d}p}{\rho} + \frac{v^2}{2} \tag{3.62}$$

is used as the independent acoustic variable. The total enthalpy occurs naturally in Crocco's form of the momentum equation (see (1.67)). In an irrotational flow, this equation reduces to

$$\frac{\partial \boldsymbol{v}}{\partial t} = -\nabla B \tag{3.63}$$

and therefore

$$B = -\frac{\partial \phi}{\partial t} \tag{3.64}$$

with $\phi(\boldsymbol{x},t)$ the velocity potential that determines the whole motion in irrotational regions of a fluid. If the mean flow is at rest in the far-field, the acoustic pressure is given by

$$p_{\mathrm{a}} = \rho_0 B = -\rho_0 \frac{\partial \phi}{\partial t} = \rho_0 \frac{\partial \psi_{\mathrm{a}}}{\partial t} . \tag{3.65}$$

To calculate the pressure in term of B elsewhere in the flow, we have to solve (3.62). Using the relation (A.2), we may rewrite (3.62) by also exploiting (1.67) as follows

$$\begin{aligned} \frac{1}{\rho}\frac{\partial p}{\partial t} &= \frac{\partial B}{\partial t} - \boldsymbol{v} \cdot \frac{\partial \boldsymbol{v}}{\partial t} \\ &= \frac{\partial B}{\partial t} - \boldsymbol{v} \cdot \left(-\nabla B - \boldsymbol{\omega} \times \boldsymbol{v} - \nu \nabla \times \boldsymbol{\omega} + \frac{4}{3}\nu \nabla\nabla \cdot \boldsymbol{v}\right) \\ &= \frac{DB}{Dt} + \nu \boldsymbol{v} \cdot \left(\nabla \times \boldsymbol{\omega} - \frac{4}{3}\nu \nabla\nabla \cdot \boldsymbol{v}\right) . \end{aligned} \tag{3.66}$$

Neglecting the viscous term as justified in high Reynolds number flows, we obtain the following general relation between p and B by

$$\frac{1}{\rho}\frac{\partial p}{\partial t} = \frac{DB}{Dt} . \tag{3.67}$$

Now, multiplying Crocco's equation (neglecting the viscous terms) by the density ρ and taking the divergence, results in

$$\nabla \cdot \left(\rho \frac{\partial \boldsymbol{v}}{\partial t}\right) + \nabla \cdot \rho \nabla B = -\nabla \big(\rho\, \boldsymbol{\omega} \times \boldsymbol{v}\big) . \tag{3.68}$$

Using the conservation of mass in the form of

$$\nabla \cdot \boldsymbol{v} = -\frac{1}{\rho}\frac{D\rho}{Dt}\,,$$

we may rewrite the first term in (3.68) as

$$\begin{aligned}
\nabla \cdot \left(\rho \frac{\partial \boldsymbol{v}}{\partial t}\right) &= \nabla \rho \cdot \frac{\partial \boldsymbol{v}}{\partial t} + \rho \frac{\partial}{\partial t}(\nabla \cdot \boldsymbol{v}) && (3.69)\\
&= \nabla \rho \cdot \frac{\partial \boldsymbol{v}}{\partial t} - \rho \frac{\partial}{\partial t}\left(\frac{1}{\rho}\frac{D\rho}{Dt}\right)\\
&= \nabla \rho \cdot \frac{\partial \boldsymbol{v}}{\partial t} - \rho \frac{\partial}{\partial t}\left(\frac{1}{\rho}\frac{\partial\rho}{\partial t}\right) - \frac{\partial \boldsymbol{v}}{\partial t}\cdot \nabla \rho - \rho \boldsymbol{v} \cdot \nabla \left(\frac{1}{\rho}\frac{\partial \rho}{\partial t}\right)\\
&= -\rho \frac{D}{Dt}\left(\frac{1}{\rho}\frac{\partial \rho}{\partial t}\right)\\
&= -\rho \frac{D}{Dt}\left(\frac{1}{\rho c^2}\frac{\partial p}{\partial t}\right)\\
&= -\rho \frac{D}{Dt}\left(\frac{1}{c^2}\frac{DB}{Dt}\right)\,. && (3.70)
\end{aligned}$$

This relation is now substituted into (3.68) to achieve at the *equation of vortex sound*

$$\frac{D}{Dt}\left(\frac{1}{c^2}\frac{DB}{Dt}\right) - \frac{1}{\rho}\nabla \cdot \rho \nabla B = \frac{1}{\rho}\nabla\big(\rho\,\boldsymbol{\omega} \times \boldsymbol{v}\big)\,. \tag{3.71}$$

This PDE clearly states that homentropic flow can generate sound only if moving vorticity is present. The differential operator on the left hand side describes propagation of sound through nonuniform flow.

3.4. Perturbation equations for low Mach number flows

The acoustic/viscous splitting technique for the prediction of flow induced sound was first introduced in [16], and afterwards many groups presented alternative and improved formulations for linear and non linear wave propagation [17, 18, 19, 20]. These formulations are all based on the idea, that the flow field quantities are split into compressible and incompressible parts.

For our derivation, we introduce a generic splitting of physical quantities to the conservation equations. For this purpose, we choose a combination of the two splitting approaches introduced above and define the following

$$\begin{aligned}
p &= \bar{p} + p_{\mathrm{ic}} + p_{\mathrm{c}} = \bar{p} + p_{\mathrm{ic}} + p_{\mathrm{a}} && (3.72)\\
\boldsymbol{v} &= \bar{\boldsymbol{v}} + \boldsymbol{v}_{\mathrm{ic}} + \boldsymbol{v}_{\mathrm{c}} = \bar{\boldsymbol{v}} + \boldsymbol{v}_{\mathrm{ic}} + \boldsymbol{v}_{\mathrm{a}} && (3.73)\\
\rho &= \rho_0 + \rho_1 + \rho_{\mathrm{a}}\,. && (3.74)
\end{aligned}$$

Thereby the field variables are split into mean and fluctuating parts just like in the LEE. In addition the fluctuating field variables are split into acoustic and non-acoustic components. Finally, the density correction ρ_1 is build in as introduced above. This choice is motivated by the following assumptions

- The acoustic field is a fluctuating field.

- The acoustic field is irrotational, i.e. $\nabla \times \boldsymbol{v}_\mathrm{a} = 0$.

- The acoustic field requires compressible media and an incompressible pressure fluctuation is not equivalent to an acoustic pressure fluctuation.

By doing so, we arrive for an incompressible flow at the following perturbation equations[1]

$$\frac{\partial p_\mathrm{a}}{\partial t} + \overline{\boldsymbol{v}} \cdot \nabla p_\mathrm{a} + \rho_0 c_0^2 \nabla \cdot \boldsymbol{v}_\mathrm{a} = -\frac{\partial p_\mathrm{ic}}{\partial t} - \overline{\boldsymbol{v}} \cdot \nabla p_\mathrm{ic} \qquad (3.75)$$

$$\rho_0 \frac{\partial \boldsymbol{v}_\mathrm{a}}{\partial t} + \rho_0 \nabla \left(\overline{\boldsymbol{v}} \cdot \boldsymbol{v}_\mathrm{a} \right) + \nabla p_\mathrm{a} = 0 \qquad (3.76)$$

with spatial constant mean density ρ_0 and speed of sound c_0. This system of partial differential equations is equivalent to the previously published ones [18]. The source term is the substantial derivative of the incompressible flow pressure p_ic. Using the acoustic scalar potential ψ_a and assuming a spacial constant mean density and speed of sound, we may rewrite (3.76) by

$$\nabla \left(\rho_0 \frac{\partial \psi_\mathrm{a}}{\partial t} + \rho_0 \, \overline{\boldsymbol{v}} \cdot \nabla \psi_\mathrm{a} - p_\mathrm{a} \right) = 0 \, , \qquad (3.77)$$

and arrive at

$$p_\mathrm{a} = \rho_0 \frac{\partial \psi_\mathrm{a}}{\partial t} + \rho_0 \, \overline{\boldsymbol{v}} \cdot \nabla \psi_\mathrm{a} \, . \qquad (3.78)$$

Now, we substitute (3.78) into (3.75) and arrive at

$$\frac{1}{c_0^2} \frac{D^2 \psi_\mathrm{a}}{Dt^2} - \Delta \psi_\mathrm{a} = -\frac{1}{\rho_0 c_0^2} \frac{D p_\mathrm{ic}}{Dt} \, ; \quad \frac{D}{Dt} = \frac{\partial}{\partial t} + \overline{\boldsymbol{v}} \cdot \nabla \, . \qquad (3.79)$$

This convective wave equation fully describes acoustic sources generated by incompressible flow structures and its wave propagation through flowing media. In addition, instead of the original unknowns p_a and $\boldsymbol{v}_\mathrm{a}$ we have know just the scalar unknown ψ_a. In accordance to the acoustic perturbation equations (APE), we name this resulting partial differential equation for the acoustic scalar potential as *Perturbed Convective Wave Equation* (PCWE).

Finally, it is of great interest that by neglecting the mean flow $\bar{\boldsymbol{v}}$ in (3.75), we arrive at the linearized conservation equations of acoustics with $\partial p_\mathrm{ic}/\partial t$ as a source term

$$\frac{1}{\rho_0 c_0^2} \frac{\partial p_\mathrm{a}}{\partial t} + \nabla \cdot \boldsymbol{v}_\mathrm{a} = \frac{-1}{\rho_0 c_0^2} \frac{\partial p_\mathrm{ic}}{\partial t} \qquad (3.80)$$

$$\frac{\partial \boldsymbol{v}_\mathrm{a}}{\partial t} + \frac{1}{\rho_0} \nabla p_\mathrm{a} = 0 \, . \qquad (3.81)$$

[1] For a detailed derivation of perturbation equations both for compressible as well as incompressible flows, we refer to [21]

As in the standard acoustic case, we apply $\partial/\partial t$ to (3.80) and $\nabla\cdot$ to (3.81) and subtract the two resulting equations to arrive at

$$\frac{1}{c_0^2}\frac{\partial^2 p_\mathrm{a}}{\partial t^2} - \nabla\cdot\nabla p_\mathrm{a} = \frac{-1}{c_0^2}\frac{\partial^2 p_\mathrm{ic}}{\partial t^2}\,. \tag{3.82}$$

We call this partial differential equation the aeroacoustic wave equation (AWE). Please note, that this equation can also be obtained by starting at Lighthill's inhomogeneous wave equation for incompressible flow, where we can substitute the second spatial derivative of Lighthill's tensor by the Laplacian of the incompressible flow pressure (see (3.22)). Using the decomposition of the fluctuating pressure p'

$$p' = p_\mathrm{ic} + p_\mathrm{a}\,.$$

results again into (3.82).

3.5. Comparison of Different Aeroacoustic Analogies

As a demonstrative example to compare the different acoustic analogies, we choose a cylinder in a cross flow, as displayed in Fig. 3.4. Thereby, the computational grid is just up to the

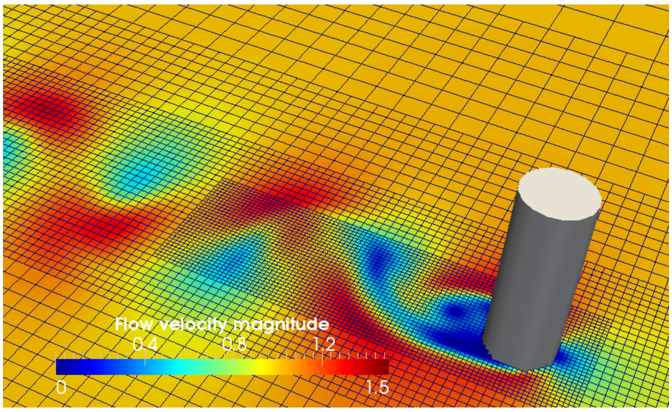

Figure 3.4.: Computational setup for flow computation.

height of the cylinder and together with the boundary conditions (bottom and top as well as span-wise direction symmetry boundary condition), we obtain a pseudo two-dimensional flow field. The diameter of the cylinder D is 1 m resulting with the inflow velocity of 1 m/s and chosen viscosity in a Reynolds number of 250 and Mach number of 0.2. From the flow simulations, we obtain a shedding frequency of 0.2 Hz (Strouhal number of 0.2). The acoustic mesh is chosen different from the flow mesh, and resolves the wavelength of two times the shedding frequency with 10 finite elements of second order. At the outer boundary of the acoustic domain we add a perfectly matched layer to efficiently absorb the outgoing waves. For the acoustic field computation we use the following formulations:

- Lighthill's acoustic analogy with Lighthill's tensor $[\boldsymbol{L}]$ according to (3.12) as source term

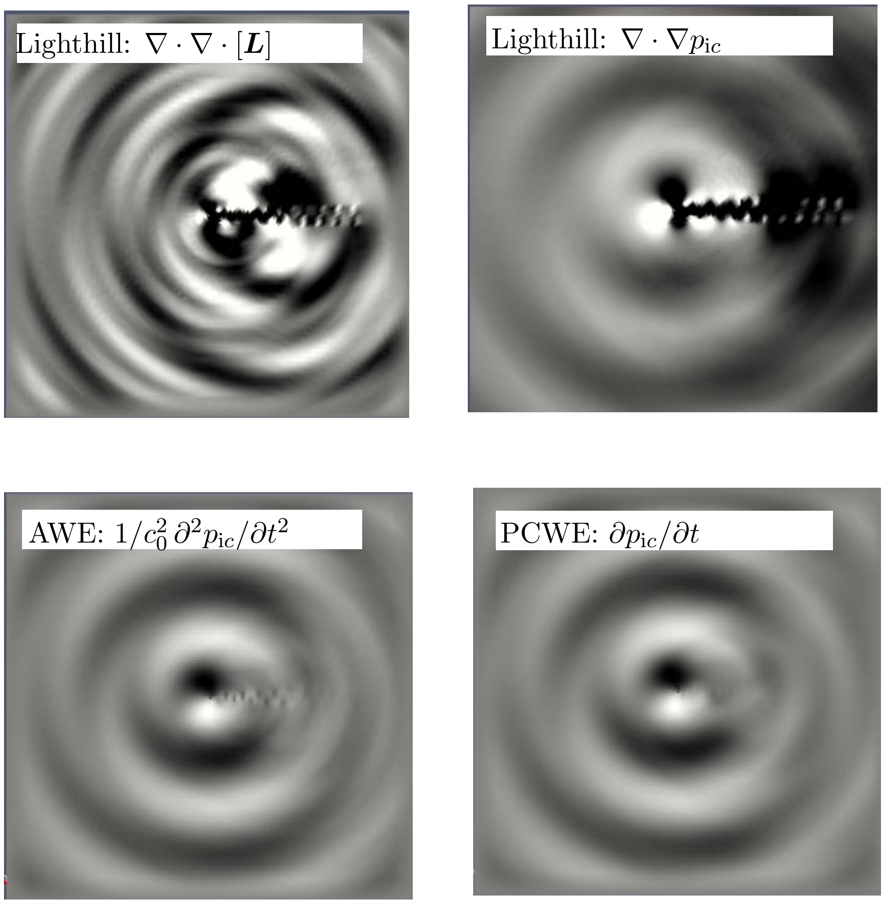

Figure 3.5.: Computed acoustic field with the different formulations.

- Lighthill's acoustic analogy with the Laplacian of the incompressible flow pressure $p_{\rm ic}$ as source term (see (3.22))

- the aeroacoustic wave equation (AWE) according to (3.82)

- Perturbed Convective Wave Equation (PCWE) according to (3.79); for comparison, we set the mean flow velocity $\bar{\boldsymbol{v}}$ to zero.

Figure 3.5 displays the acoustic field for the different formulations. One can clearly see that the acoustic field of PE (for comparison with the other formulations we have neglected the convective terms) meets very well the expected dipole structure and is free from dynamic flow disturbances. Furthermore, the acoustic field of AWE is quite similar and exhibits almost no dynamic flow disturbances. Both computations with Lighthill's analogy show flow disturbances, whereby the formulation with the Laplacian of the incompressible flow pressure as source term shows qualitative better result as the classical formulation based on the incompressible flow velocities.

3.6. Towards general aeroacoustics

In 2003, Goldstein proposed a method to split flow variables $(p, \boldsymbol{u}, ...)$ into a base flow (non-radiating) and a remaining component (acoustic, radiating fluctuations) [22]

$$\star = \tilde{\star} + \star' \,. \tag{3.83}$$

Applying the decomposition to the right hand side of the wave equation (the left hand side of the equation is already treated in this manner during the derivation of the acoustic analogy) leads to

$$\Box p' = \mathbf{RHS}(\tilde{p}, \tilde{\boldsymbol{v}}, \tilde{\rho}, p', \boldsymbol{v}', \rho', ...) \,. \tag{3.84}$$

Now interaction terms can be moved to the differential operator to take, e.g., convection and refraction effects into account, and even nonlinear interactions can be considered. Therefore, we propose the three steps to relax the Mach number constraint imposed by the incompressible flow simulation:

1. Perform a compressible flow simulation, which incorporates two-way coupling of flow and acoustics.
2. Filtering of the flow field, such that we obtain a pure non-radiating field from which we compute the acoustic sources.
3. Solve with an appropriate wave operator for the radiating field

$$\Box p' = \mathbf{RHS}(\tilde{p}, \tilde{\boldsymbol{v}}, \tilde{\rho}, ...) \,. \tag{3.85}$$

The non-radiating base flow is obtained by applying a Helmholtz-Hodge decomposition (see Sec. 1.6). For the computation of the wave propagation, we apply the equation of vortex sound (3.71). Assuming a homogeneous medium, we solve

$$\frac{1}{c_0^2}\frac{D}{Dt^2}B - \nabla \cdot \nabla B = \nabla \cdot (\boldsymbol{\omega} \times \boldsymbol{v}) = \nabla \cdot \boldsymbol{La}(\boldsymbol{v}) \,, \tag{3.86}$$

with a constant isentropic speed of sound c_0 and density ρ_0. The wave operator is of convective type, where the total derivative (material derivative) is defined as $\frac{D}{Dt} = \frac{\partial}{\partial t} \star + (\tilde{\boldsymbol{v}} \cdot \nabla)\star$. The aeroacoustic source term is known as the divergence of the Lamb vector $\boldsymbol{La}$

$$\boldsymbol{La}(\boldsymbol{v}) = (\boldsymbol{\omega} \times \boldsymbol{v}) = (\boldsymbol{\omega} \times \tilde{\boldsymbol{v}}) + \left(\boldsymbol{\omega} \times \boldsymbol{v}'\right) \,. \tag{3.87}$$

The second term in (3.87) is now no more a source term, but an interaction term between the base and radiating flow. In our formulation, the Lamb vector in terms of the non-radiating base flow $\tilde{\boldsymbol{v}}$ reads as follows

$$\boldsymbol{La}(\tilde{\boldsymbol{v}}) = (\boldsymbol{\omega} \times \tilde{\boldsymbol{v}}) \,, \tag{3.88}$$

and we will not consider the second term in (3.87) within the wave operator.

Naturally, the incompressibility condition (regarding the concept of a non-radiating base flow of Goldstein) leads to the Helmholtz-Hodge decomposition of the flow field. We propose an additive splitting on the bounded problem domain Ω of the velocity field $\boldsymbol{v} \in \mathrm{L}^2(\Omega)$ in L^2-orthogonal velocity components

$$\boldsymbol{v} = \boldsymbol{v}_\mathrm{v} + \boldsymbol{v}_\mathrm{c} + \boldsymbol{v}_\mathrm{h} = \nabla \times \boldsymbol{A} + \nabla \phi_\mathrm{c} + \boldsymbol{v}_\mathrm{h}\,, \tag{3.89}$$

where $\boldsymbol{v}_\mathrm{v}$ represents the solenoidal (vortical, non-radiating base flow) part, $\boldsymbol{v}_\mathrm{c}$ the irrotational (radiating) part and $\boldsymbol{v}_\mathrm{h}$ the harmonic (divergence-free and curl-free) part of the flow velocity. The scalar potential ϕ_c is associated with the compressible part and the property $\nabla \times \boldsymbol{v}_\mathrm{c} = 0$, whereas the vector potential $\boldsymbol{A}$ describes the vortical flow (solenoidal part of the velocity field), satisfying $\nabla \cdot \boldsymbol{v}_\mathrm{v} = 0$.

Based on the decomposition (3.89) we apply the curl to (3.89) and obtain the vector valued curl-curl equation with the vorticity $\boldsymbol{\omega} = \nabla \times \boldsymbol{v}$ as forcing

$$\nabla \times \nabla \times \boldsymbol{A} = \nabla \times \boldsymbol{v} = \nabla \times \boldsymbol{v}_\mathrm{v} = \boldsymbol{\omega}\,. \tag{3.90}$$

To obtain a unique solution according to the Helmholtz-Hodge decomposition (see Sec. 1.6), we apply homogeneous boundary condition according to

$$\boldsymbol{n} \times \boldsymbol{A} = \boldsymbol{0}$$

on the boundary Γ. The function space $\mathcal{W}$ for the vector potential

$$\mathcal{W} = \{\boldsymbol{\varphi} \in H(curl, \Omega) | \boldsymbol{n} \times \boldsymbol{\varphi} = \boldsymbol{0} \text{ on } \Gamma_{1,2,3,4}\}$$

requires a finite element discretization with edge elements (Nédélec elements) [23].

We demonstrate the proposed method for the aeroacoustic benchmark case [24], cavity with a lip. The geometrical properties are given in Figs. 3.6 and 3.7, with all spatial dimensions in mm.

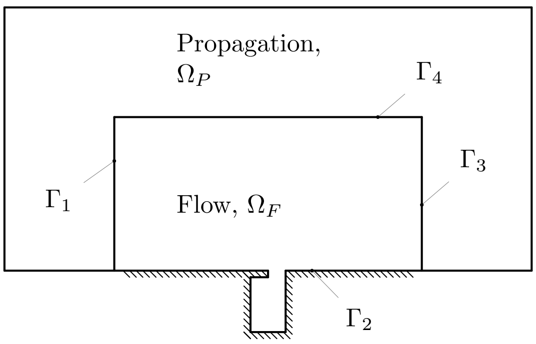

Figure 3.6.: The flow domain Ω_F is a subdomain of the acoustic domain Ω_A, which includes the flow domain as its source domain and the propagation domain Ω_P.

The deep cavity has a reduced cross-section at the orifice (Helmholtz resonator like geometry) and the cavity separates two flat plate configurations. The Helmholtz resonance of the cavity is at about 4.4 kHz. The flow, with a free-stream velocity of $U_\infty = 50\,\mathrm{m/s}$, develops over the plate up to a boundary layer thickness of $\delta = 10\,\mathrm{mm}$. For this configuration we expect the first shear layer mode at about $f_\mathrm{s1} = 1.7\,\mathrm{kHz}$.

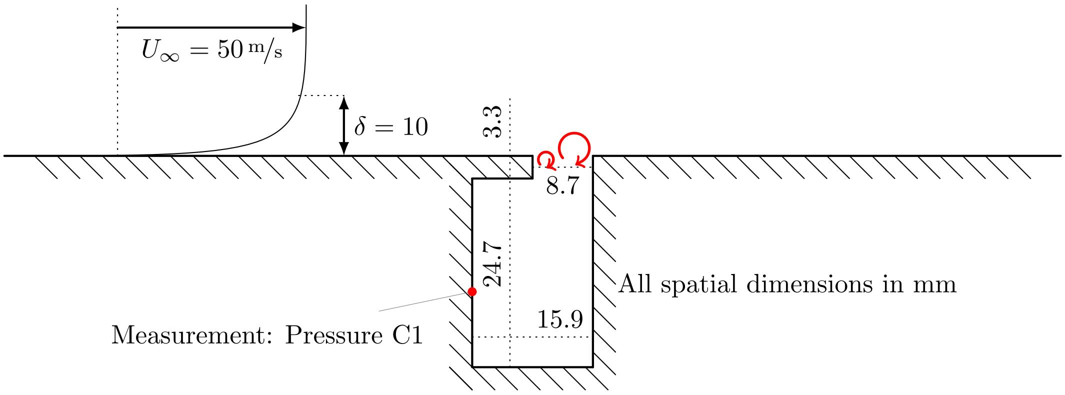

Figure 3.7.: The geometry and the flow configuration of the benchmark problem, cavity with a lip.

The unsteady, compressible, and laminar flow simulation is performed with a prescribed velocity profile $\boldsymbol{v} = \boldsymbol{v}_{\mathrm{in}}$ at the inlet Γ_1, a no slip and no penetration condition $\boldsymbol{v} = \boldsymbol{0}$ for the wall Γ_2, an enforced reference pressure $p = p_{\mathrm{ref}}$ at the outlet Γ_3, and a symmetry condition $\boldsymbol{v} \cdot \boldsymbol{n} = 0$ at the top Γ_4 (see Fig. 3.6). Thereby, the commercial CFD software Ansys-Fluent has been used.

The compressible flow simulation predicts the first shear layer mode at $f_{\mathrm{s1}} = 1.7\,\mathrm{kHz}$ accurately (see Fig. 3.8), which is also confirmed by measurements [25]. An incompressible simulation misinterprets the physics and predicts a shear layer mode of second type [26]. However, Fig. 3.8 also shows a strong peak at 1400 Hz and two minor peaks at around

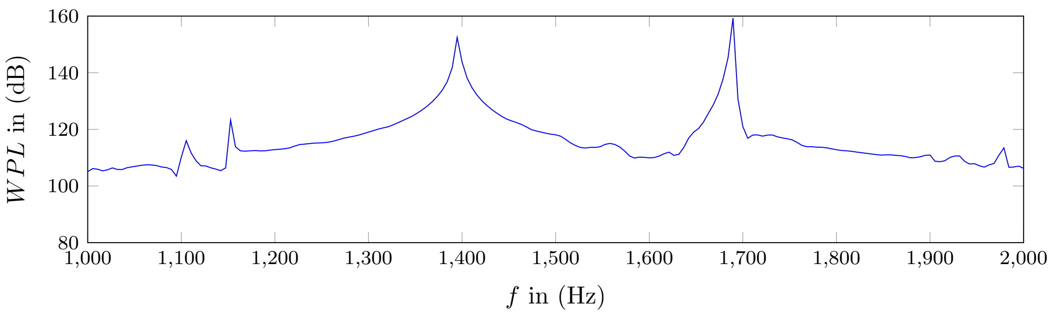

Figure 3.8.: The wall pressure level (WPL) of the compressible flow simulation at the observation point C1 in the cavity. The physical 1^{st} shear layer mode at 1680 Hz and the artificial computational domain resonances are located around 1100Hz. The reference pressure is $20\,\mu\mathrm{Pa}$.

1150 Hz. The artificial computational domain resonances are excited by compressible effects. This shows how important it is to model boundaries with respect to the physical phenomena.

A direct numerical simulation using a commercial flow solver, resolving flow and acoustic, suffers the following main drawbacks. First, transmission boundaries for vortical and wave structures are limited and often inaccurate. In computational fluid dynamics the boundaries are optimized to propagate vortical structures without reflection. But in contrast to that, the radiation condition of waves are not modelled precisely and, as depicted in Fig. 3.9, artificial computational domain resonances superpose the dominant flow field. The state of the art

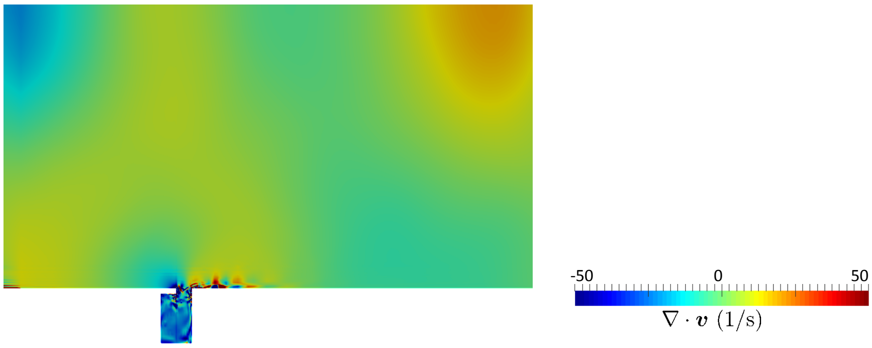

Figure 3.9.: The rate of expansion $\nabla \cdot \boldsymbol{v}$ of the compressible flow simulation at a representative time step. The figure demonstrates the presence of standing waves due to the boundary conditions of the compressible flow simulation.

modelling approach in flow simulation utilizes sponge layer techniques, to damp acoustic waves towards the boundaries, so that they have no influence on the simulation with respect to the wave modelling. Second, low order accuracy of currently available commercial flow simulation tools and the numerical damping dissipates the waves before they are propagated into the far field. Third, a relatively high computational cost to resolve both flow and acoustics exists.

For each time step of the compressible flow computation, we solve (3.90) and obtain the vortical velocity field. As displayed in Fig. 3.10, no singularities at the reentrant corners arise and the overall extracted non-radiating velocity field contains all divergence-free components. This method tackles the compressible phenomena inside the domain Ω_{F} by filtering the domain

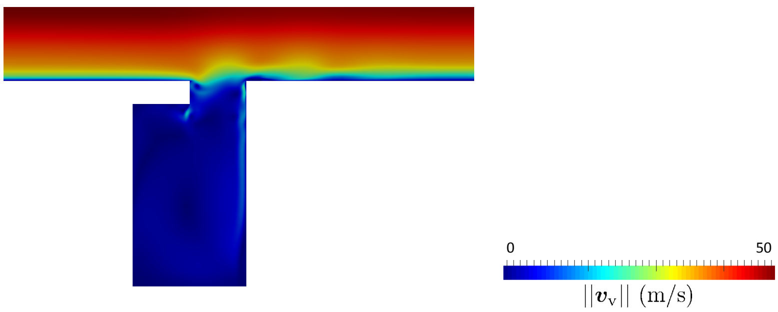

Figure 3.10.: The magnitude of the incompressible component of the flow velocity captures the vortical flow features of the simulation.

artifacts of the compressible flow field such that the computed sources are not corrupted. Figure 3.11 illustrates the shape and nature of the Lamb vector for a characteristic time step. As one can see, there is almost no visible difference in the source term. Therefore, we have performed a Fourier-transform and display in Fig. 3.12 the $x-$ and $y-$ components of the obtained Lamb vectors in the frequency domain at the first shear layer mode (1660 Hz). Now, the difference in the spatial distribution gets visible.

The acoustic simulation utilizes the equation of vortex sound (3.86) to compute the acoustic propagation applying the finite element method by using the in-house solver CFS++ [23].

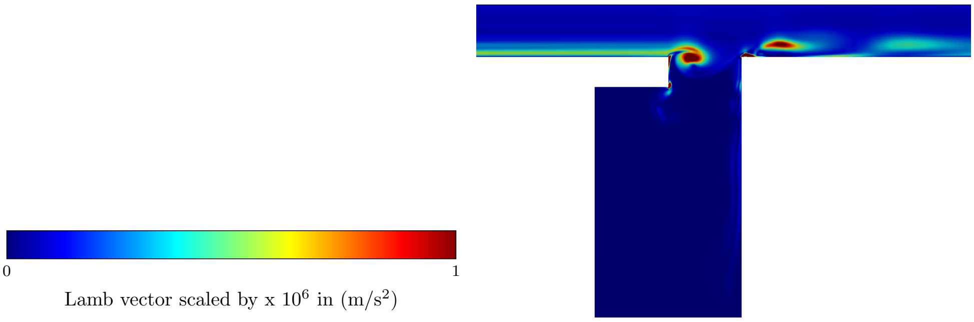

(a) $||\boldsymbol{La}(\tilde{\boldsymbol{v}}) = \boldsymbol{\omega} \times \tilde{\boldsymbol{v}}||$

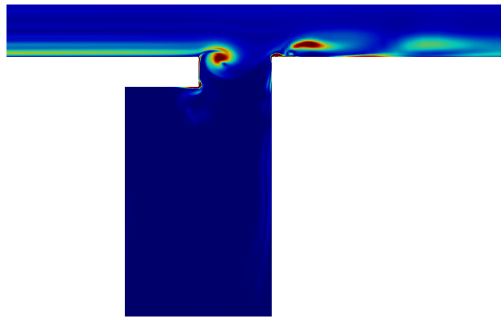

(b) $||\boldsymbol{La}(\boldsymbol{v}) = \boldsymbol{\omega} \times \boldsymbol{v}||$

Figure 3.11.: Comparison of the Lamb vector for the corrected and the non-corrected calculation.

The Doppler effect is included in the convective property of the wave operator, upstreams the wavefronts reduce their wavelength and downstream the distance between the peaks of the wavefronts are enlarged. The finite element domain consists of three sub-domains being independently discretized and connected by non-conforming Nitsche-type Mortar interfaces [23]. The acoustic sources are prescribed in the source domain and a final outer perfectly matching layer ensures accurate free field radiation. Two different aeroacoustic source variants are investigated, the uncorrected Lamb vector $\boldsymbol{La}(\boldsymbol{v})$ (field quantities directly from the flow simulation) and the corrected Lamb vector $\boldsymbol{La}(\tilde{\boldsymbol{v}})$ based on the Helmholtz-Hodge decomposition in the vector potential formulation. Figure 3.13 compares the resulting acoustic fields. As expected, the acoustic field computed by the corrected source term is strongly reduced in amplitude and shows a typically wave propagation, whereas Fig. 3.13a shows perturbations.

In the far-field, the relation (3.65) allows to compute the acoustic pressure and thereby the sound pressure level (SPL) by

$$SPL = 20 \log \left(\frac{\rho_0 \hat{B}}{p_{\mathrm{a,\,ref}}} \right) \tag{3.91}$$

with $\hat{B}$ the Fourier-transformed total enthalpy and $p_{\mathrm{a,\,ref}}$ being $20\,\mu$Pa. The plotted sound spectra of the computations in the far field as shown in Fig.3.14 reveal that the SPL of the non-corrected source terms are much higher. Furthermore, the spectrum obtained by the corrected source term mainly reveals the physical 1^{st} shear layer mode and strongly suppresses all artificial domain resonance modes. Table 3.1 quantifies the obtained results in the far field, where the computed 2D acoustic sound pressure has been scaled according to

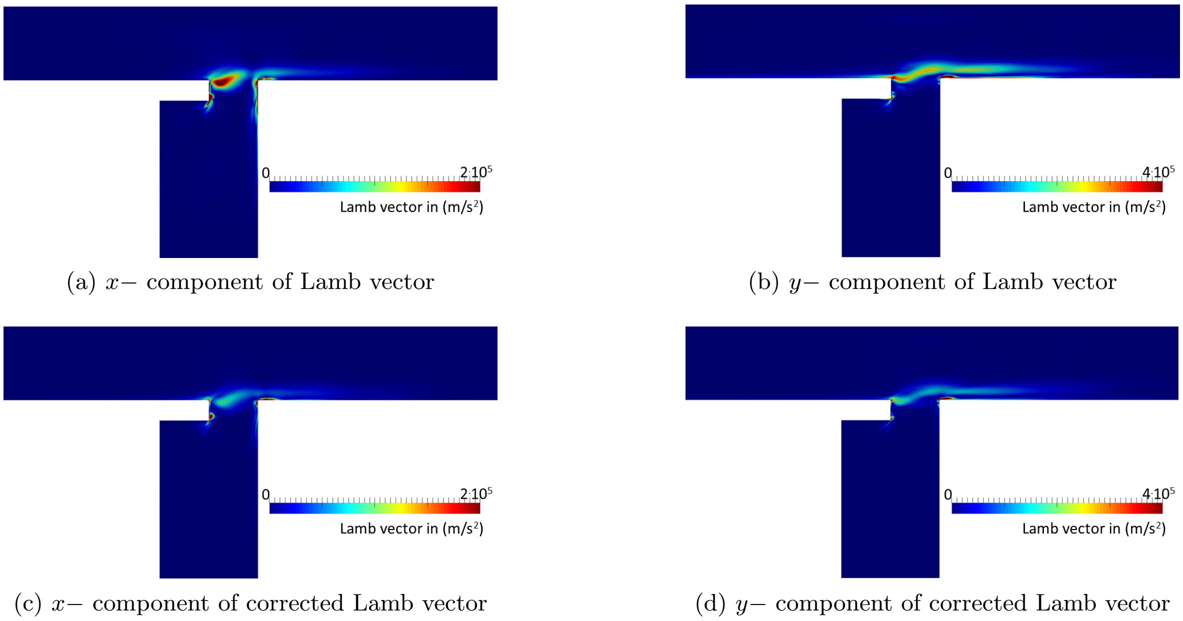

(a) $x-$ component of Lamb vector

(b) $y-$ component of Lamb vector

(c) $x-$ component of corrected Lamb vector

(d) $y-$ component of corrected Lamb vector

Figure 3.12.: Comparison of the Lamb vector for the corrected and the non-corrected calculation at the first shear layer mode.

[27] for comparison with the measured data. Thereby, the computations of the non-corrected source terms overestimate the experimental result by 22 dB. In the case of the corrected source terms, the overestimation is just 4 dB. These results strongly demonstrates the applicability

	f_{s1}/Hz	SPL_{s1}/dB
Experiment	1650	30
Simulation $\boldsymbol{La}(\tilde{\boldsymbol{v}}) = \boldsymbol{\omega} \times \tilde{\boldsymbol{v}}$	1660	34
Simulation $\boldsymbol{La}(\boldsymbol{v}) = \boldsymbol{\omega} \times \boldsymbol{v}$	1660	52

Table 3.1.: Comparison of the pressure outside the cavity

of our Helmholtz-Hodge decomposition approach.

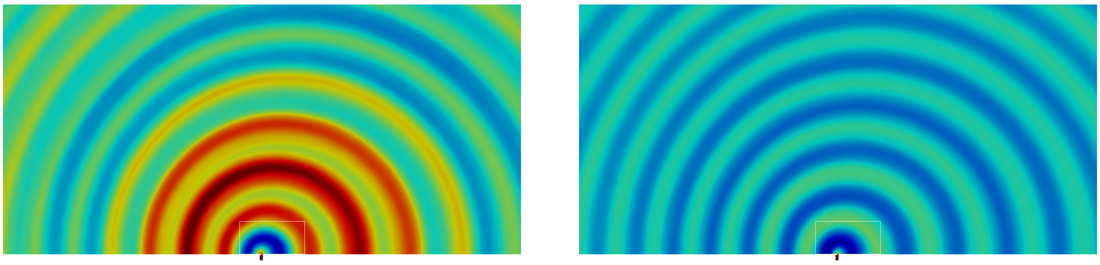

(a) $\boldsymbol{La}(\boldsymbol{v}) = \boldsymbol{\omega} \times \boldsymbol{v}$, not corrected (b) $\boldsymbol{La}(\tilde{\boldsymbol{v}}) = \boldsymbol{\omega} \times \tilde{\boldsymbol{v}}$, corrected

Figure 3.13.: Field of the total enthalpy fluctuation H at a characteristic time. (a) Aeroacoustic sources are due to a compressible flow simulation without applying the correction. (b) Aeroacoustic sources of the wave equation are due to a compressible flow simulation applying the correction.

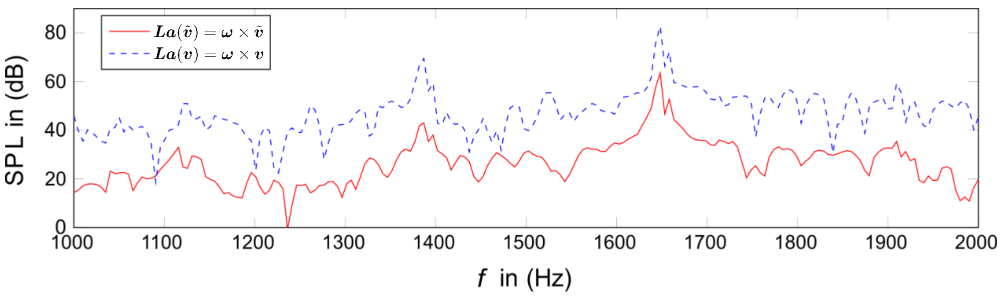

Figure 3.14.: Comparison of the SPL level outside the cavity. The spectrum of the corrected Lamb vector formulation reveals that only the shear layer mode is present.

Appendices

A. Spectial properties

Assuminge a physical quantity ξ to be only a function of η

$$\xi = f(\eta)\,,$$

then the follwing properties holds

$$\nabla \int \frac{\mathrm{d}\eta}{\xi(\eta)} = \frac{1}{\xi(\eta)}\,\nabla\eta \tag{A.1}$$

$$\frac{\partial}{\partial t} \int \frac{\mathrm{d}\eta}{\xi(\eta)} = \frac{1}{\xi(\eta)}\,\frac{\partial\eta}{\partial t}\,. \tag{A.2}$$

This can be easily proofed, by defining $F(\eta)$ as the antiderivative of $f(\eta)$. Then, we have

$$\nabla \int \frac{\mathrm{d}\eta}{\xi(\eta)} = \nabla\big(F(\eta) + const.\big) \tag{A.3}$$

$$= F'\,\nabla\eta = \frac{1}{\xi(\eta)}\,\nabla\eta\,. \tag{A.4}$$

A similar proof is given for (A.2).

B. Vector identities and operations in different coordinate systems

The nabla operator is defined by

$$\nabla = \frac{\partial}{\partial x}\,\boldsymbol{e}_x + \frac{\partial}{\partial y}\,\boldsymbol{e}_y + \frac{\partial}{\partial z}\,\boldsymbol{e}_z \tag{B.1}$$

with the unit vectors $\boldsymbol{e}_x$, $\boldsymbol{e}_y$ and $\boldsymbol{e}_z$. Thereby, the gradient of a scalar function ϕ results in a vector field and computes by

$$\nabla\phi = \begin{pmatrix} \frac{\partial\phi}{\partial x} \\ \frac{\partial\phi}{\partial y} \\ \frac{\partial\phi}{\partial z} \end{pmatrix}. \tag{B.2}$$

The divergence of a vector field results in a scalar value

$$\nabla\cdot\boldsymbol{u} = \frac{\partial u_x}{\partial x} + \frac{\partial u_y}{\partial y} + \frac{\partial u_z}{\partial z}. \tag{B.3}$$

Finally, the curl of a vector $\boldsymbol{u}$ computes as

$$\nabla\times\boldsymbol{u} = \begin{pmatrix} \boldsymbol{e}_x & \boldsymbol{e}_y & \boldsymbol{e}_z \\ \frac{\partial}{\partial x} & \frac{\partial}{\partial y} & \frac{\partial}{\partial z} \\ u_x & u_y & u_z \end{pmatrix} = \begin{pmatrix} \frac{\partial u_z}{\partial y} - \frac{\partial u_y}{\partial z} \\ \frac{\partial u_x}{\partial z} - \frac{\partial u_z}{\partial x} \\ \frac{\partial u_y}{\partial x} - \frac{\partial u_x}{\partial y} \end{pmatrix}. \tag{B.4}$$

In addition, the gradient of a vector $\boldsymbol{u}$ computes by

$$\nabla\boldsymbol{u} = \frac{\partial u_i}{\partial x_j} = \begin{pmatrix} \frac{\partial u_x}{\partial x} & \frac{\partial u_x}{\partial y} & \frac{\partial u_x}{\partial z} \\ \frac{\partial u_y}{\partial x} & \frac{\partial u_y}{\partial y} & \frac{\partial u_y}{\partial z} \\ \frac{\partial u_z}{\partial x} & \frac{\partial u_z}{\partial y} & \frac{\partial u_z}{\partial z} \end{pmatrix}. \tag{B.5}$$

By using the definitions of gradient, divergence, and curl, the following relations hold

$$\nabla(\xi\eta) = \xi\nabla\eta + \eta\nabla\xi \tag{B.6}$$

$$\nabla\cdot(\xi\boldsymbol{u}) = \xi\nabla\cdot\boldsymbol{u} + \boldsymbol{u}\cdot\nabla\xi \tag{B.7}$$

$$\nabla\cdot(\boldsymbol{u}_1\times\boldsymbol{u}_2) = \boldsymbol{u}_2\cdot\nabla\times\boldsymbol{u}_1 - \boldsymbol{u}_1\cdot\nabla\times\boldsymbol{u}_2 \tag{B.8}$$

$$\nabla\times(\xi\boldsymbol{u}) = \xi\nabla\times\boldsymbol{u} - \boldsymbol{u}\times\nabla\xi \tag{B.9}$$

$$\nabla\cdot\nabla\boldsymbol{u} = \nabla(\nabla\cdot\boldsymbol{u}) - \nabla\times(\nabla\times\boldsymbol{u}) \tag{B.10}$$

$$\nabla\times(\boldsymbol{u}\times\boldsymbol{v}) = (\boldsymbol{v}\cdot\nabla)\,\boldsymbol{u} - \boldsymbol{v}\,(\nabla\cdot\boldsymbol{u}) - (\boldsymbol{u}\cdot\nabla)\,\boldsymbol{v} + \boldsymbol{u}\,(\nabla\cdot\boldsymbol{v}) \tag{B.11}$$

$$\xi\,\boldsymbol{u}\cdot\nabla\boldsymbol{u} = \nabla\cdot(\xi\boldsymbol{u}\boldsymbol{u}) - \boldsymbol{u}\nabla\cdot\xi\boldsymbol{u} \tag{B.12}$$

$$\boldsymbol{u}\cdot\nabla\boldsymbol{u} = \nabla\times\boldsymbol{u}\,\times\boldsymbol{u} + \nabla\frac{1}{2}u^2 \tag{B.13}$$

$$\nabla\cdot(\boldsymbol{v}\otimes\boldsymbol{v}) = \boldsymbol{v}\cdot\nabla\boldsymbol{v} + \boldsymbol{v}\nabla\cdot\boldsymbol{v}\,. \tag{B.14}$$

These relations combine the essential differential operators and build up a basis for the description of physical fields.

Furthermore, we introduce the Laplace operator on a scalar

$$\nabla \cdot \nabla \phi = \triangle \phi = (\nabla \cdot \nabla)\phi = \frac{\partial^2 \phi}{\partial x^2} + \frac{\partial^2 \phi}{\partial y^2} + \frac{\partial^2 \phi}{\partial z^2}\,, \tag{B.15}$$

and for a vector $\boldsymbol{u}$

$$(\nabla \cdot \nabla)\boldsymbol{u} = \triangle \boldsymbol{u} = \begin{pmatrix} \frac{\partial^2 u_x}{\partial x^2} + \frac{\partial^2 u_x}{\partial y^2} + \frac{\partial^2 u_x}{\partial z^2} \\ \frac{\partial^2 u_y}{\partial x^2} + \frac{\partial^2 u_y}{\partial y^2} + \frac{\partial^2 u_y}{\partial z^2} \\ \frac{\partial^2 u_z}{\partial x^2} + \frac{\partial^2 u_z}{\partial y^2} + \frac{\partial^2 u_z}{\partial z^2} \end{pmatrix}. \tag{B.16}$$

The following operations always result in zero

$$\nabla \times (\nabla \phi) = 0\,; \quad \nabla \cdot (\nabla \times \nabla \boldsymbol{u}) = 0\,. \tag{B.17}$$

In a next step, we will define the above introduced vector operations in the cylindrical coordinate system. In doing so, we have (see Fig. B.1a)

$$x = r\cos\varphi\,; \quad y = r\sin\varphi\,; \quad z = z\,, \tag{B.18}$$

and therefore

$$\boldsymbol{u} = u_r\boldsymbol{e}_r + u_\varphi\boldsymbol{e}_\varphi + u_z\boldsymbol{e}_z \tag{B.19}$$

$$\boldsymbol{e}_r = \cos\varphi\,\boldsymbol{e}_x + \sin\varphi\,\boldsymbol{e}_y + \boldsymbol{e}_z \tag{B.20}$$

$$\boldsymbol{e}_\varphi = -\sin\varphi\,\boldsymbol{e}_x + \cos\varphi\,\boldsymbol{e}_y \tag{B.21}$$

$$\boldsymbol{e}_z = \boldsymbol{e}_z \tag{B.22}$$

$$\nabla = \boldsymbol{e}_r\frac{\partial}{\partial r} + \frac{\boldsymbol{e}_\varphi}{r}\frac{\partial}{\partial \varphi} + \boldsymbol{e}_z\frac{\partial}{\partial z}\,. \tag{B.23}$$

Therefore, we obtain for the gradient, divergence and curl operations in cylindrical coordi-

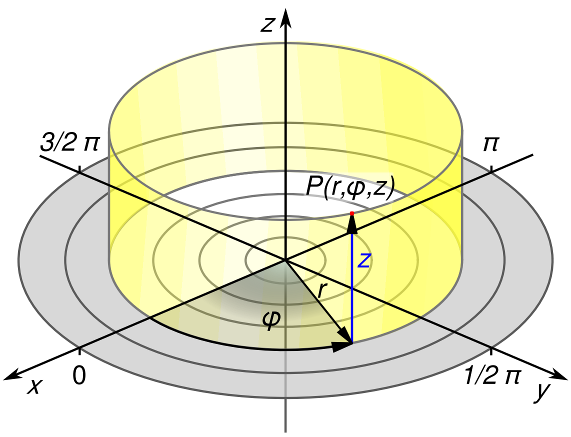

(a) Cylindrical coordinate system.

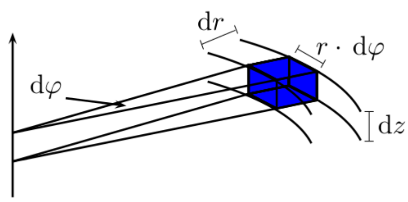

(b) Volume element.

Figure B.1.: Cylindrical coordinate systems.

nates the following formula

$$\nabla\phi = \begin{pmatrix} \frac{\partial\phi}{\partial r} \\ \frac{1}{r}\frac{\partial\phi}{\partial\varphi} \\ \frac{\partial\phi}{\partial z} \end{pmatrix} \tag{B.24}$$

$$\nabla\cdot\boldsymbol{u} = \frac{1}{r}\frac{\partial(ru_r)}{\partial r} + \frac{1}{r}\frac{\partial u_\varphi}{\partial\varphi} + \frac{\partial u_z}{\partial z} \tag{B.25}$$

$$\nabla\times\boldsymbol{u} = \frac{1}{r}\begin{pmatrix} \boldsymbol{e}_r & r\boldsymbol{e}_\varphi & \boldsymbol{e}_z \\ \frac{\partial}{\partial r} & \frac{\partial}{\partial\varphi} & \frac{\partial}{\partial z} \\ u_r & ru_\varphi & u_z \end{pmatrix} = \begin{pmatrix} \frac{1}{r}\left(\frac{\partial u_z}{\partial\varphi} - \frac{\partial(ru_\varphi)}{\partial r}\right) \\ r\frac{\partial u_r}{\partial z} - r\frac{\partial u_z}{\partial r} \\ \frac{1}{r}\left(\frac{\partial(ru_\varphi)}{\partial r} - \frac{\partial u_r}{\partial\varphi}\right) \end{pmatrix}. \tag{B.26}$$

Furthermore, the Laplacian of a scalar function ϕ computes by

$$\nabla\cdot\nabla\phi = \frac{1}{r}\frac{\partial}{\partial r}\left(r\frac{\partial\phi}{\partial r}\right) + \frac{1}{r^2}\frac{\partial^2\phi}{\partial\varphi^2} + \frac{\partial^2\phi}{\partial z^2}. \tag{B.27}$$

Performing an integration in cylindrical coordinates, needs a transformation for the volume element (see Fig. B.1b)

$$\mathrm{d}\Omega = r\,\mathrm{d}r\,\mathrm{d}\varphi\,\mathrm{d}z\,. \tag{B.28}$$

Therefore, we obtain

$$\int_\Omega f(x,y,z)\,\mathrm{d}x\,\mathrm{d}y\,\mathrm{d}z = \int_z\int_r\int_\varphi f(r,\varphi,z)\,r\,\mathrm{d}\varphi\,\mathrm{d}r\,\mathrm{d}z\,. \tag{B.29}$$

Furthermore, we also provide all these relations for spherical coordinates. Thereby, we have

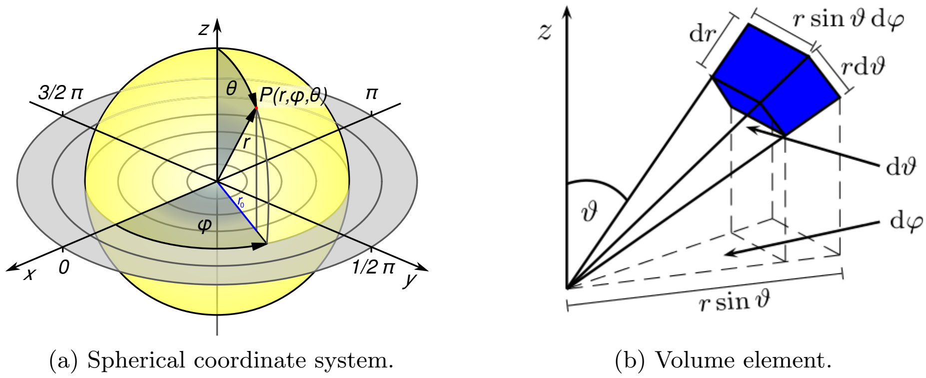

(a) Spherical coordinate system. (b) Volume element.

Figure B.2.: Spherical coordinate systems

the relations (see Fig. B.2a)

$$x = r\cos\varphi\sin\vartheta\,;\quad y = r\sin\varphi\sin\vartheta\,;\quad z = r\cos\vartheta\,, \tag{B.30}$$

and therefore

$$\begin{aligned}
\boldsymbol{u} &= u_r \boldsymbol{e}_r + u_\varphi \boldsymbol{e}_\varphi + u_\vartheta \boldsymbol{e}_\vartheta && \text{(B.31)}\\
\boldsymbol{e}_r &= \sin\vartheta\,(\cos\varphi\,\boldsymbol{e}_x + \sin\varphi\,\boldsymbol{e}_y) + \cos\vartheta \boldsymbol{e}_z && \text{(B.32)}\\
\boldsymbol{e}_\varphi &= -\sin\varphi\,\boldsymbol{e}_x + \cos\varphi\,\boldsymbol{e}_y && \text{(B.33)}\\
\boldsymbol{e}_\vartheta &= \cos\vartheta\,(\cos\varphi\,\boldsymbol{e}_x + \sin\varphi\,\boldsymbol{e}_y) - \sin\vartheta \boldsymbol{e}_z && \text{(B.34)}\\
\boldsymbol{e}_z &= \boldsymbol{e}_z && \text{(B.35)}\\
\nabla &= \boldsymbol{e}_r \frac{\partial}{\partial r} + \frac{\boldsymbol{e}_\vartheta}{r}\frac{\partial}{\partial \vartheta} + \frac{\boldsymbol{e}_\varphi}{r\sin\vartheta}\frac{\partial}{\partial\varphi}\,. && \text{(B.36)}
\end{aligned}$$

Therefore, we obtain for the gradient, divergence and curl operations in spherical coordinates the following formula

$$\nabla\phi = \begin{pmatrix} \frac{\partial\phi}{\partial r} \\ \frac{1}{r}\frac{\partial\phi}{\partial\vartheta} \\ \frac{1}{r\sin\vartheta}\frac{\partial\phi}{\partial\varphi} \end{pmatrix} \tag{B.37}$$

$$\nabla\cdot\boldsymbol{u} = \frac{1}{r^2}\frac{\partial(r^2 u_r)}{\partial r} + \frac{1}{r\sin\vartheta}\frac{\partial\sin\vartheta u_\vartheta}{\partial\vartheta} + \frac{1}{r\sin\vartheta}\frac{\partial u_\varphi}{\partial\varphi} \tag{B.38}$$

$$\nabla\times\boldsymbol{u} = \frac{1}{r^2\sin\vartheta}\begin{pmatrix} \boldsymbol{e}_r & r\boldsymbol{e}_\vartheta & r\sin\vartheta\,\boldsymbol{e}_\varphi \\ \frac{\partial}{\partial r} & \frac{\partial}{\partial\vartheta} & \frac{\partial}{\partial\varphi} \\ u_r & ru_\vartheta & r\sin\vartheta u_\varphi \end{pmatrix} = \begin{pmatrix} \frac{1}{r^2\sin\vartheta}\left(\frac{\partial(r\sin\vartheta\,u_\varphi)}{\partial\vartheta} - \frac{\partial(ru_\vartheta)}{\partial\varphi}\right) \\ r\left(\frac{\partial u_r}{\partial\varphi} - \frac{\partial(r\sin\vartheta\,u_\varphi)}{\partial r}\right) \\ r\sin\vartheta\left(\frac{\partial(ru_\vartheta)}{\partial r} - \frac{\partial u_r}{\partial\vartheta}\right) \end{pmatrix} \tag{B.39}$$

Furthermore, the Laplacian of a scalar function ϕ computes by

$$\nabla\cdot\nabla\phi = \triangle\phi = \frac{1}{r^2}\frac{\partial}{\partial r}\left(r^2\frac{\partial\phi}{\partial r}\right) + \frac{1}{r^2\sin\vartheta}\frac{\partial}{\partial\vartheta}\left(\sin\vartheta\frac{\partial\phi}{\partial\vartheta}\right) + \frac{1}{r^2\sin^2\vartheta}\frac{\partial^2\phi}{\partial\varphi^2}\,. \tag{B.40}$$

Performing an integration in the spherical coordinate system, the volume element transforms (see Fig. B.2b)

$$\mathrm{d}\Omega = (r\,\mathrm{d}\vartheta)\,(\,\mathrm{d}r)\,(r\sin\vartheta\,\mathrm{d}\varphi) = r^2\sin\vartheta\;\mathrm{d}r\,\mathrm{d}\varphi\,\mathrm{d}\vartheta\,, \tag{B.41}$$

and therefore the integral

$$\int\limits_\Omega f(x,y,z)\,\mathrm{d}x\,\mathrm{d}y\,\mathrm{d}z = \int\limits_r\int\limits_\varphi\int\limits_\vartheta f(r,\varphi,\vartheta)\,r^2\sin\vartheta\,\mathrm{d}\vartheta\,\mathrm{d}\varphi\,\mathrm{d}r\,. \tag{B.42}$$

Important is also the Helmholtz decomposition, which states that each vector field $\boldsymbol{v}$ (e.g., the flow velocity) can be decomposed in an irrotational field described by the gradient of a scalar potential ϕ and in a solenoidal field $\boldsymbol{u}$ described by a vector potential $\boldsymbol{A}$

$$\boldsymbol{v} = \nabla\times\boldsymbol{A} + \nabla\phi\,. \tag{B.43}$$

Furthermore, the integral theorem of Gauss (also known as the divergence theorem) transforms a volume integral to a surface integral

$$\int\limits_\Omega \nabla\cdot u\;\mathrm{d}\boldsymbol{x} = \oint\limits_{\Gamma(\Omega)} \boldsymbol{u}\cdot\,\mathrm{d}\boldsymbol{s} = \oint\limits_{\Gamma(\Omega)} \boldsymbol{u}\cdot\boldsymbol{n}\;\mathrm{d}s\,. \tag{B.44}$$

The theorem of Stokes transforms a surface integral to a line integral

$$\int_{\Gamma} \nabla \times \boldsymbol{u} \cdot \mathrm{d}\boldsymbol{s} = \oint_{C(\Gamma)} \boldsymbol{u} \cdot \mathrm{d}\boldsymbol{l}\,. \tag{B.45}$$

Finally, we want to define the integration by parts and its extension to Green's integral formula. Let $\Omega \subset \mathcal{R}^n$, $n = 2, 3$ be a domain with smooth boundary Γ. Then, for any $u, v \in H^1(\Omega)$ the following relation holds (definition of functional spaces, e.g., H^1 see [28])

$$\int_{\Omega} \frac{\partial u}{\partial x_i} v \, d\Omega = \int_{\Gamma} uv \, \boldsymbol{n} \cdot \boldsymbol{e}_i \, ds - \int_{\Omega} u \frac{\partial v}{\partial x_i} \, d\Omega\,. \tag{B.46}$$

In (B.46) $\boldsymbol{n}$ denotes the outer normal of the considered domain Ω with boundary Γ. By a multiple application of (B.46), we arrive at **Green's formula**

$$\int_{\Omega} \triangle u \, v \, d\Omega = \int_{\Gamma} \frac{\partial u}{\partial \boldsymbol{n}} v \, ds - \int_{\Omega} \nabla u \cdot \nabla v \, d\Omega \tag{B.47}$$

for all $u \in H^2(\Omega)$ and $v \in H^1(\Omega)$.

C. Tensors and Index Notation

Tensors are simply speaking a linear mapping. E.g., a second order tensor $[\boldsymbol{A}]$ is a linear mapping that associates a given vector $\boldsymbol{u}$ with a second vector $\boldsymbol{v}$ by

$$\boldsymbol{v} = [\boldsymbol{S}]\boldsymbol{u}\,.$$

The term linear in the above relation implies that given two arbitrary vectors $\boldsymbol{u}$ and $\boldsymbol{v}$ and two arbitrary scalars α, β, then the following relation holds

$$[\boldsymbol{S}]\,(\alpha\boldsymbol{u} + \beta\boldsymbol{v}) = \alpha[\boldsymbol{S}]\boldsymbol{u} + \beta[\boldsymbol{S}]\boldsymbol{v}\,.$$

The extension to tensors of higher rank is straight forward. E.g., Hook's law maps the mechanical strain tensor $[\boldsymbol{S}]$ by the 4th order elasticity tensor $[\boldsymbol{c}]$ to the mechanical stress tensor $[\boldsymbol{\sigma}]$

$$[\boldsymbol{\sigma}] = [\boldsymbol{c}]\,[\boldsymbol{S}]\,.$$

Now, index notation is a powerful tool to write complex operations of vectors and tensors in a more readable way. However, there are times when the more conventional vector notation is more useful. It is therefore important to be able to easily convert back and forth between the two notations. Table C.1 describes our notation[1]. An index can be a *free* or a *dummy*

Table C.1.: Vector and index notation.

	Vector	Index	Rank
Scalar	ξ	ξ	0
Vector	$\boldsymbol{u}$	u_i	1
Tensor (2nd order)	$[\boldsymbol{A}]$	A_{ij}	2
Tensor (3nd order)	$[\boldsymbol{B}]$	B_{ijk}	3
Tensor (4nd order)	$[\boldsymbol{C}]$	C_{ijkl}	4

index. For free indices, the following rules are defined:

- The number of free indices equals the rank as displayed in Tab. C.1. Thereby, a scalar is a tensor with rank 0, and a vector is a tensor of rank 1. Tensors may assume a rank of any integer greater than or equal to zero. Please note that it is just allowed to sum together tensors with equal rank.

[1] Our notation does not differ between tensors of different orders.

- A free index appears once and only once within each additive term and remains within the expression after the operation has been performed, e.g.

$$a_i = \epsilon_{ijk} b_j c_k + A_{ij} d_j \,. \tag{C.1}$$

- The same letter must be used for the free index in every additive term.

- The first free index in a term corresponds to the row, and the second corresponds to the column. Thus, a vector (which has only one free index) is written as a column of three rows

$$\boldsymbol{u} = u_i = \begin{pmatrix} u_1 \\ u_2 \\ u_3 \end{pmatrix}$$

  and a second order tensor as

$$[\boldsymbol{A}] = A_{ij} = \begin{pmatrix} A_{11} & A_{12} & A_{13} \\ A_{21} & A_{22} & A_{23} \\ A_{31} & A_{32} & A_{33} \end{pmatrix}$$

A dummy index defines an index, which does not appear in the final expression any more. The rules are as follows:

- A dummy index appears twice within an additive term of an expression. For the example above (see (C.1)), the dummy indices are j and k.

- A dummy index implies a summation over the range of the index, e.g.

$$a_{ii} = a_{11} + a_{22} + a_{33} \,.$$

For many operations we use the Kronecker delta (2nd order tensor)

$$\delta_{ij} = \begin{pmatrix} 1 & 0 & 0 \\ 0 & 1 & 0 \\ 0 & 0 & 1 \end{pmatrix} \tag{C.2}$$

and the alternating unit tensor (3rd order tensor)

$$\epsilon_{ijk} = \begin{cases} 1 & \text{if } ijk = 123,\ 231 \text{ or } 312 \\ 0 & \text{if any two indices are the same} \\ -1 & \text{if } ijk = 132,\ 213 \text{ or } 321 \end{cases} \tag{C.3}$$

Thereby, the following relation can be explored

$$\epsilon_{ijk} = \frac{1}{2}(i-j)\,(j-k)\,(k-i)\,.$$

With these definitions, we may write vector and tensor operations using index notation. Here, we list the most useful ones:

- Scalar product of two vectors

$$\boldsymbol{a} \cdot \boldsymbol{b} = c \ \rightarrow \ a_i b_i = c \tag{C.4}$$

- Vector product of two vectors

$$\boldsymbol{a} \times \boldsymbol{b} = \boldsymbol{c} \ \rightarrow \ \epsilon_{ijk} a_j b_k = c_i \tag{C.5}$$

- Gradient of a scalar

$$\nabla \phi = \boldsymbol{u} \ \rightarrow \ \frac{\partial \phi}{\partial x_i} = u_i \tag{C.6}$$

- Gradient of a vector

$$\nabla \boldsymbol{a} = \begin{pmatrix} \frac{\partial a_1}{\partial x_1} & \frac{\partial a_2}{\partial x_1} & \frac{\partial a_3}{\partial x_1} \\ \frac{\partial a_1}{\partial x_2} & \frac{\partial a_2}{\partial x_2} & \frac{\partial a_3}{\partial x_2} \\ \frac{\partial a_1}{\partial x_3} & \frac{\partial a_2}{\partial x_3} & \frac{\partial a_3}{\partial x_3} \end{pmatrix} \ \rightarrow \ \frac{\partial a_i}{\partial x_j} \tag{C.7}$$

- Gradient of a second order tensor

$$\nabla [\boldsymbol{A}] = \frac{\partial [\boldsymbol{A}]}{\partial \boldsymbol{x}} = \sum_{i,j,k=1}^{3} \frac{\partial A_{ij}}{\partial x_k} \boldsymbol{e}_i \otimes \boldsymbol{e}_j \otimes \boldsymbol{e}_k \tag{C.8}$$

- Divergence of a vector

$$\nabla \cdot \boldsymbol{a} = b \ \rightarrow \ \frac{\partial a_i}{\partial x_i} = b \tag{C.9}$$

- Divergence of a second order tensor

$$\nabla \cdot [\boldsymbol{A}] = \sum_{i,j=1}^{3} \frac{\partial A_{ij}}{\partial x_j} \boldsymbol{e}_i \tag{C.10}$$

- Curl of a vector

$$\nabla \times \boldsymbol{a} = \boldsymbol{b} \ \rightarrow \ \epsilon_{ijk} \frac{\partial a_k}{\partial x_j} = b_i \tag{C.11}$$

- Double product or double contraction of two second order tensors

$$[\boldsymbol{A}] : [\boldsymbol{B}] = c \ \rightarrow \ A_{ij} B_{ij} = c \tag{C.12}$$

  or of a fourth order tensor with a second order tensors, e.g. Hooks law

$$[\boldsymbol{\sigma}] = [\boldsymbol{c}] : [\boldsymbol{S}] \tag{C.13}$$

- Dyadic or tensor product

$$\boldsymbol{a} \otimes \boldsymbol{b} = [\boldsymbol{C}] \ \rightarrow \ a_i b_j = C_{ij} \tag{C.14}$$

$$[\boldsymbol{A}] \otimes \boldsymbol{b} = [\boldsymbol{C}] \ \rightarrow \ A_{ij} b_k = C_{ijk} \tag{C.15}$$

$$[\boldsymbol{A}] \otimes [\boldsymbol{B}] = [\boldsymbol{D}] \ \rightarrow \ A_{ij} B_{kl} = D_{ijkl} \tag{C.16}$$

- Product of two tensors

$$[\boldsymbol{A}][\boldsymbol{B}] = [\boldsymbol{C}] \;\rightarrow\; A_{ij}B_{jk} = C_{ik} \tag{C.17}$$

  Note that only the inner index is to be summed.

- Trace of a tensor

$$\mathrm{tr}\,([\boldsymbol{A}]) = b \;\rightarrow\; A_{ii} = b \tag{C.18}$$

D. Generalized Functions

In reality, dissipative effects cause discontinuities to be smooth and real signals to decay for $t \to \infty$. However, in idealized models, we often cannot describe the properties by ordinary functions. Two simple examples: (1) a point source is zero everywhere except in one point, where it is infinitely large; (2) the function $\sin \omega t$ is not a decaying function, which in the classical sense cannot be Fourier-transformed.

So, in general we can state that our mathematical apparatus for functions is too restricted and so it makes sense to extend it to so called *generalized functions*.

D.1. Basics

Definition (Lebesgue). A function $f(\boldsymbol{x})$ is locally integrable in R^n if

$$\int\limits_{\Omega} |f(\boldsymbol{x})| \,\mathrm{d}\boldsymbol{x}$$

exists for every bounded volume Ω in R^n. A function $f(\boldsymbol{x})$ is locally integrable on a hypersurface in R^n if

$$\int\limits_{\Gamma} |f(\boldsymbol{x})| \,\mathrm{d}\boldsymbol{s}$$

exists for every bounded region Γ in R^n.

Definition. The support denoted by *supp* of a function $f(\boldsymbol{x})$ is the closure of the set of all points $\boldsymbol{x}$ such that $f(\boldsymbol{x}) \neq 0$. If $\mathit{supp}\, f$ is a bounded set, then f is said to have compact support (see Fig. D.1a).

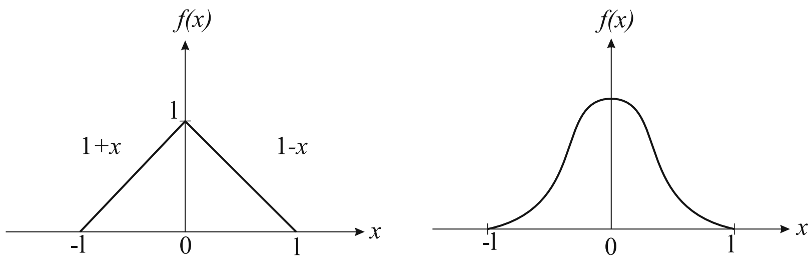

(a) Function with compact support. (b) Infinitely differentiable functions with compact support.

Figure D.1.: Special properties of functions.

We know that the delta function $\delta(\boldsymbol{x})$ becomes meaningful, if it is first multiplied by a sufficient smooth auxiliary function and then integrated over the entire space, e.g. in the one-dimensional space

$$\int_{-\infty}^{\infty} \delta(x)\phi(x) \; \mathrm{d}x = \phi(0) \, .$$

Therefore, we will follow the **Schwartz-Sobolev** approach, which includes the following steps: (1) operators on ordinary functions such as differentiation and Fourier transform are extended by first writing these operators as *functionals* for ordinary functions; (2) extend it for all generalized functions, e.g., also for the delta function, etc. In doing so, we first define the space D of all test functions $\phi(x)$, which are infinitely differentiable functions with bounded support. The prototype of such a test function belonging to D is

$$\phi(x) = \begin{cases} e^{-\frac{a^2}{a^2-r^2}} & r < a \\ 0 & r > a \end{cases}$$

as displayed in Fig. D.1b (for details see [29]). A linear functional of f on the space D is an operation by which we assign to every test function $\phi(x)$ a real (complex) number - a functional - denoted by

$$< f, \phi > = \int_{-\infty}^{\infty} f \, \phi \; \mathrm{d}x$$

such that

$$< f, c_1\phi_1 + c_2\phi_2 > = c_1 < f, \phi_1 > + c_2 < f, \phi_2 >$$

for arbitrary test functions ϕ_1, ϕ_2 and real numbers c_1. c_2.

Definition. A linear functional on D is *continuous*, iff the sequence of numbers $< f, \phi_m >$ converges to $< f, \phi >$, when the sequence of test functions $\{\phi_m\}$ converges to the test function ϕ. Thus

$$\lim_{m\to\infty} < f, \phi_m > = < f, \lim_{m\to\infty} \phi_m > \; .$$

Definition. A continuous linear functional on the space D of test functions is called a *distribution.*

So, every locally integrable function $f(x)$ generates a distribution through the formula

$$< f, \phi > = \int_{R^n} f(x)\phi(x) \; \mathrm{d}x \, ,$$

and is denoted a *regular* distribution. All other distributions are called *singular*, e.g. a distribution with the singular function δ. The space of all distributions on D is denoted by D', which is larger as D and which is also a linear space (see Fig. D.2). It forms a generalization of the class of locally integrable functions because it contains functions such as $\delta(x)$ that are not locally integrable. For this reason distributions are also called *generalized functions.* We shall use the term *distribution* and *generalized functions* interchangeably.

Example: The Heaviside distribution in R^n is

$$< H_\Omega, \phi > = \int_\Omega \phi(x) \; \mathrm{d}x \;\; \text{where } H_\Omega(x) = \begin{cases} 1, & x \in \Omega \\ 0 & x \notin \Omega \end{cases}$$

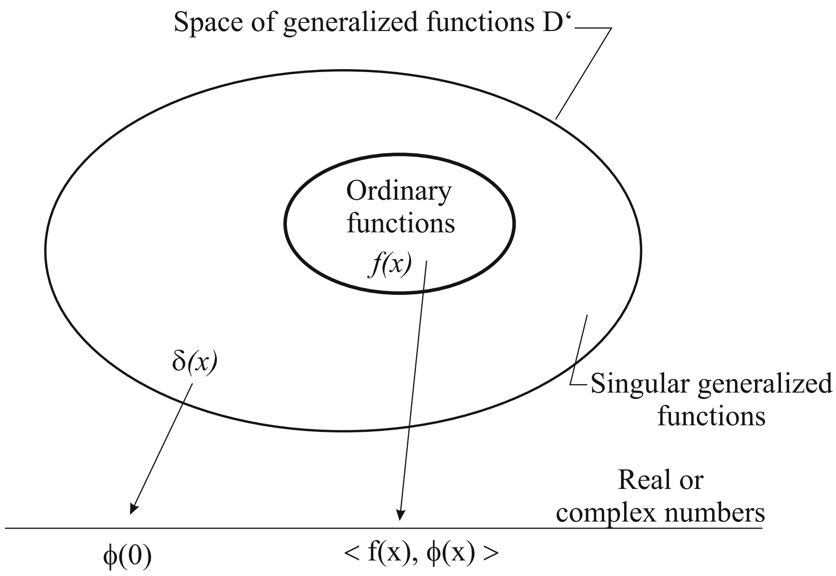

Figure D.2.: Generalized functions are continuous linear functionals on space D of test functions.

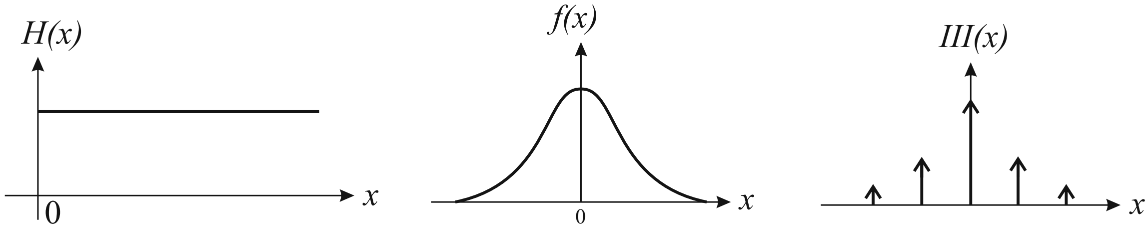

(a) Heaviside functions. (b) Sampling function with compact support.

Figure D.3.: Special functions.

For R^1 it becomes (see function in Fig. D.3a)

$$< H, \phi > = \int\limits_0^\infty \phi(x)\ \mathrm{d}x\,.$$

Since $H(x)$ is a piecewise continuous function, this is a regular distribution.

Example: An infinite sequence of delta functions is described by

$$III(x) = \sum_{n=-\infty}^{\infty} \delta(x-n)\,.$$

This is called the sampling or replicating function (see Fig. D.3b) because it gives information about the function $f(x)$ at $x = n$

$$< III(x), f(x) > = \sum_{n=-\infty}^{\infty} f(x)\delta(x-n)\,.$$

Since the delta function is not locally integrable, this distribution is a singular distribution.

D.2. Special properties

In the following, we will derive important properties of generalized functions.

D.2.1. Shift operator

Let $f(x)$ be an ordinary function, which we shift by a value of h. Then, the linear functional on the space of test functions computes as

$$< f(x+h), \phi(x) > = \int_{-\infty}^{\infty} f(x+h)\phi(x)\ \mathrm{d}x = \int_{-\infty}^{\infty} f(x)\phi(x-h)\ \mathrm{d}x\,.$$

This rule can now be used for all generalized functions in D', e.g. for the delta function $\delta(x)$

$$< \delta(x+h), \phi(x) > = \int_{-\infty}^{\infty} \delta(x+h)\phi(x)\ \mathrm{d}x = \int_{-\infty}^{\infty} \delta(x)\phi(x-h)\ \mathrm{d}x = \phi(-h)\,.$$

D.2.2. Linear change of variables

Let $< f, \phi >$ be a regular distribution generated by the function $f(x)$ that is locally integrable in R^n. Now, let $x = Ay - a$, where A is a $n \times n$ matrix with $det(A) \neq 0$ and a a constant vector, be a non-singular linear transformation of the space R^n onto itself. Then we have

$$\begin{aligned} < f(Ay-a), \phi(y) > &= \int_{R^n} f(Ay-a)\phi(y)\,\mathrm{d}y \\ &= \frac{1}{|det(A)|} \int_{R^n} f(x)\phi\left(A^{-1}(x+a)\right)\ \mathrm{d}x \\ &= \frac{1}{|det(A)|}\ < f(x), \phi\left(A^{-1}(x+a)\right) >\,, \end{aligned} \tag{D.1}$$

where A^{-1} is the inverse of the matrix A. In special, we have for the delta function

$$< \delta(ax), \phi(x) > = \frac{1}{|a|}\ < \delta(x), \phi(x) >\ . \tag{D.2}$$

So we can simply write $\delta(ax) = (1/|a|)\delta(x)$.

D.2.3. Derivatives of generalized functions

Let $f(x)$ be an ordinary function out of D, e.g. $f \in C^1$. Then we can write

$$< f'(x), \phi(x) > = \int_{-\infty}^{\infty} f'(x)\phi(x)\ \mathrm{d}x\,.$$

Performing an integration by parts results in

$$< f'(x), \phi(x) > = \underbrace{f(x)\phi(x)|_{-\infty}^{\infty}}_{=0 \text{ due to local support of } \phi(x)} - \int_{-\infty}^{\infty} f(x)\,\phi'(x)\ \mathrm{d}x\,. \tag{D.3}$$

This result can be extended to define the derivatives of all generalized functions in D'

$$< f^n(x), \phi(x) >= (-1)^n \ < f(x), \phi^n(x) > , \tag{D.4}$$

which states that generalized functions have derivatives of all orders.

Example: The derivative of the delta function $\delta'(x)$ has the property

$$< \delta'(x), \phi(x) >= - \int\limits_{-\infty}^{\infty} \delta(x)\phi'(x) \ \mathrm{d}x = -\phi'(0) \, . \tag{D.5}$$

Example: The derivative of the Heaviside function computes as

$$\begin{aligned} < H'(x), \phi(x) > \quad &= \quad \int\limits_{-\infty}^{\infty} H'(x)\phi(x) \ \mathrm{d}x \\ &= \quad - < H(x), \phi'(x) > \\ &= \quad \int\limits_{0}^{\infty} \phi'(x) \ \mathrm{d}x = - \left. \phi(x) \right|_0^\infty \\ &= \quad \phi(0) = < \delta(x), \phi(x) > \ . \end{aligned} \tag{D.6}$$

D.2.4. Multidimensional delta function

In multidimensional, $\delta(\boldsymbol{x})$ has a simple interpretation by

$$< \delta(\boldsymbol{x}), \phi(\boldsymbol{x}) >= \int\limits_{-\infty}^{\infty} \delta(\boldsymbol{x})\phi(\boldsymbol{x}) \ \mathrm{d}\boldsymbol{x} = \phi(\boldsymbol{0}) \, .$$

Thus,

$$\delta(\boldsymbol{x}) = \delta(x_1)\, \delta(x_2)\, \delta(x_3) ... \delta(x_n) \, ,$$

where $\boldsymbol{x} = (x_1, x_2, .., x_n)$. Of great interest are applications of $\delta(f)$ and $\delta'(f)$, where $f = 0$ is a surface in the three-dimensional space as displayed in Fig. D.4. Then, for a test function $\phi(\boldsymbol{x})$ defined in Ω and on Γ we have the following properties

$$\int\limits_{-\infty}^{\infty} \phi(\boldsymbol{x}) \nabla H(f) \ \mathrm{d}\boldsymbol{x} \quad = \quad \oint\limits_{\Gamma} \phi(\boldsymbol{x}) \boldsymbol{n} \, \mathrm{d}s = \oint\limits_{\Gamma} \phi(\boldsymbol{x}) \, \mathrm{d}\boldsymbol{s} \tag{D.7}$$

$$\int\limits_{-\infty}^{\infty} \phi(\boldsymbol{x}) \frac{\partial H(f)}{\partial x_j} \ \mathrm{d}\boldsymbol{x} \quad = \quad \oint\limits_{\Gamma} \phi(\boldsymbol{x}) n_j \, \mathrm{d}s = \oint\limits_{\Gamma} \phi(\boldsymbol{x}) \, \mathrm{d}s_j \, . \tag{D.8}$$

In the following, we want to proof these properties. First of all, we may write by the chain rule of differentiation

$$\frac{\partial H(f)}{\partial x_j} = \underbrace{\frac{\partial H(f)}{\partial f}}_{=\delta(f)} \frac{\partial f}{\partial x_j} \ \Rightarrow \ \nabla H(f) = \delta(f) \, \nabla f \, .$$

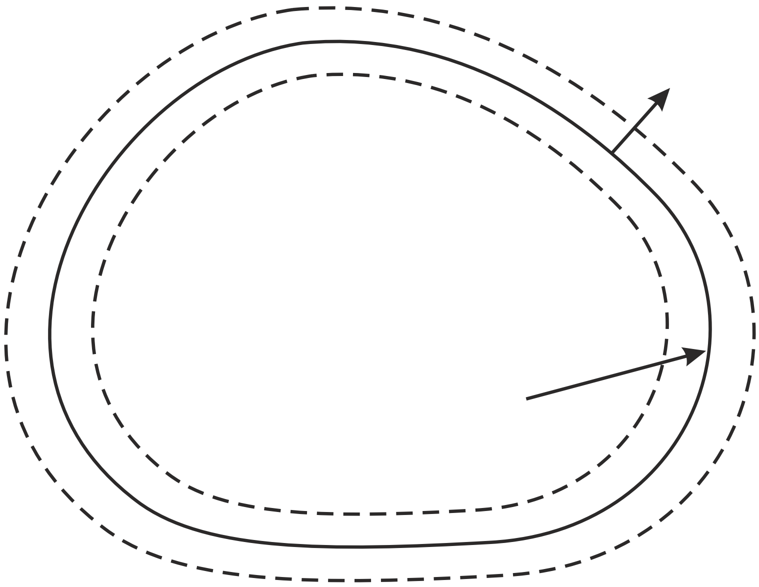

Figure D.4.: Surface defined by $f = 0$.

Thereby, the gradient of f points in the direction of $\boldsymbol{n}$. In a next step, we will decompose the volume element into a surface element $\mathrm{d}s$ and a line element $\mathrm{d}l_\perp$ in the direction of $\boldsymbol{n}$, and write

$$\mathrm{d}\boldsymbol{x} = \mathrm{d}l_\perp \; \mathrm{d}s \,.$$

Since, f is zero on the surface Γ, a Taylor expansion up to first order results in

$$f = \left(\frac{\partial f}{\partial l_\perp} \right)_\Gamma l_\perp = |\nabla f| \, l_\perp \,.$$

Using this relation and the property (D.2), we may write

$$\delta(f) = \delta(|\nabla f| l_\perp) = \frac{\delta(l_\perp)}{|\nabla f|} \,.$$

Hence, we obtain

$$\begin{aligned} \int_{-\infty}^{\infty} \phi(\boldsymbol{x}) \nabla H(f) \; \mathrm{d}\boldsymbol{x} &= \int_{-\infty}^{\infty} \phi(\boldsymbol{x}) \nabla f \, \delta(f) \; \mathrm{d}\boldsymbol{x} \\ &= \int_{-\infty}^{\infty} \phi(\boldsymbol{x}) \underbrace{\frac{\nabla f}{|\nabla f|}}_{\boldsymbol{n}} \delta(l_\perp) \; \mathrm{d}l_\perp \; \mathrm{d}s \\ &= \oint_\Gamma \phi(\boldsymbol{x}) \boldsymbol{n} \, \mathrm{d}s \,, \end{aligned} \tag{D.9}$$

since $\boldsymbol{n} = \nabla f / |\nabla f|$.

Bibliography

[1] T. J. R. Hughes, W. K. Liu, and T. K. Zimmermann. Lagrangian-Eulerian finite element formulation for incompressible viscous flows. *Computer Methods in Applied Mechanics and Engineering*, 29(3):329–349, 1981.

[2] F. Durst. *Grundlagen der Strömungsmechanik*. Springer, 2006.

[3] H. Schlichting and K. Gersten. *Grenzschicht-Theorie (Boundary layer theory)*. Springer, 2006.

[4] M. S. Howe. *Theory of Vortex Sound*. Cambridge Texts in Applied Mathematics, 2003.

[5] G. K. Batchelor. *An introduction to fluid dynamics)*. Cambridge University Press, 1967.

[6] S. Glegg and W. Devenport. *Aeroacoustics of low Mach number flows*. Academic Press, 2017.

[7] M.J. Lighthill. On sound generated aerodynamically I. General theory. *Proc. Roy. Soc. Lond.*, (A 211):564–587, 1952.

[8] D. G. Crighton, A. P. Dowling, J. E. Ffowcs-Williams, M. Heckl, and F. G. Leppington. *Modern methods in analytical acoustics*. Springer Lecture Notes, 1992.

[9] O. M. Phillips. On the generation of sound by supersonic turbulent shear layers. *J. Fluid Mech.*, 9:1–18, 1960.

[10] G. M. Lilley. On the noise from jets. Technical report, AGARD CP-131, 1974.

[11] M. E. Goldstein. *Aeroacoustics*. McGraw-Hill, 1976.

[12] S. C. Crow. Aerodynamic sound emmission as a singular perturbation problem. *Studies of Applied Mathematics*, 49:21–44, 1970.

[13] N. Curle. The influence of solid boundaries upon aerodynamic sound. *J. Proc. Roy. Soc. London*, A:231–505, 1955.

[14] J E. Ffowcs-Williams and D. L. Hawkings. Sound radiation from turbulence and surfaces in arbitrary motion. *Phil. Trans. Roy. Soc.*, pages 321–342, 1969.

[15] H. Lamb. *Hydrodynamics*. Cambridge University Press, 1932.

[16] J. C. Hardin and D. S. Pope. An acoustic/viscous splitting technique for computational aeroacoustics. *heoretical and Computational Fluid Dynamics*, pages 323–340, 1994.

[17] W. Z. Shen, J. N. Sørensen. Aeroacoustic modelling of low-speed flows. *Theoretical and Computational Fluid Dynamics*, 13:271–289, 1999.

[18] R. Ewert and W. Schröder. Acoustic perturbation equations based on flow decomposition via source filtering. *Journal of Computational Physics*, 188:365–398, 2003.

[19] J.H. Seo and Y.J. Moon. Perturbed compressible equations for aeroacoustic noise prediction at low mach numbers. *AIAA Journal*, 43:1716–1724, 2005.

[20] C.D. Munz, M. Dumbser, and S. Roller. Linearized acoustic perturbation equations for low Mach number flow with variable density and temperature. *Journal of Computational Physics*, 224:352 – 364, 2007.

[21] A.Hüppe. *Spectral Finite Elements for Acoustic Field Computation.* PhD thesis, University of Klagenfurt, Austria, 2013.

[22] M. E. Goldstein. A generalized acoustic analogy. *Journal of Fluid Mechanics*, 488:315–333, 2003.

[23] M. Kaltenbacher. *Numerical Simulation of Mechatronic Sensors and Actuators: Finite Elements for Computational Multiphysics.* Springer, 3 edition, 2015.

[24] B. Henderson. Automobile noise involving feedback- sound generation by low speed cavity flows. Technical report, In: Third Computational Aeroacoustic(CAA) Workshop on Benchmark Problems, 2000.

[25] T. Seitz. Experimentelle Untersuchungen der Schallabstrahlung bei der Überströmung einer Kavität. Master's thesis, Friedrich Alexander Universität Erlangen, 2005.

[26] B. Farkas and G. Paal. Numerical study on the flow over a simplified vehicle door gap an old benchmark problem is revisited. *Period. Polytech. Civil Eng.*, 59(3):337–346, 2015.

[27] A. Oberai, F. Roknaldin, and T. J. R. Hughes. Computation of trailing-edge noise due to turbulent flow over an airfoil. *AIAA*, 40(11), 2002.

[28] M. Kaltenbacher. *Numerical Simulation of Mechatronic Sensors and Actuators: Finite Elements for Multiphysics.* Springer, Berlin, 3. edition, 2015.

[29] R. P. Kanwal. *Generalized Functions: Theory and Technique.* Academic Press, 1983.